Mechanisms Regulating Osteoblast Response to Surface Microtopography and Vitamin D

A Dissertation
Presented to
The Academic Faculty

By

Bryan Frederick Bell, Jr.

In Partial Fulfillment
of the Requirements for the Degree
Doctor of Philosophy in the
School of Materials Science and Engineering

Georgia Institute of Technology
December, 2009

Mechanisms Regulating Osteoblast Response to Surface Microtopography and Vitamin D

Approved by:

Dr. Barbara D. Boyan, Advisor
School of Biomedical Engineering
Georgia Institute of Technology

Dr. Nael McCarty
School of Medicine
Emory University

Dr. Zvi Schwartz
School of Biomedical Engineering
Georgia Institute of Technology

Dr. Anthony Norman
Department of Biochemistry
University of California, Riverside

Dr. Andrés J. García
School of Mechanical Engineering
Georgia Institute of Technology

Date Approved: September 22, 2009

ACKNOWLEDGEMENTS

First and foremost, I would like to thank my advisors Dr. Barbara Boyan and Dr. Zvi Schwartz. Dr. Boyan was kind enough to take a materials science student into a lab focused heavily on the biological side of biomaterials engineering. I had done research in the orthopaedic implant area, but I had never actually tested cell response to material surfaces. Dr. Boyan has helped teach me that understanding the underlying biology and host response is central to the proper design of biomedical devices. In addition, I would like to thank Dr. Boyan for her personal support throughout my graduate studies. Dr. Boyan allowed me the freedom to participate in business school and programs like TI:GER that have helped me develop skills that will be valuable to me in my future career. Very few advisors would allow students this freedom, so for that I am extremely thankful. I would also like to thank my co-advisor Dr. Schwartz, who helped guide me through the thesis project. He has helped me in designing experiments so that the techniques applied are consistent and repeatable. Dr, Schwartz has also pressured me to work hard and continuously try to improve the quality of my work.

I also greatly appreciate the help of my committee in shaping the direction of my thesis. Dr. Andres Garcia has helped me through the thesis work, course work, and the qualifier to think more deeply about cell-surface interactions. Dr. Nael McCarty has also been helpful to my thesis and to my understanding of biology. Dr. McCarty's biology course was my first graduate level biology and has been critical in helping me adapt to research in the Boyan lab. I would also like to thank Dr. Anthony Norman, whose papers and advice have required me to think more broadly about the roles of membrane and nuclear vitamin D receptors.

I would also like to extend my appreciation to my labmates. Sayeed Safavynia, Gary Seeba, John Douly, and Leang Chhung have all been extremely helpful in culturing

cells throughout my Ph.D. Sayeed Safavynia, Reyhaan Chaudhri, and Sharon Hyzy have been extremely supportive in their roles as lab manager over the past few years. I also have to thank the undergraduate students who have helped me over the past few years. These students include Naghmeh “Naz” Majdi, Michael Chervonski, Malcolm Blanchard, and Jonathan Martinez. Naz and Michael have contributed extensively to the KRSR, VDR, and caveolae studies presented herein this thesis. I would also like to thank Dr. Ramsey Kinney who was my labmate and also my ‘big brother’ in college. Ramsey’s opinions, though not always asked for, have been valuable in shaping some of the thoughts in this thesis. Dr. Rene Olivares-Navarrete, Dr. Liping Wang, Dr. Yun Wang, and Dr. Hai Yao have also been extremely helpful in providing advice on topics throughout the thesis. I also appreciate the support of my fellow graduate students including Jennifer Hurst-Kennedy, Brandy Rogers, Ming Zhong, Dr. Tracy Denison, Kevin Wong, Jessica Mata, Dr. Alice Zhao, Chris Lee, Jiaxian Chen, Andrew Raines, Chris Herman, Maryam Doroudi, Khairat Elbaradie, Jamie Lazin, and Reyhaan Chaudhri.

I am thankful for my friends and family who have supported me throughout the Ph.D. process. My mother and father have encouraged me when I have struggled with experiments and have been accepting when I have had to leave on holidays to go feed cells. My brother and sister have always been encouraging of my graduate studies, but have not so secretly wondered if I would ever graduate. I was also lucky enough to meet my fiancé, Ashley Struck, while in graduate school. When I met Ashley over two and a half years ago I told her that I was nearing graduation. Fortunately, she is an incredibly patient and understanding person. I am so grateful for the love and support of Ashley throughout the Ph.D. process. Finishing would have been difficult without the support of Ashley, my friends, and my family.

TABLE OF CONTENTS

LIST OF TABLES

LIST OF FIGURES

VDR KNOCKOUT OSTEOBLASTS

CAVEOLIN-1 KNOCKOUT OSTEOBLASTS

APPENDIX

SUMMARY

A comprehensive understanding of the interactions between orthopaedic and dental implant surfaces with the surrounding host tissue is essential in the design of advanced biomaterials that better promote bone growth and osseointegration of implants. Dental implants with roughened surfaces and high surface energy are well known to promote osteoblast differentiation *in vitro* and promote increased bone-to-implant contact *in vivo*. In addition, increased surface roughness increases osteoblasts response to the vitamin D metabolite $1\alpha,25(OH)_2D_3$. However, the exact mechanisms mediating cell response to surface properties and $1\alpha,25(OH)_2D_3$ are still being elucidated. The central aim of the thesis is to investigate whether integrin signaling in response to rough surface microtopography enhances osteoblast differentiation and responsiveness to $1\alpha,25(OH)_2D_3$. The hypothesis is that the integrin $\alpha_5\beta_1$ plays a role in osteoblast response to surface microtopography and that $1\alpha,25(OH)_2D_3$ acts through VDR-independent pathways involving caveolae to synergistically enhance osteoblast response to surface roughness and $1\alpha,25(OH)_2D_3$. To test this hypothesis the objectives of the studies performed in this thesis were: 1) to determine if $\alpha_5\beta_1$ signaling is required for osteoblast response to surface microstructure; 2) to determine if increased responsiveness to $1\alpha,25(OH)_2D_3$ requires the vitamin D receptor, 3) to determine if rough titanium surfaces functionalized with the peptides targeting integrins (RGD) and transmembrane proteoglycans (KRSR) will enhance both osteoblast proliferation and differentiation, and 4) to determine whether caveolae, which are associated with integrin and $1\alpha,25(OH)_2D_3$ signaling, are required for enhance osteogenic response to surface microstructure and $1\alpha,25(OH)_2D_3$.

The results demonstrate that integrins, VDR, and caveolae play important roles in mediating osteoblast response to surface properties and $1\alpha,25(OH)_2D_3$. Silencing of the β_1 integrin in osteoblast-like MG63 cells significantly reduced osteogenic response to surface topography and $1\alpha,25(OH)_2D_3$. Silencing of the α_5 subunit did not alter the response of MG63 cells to changing surface roughness or chemistry, although future work must confirm these results given similar cell surface α_5 integrin expression observed in control and α_5-silenced cells. Multifunctional RGD, KRSR, and K<u>S</u>SR coated surfaces show that RGD increased osteoblast proliferation and reduced differentiation, KRSR had no affect on osteoblast phenotype, and K<u>S</u>SR increased osteoblast differentiation. These results suggest that titanium surfaces can be modified to manipulate proliferation and differentiation and that RGD/K<u>S</u>SR functionalized surfaces could be further investigated for use as osteointegrative surfaces. The results using VDR deficient osteoblasts demonstrate that $1\alpha,25(OH)_2D_3$ acts via VDR-dependent mechanisms in cells cultured on titanium surfaces that support terminal differentiation. In caveolae deficient osteoblasts, $1\alpha,25(OH)_2D_3$ affected cell number, alkaline phosphatase activity, and TGF-β1 levels, although levels of osteocalcin and PGE_2 were not affected. These results are consistent with the hypothesis that VDR is required for the actions of $1\alpha,25(OH)_2D_3$, but that caveolae-dependent membrane $1\alpha,25(OH)_2D_3$ signaling modulates traditional VDR signaling. The exact mechanisms for this interaction remain to be shown. Overall, these results are important in better understanding the role of β_1 integrin partners in mediating osteoblast response to implant surfaces and in understanding how integrin signaling can alter osteoblast differentiation and responsiveness to $1\alpha,25(OH)_2D_3$ via genomic and non-genomic pathways.

CHAPTER 1: Introduction

Modern orthopaedic implants have been enormously successful in relieving pain and restoring basic joint function for hundreds of thousands of patients each year; however, increased patient lifetime and activity levels are creating demand for advances in device performance. Orthopaedic implant design has traditionally relied on advances in materials engineering and manufacturing processes to make biomaterials more biocompatible and less susceptible to fatigue and wear [1-3]. Approaches inspired by the underlying biology and biological response to implants have the potential to create biomaterials that actively direct host cell and tissue response to form a strong bone-implant interface [4, 5]. A comprehensive understanding of the mechanisms guiding interactions between the implant surface, attached osteoblasts, and the surrounding host tissue will allow engineers to design surfaces that better promote bone growth and osseointegration of the implant. Moreover, an increased understanding of the mechanisms regulating bone turnover and the response of osteoblasts to hormones, growth factors, or other biologics could lead to combination therapies that aid in osseointegration of implants.

The present set of studies presented herein this thesis are aimed at 1) gaining a better understanding of mechanisms underlying osteoblast response to implant surface topography and chemistry, 2) determining whether specific ligands can actively recruit osteoblasts and promote an osteogenic phenotype, and 3) exploring the mechanisms through which the vitamin D metabolite $1\alpha,25(OH)_2D_3$ can act to enhance the response of osteoblasts to surface energy and chemistry. The following sections in this chapter will explore the relevant general background material that serves as a basis for the aims of this thesis. These topics include bone anatomy and physiology, osteoblast biology,

and host response to biomaterials. There will also be discussion of current orthopaedic implant technology and advanced surface engineering techniques that can be used to improve upon current designs. Next, there will be discussion of vitamin D physiology, $1\alpha,25(OH_2)D_3$ signaling mechanisms, and the effects of $1\alpha,25(OH_2)D_3$ on osteointegration of implants. Finally, this chapter will conclude with a summary of the objectives of this thesis with regard to the highlighted clinical and scientific needs.

1.1. Bone Anatomy and Physiology

Bone is a dynamic tissue that provides critical structural, metabolic, and physiological functions for the body. Bone is the most rigid and strongest material in the body. It has yield strength between 90-140 MPa, comparable to some metals, yet its density is only 1.6 g/cm^3, making it an extraordinarily efficient structure [6, 7]. More importantly, bone constantly undergoes remodeling, a process that both repairs bone and helps it adapt to changing stress conditions. No artificial material has such resilience to decades of fatigue loading. Bone protects vital internal organs and the long bones house bone marrow, which is the source of haematopoiesis. Bones provide the shape and structure through which muscles are able to transmit force to create movement. Bone also serves as a reservoir for calcium and phosphorus, which can be released through bone resorption to help maintain overall mineral ion homeostasis.

Bone is a highly organized nanocomposite material made up primarily of collagen I, carbonate-substituted hydroxyapatite [$Ca_{10}(PO_4)_6OH_2$], water, and cells [8]. The hierarchical organization of bone makes it strong, tough, and lightweight, and provides a structure through which cells can maintain and remodel bone. The hierarchical nature of bone is shown in Figure 1-1 on the following page [9]. At the macroscopic level, bones are composed of either cortical or cancellous bone. Cortical bone is highly compact and composes the outer layer of all bones as well as the diaphysis of long bones [8].

Cortical bone makes up more than 80% of total bone mass and gives bone much of its resistance to bending, compressive, and torsional forces [6, 8]. Cancellous, or trabecular bone, is composed of a porous network of bone spicules that align along directions of stress in the metaphyses and epiphyses of long bones or in the interior of vertebrae. Trabecular bone is roughly four times less dense than cortical bone and undergoes much more turnover due to its high surface area. Because of this difference in turnover, trabecular bone is more susceptible than cortical bone to bone mass loss caused by osteoporosis [10].

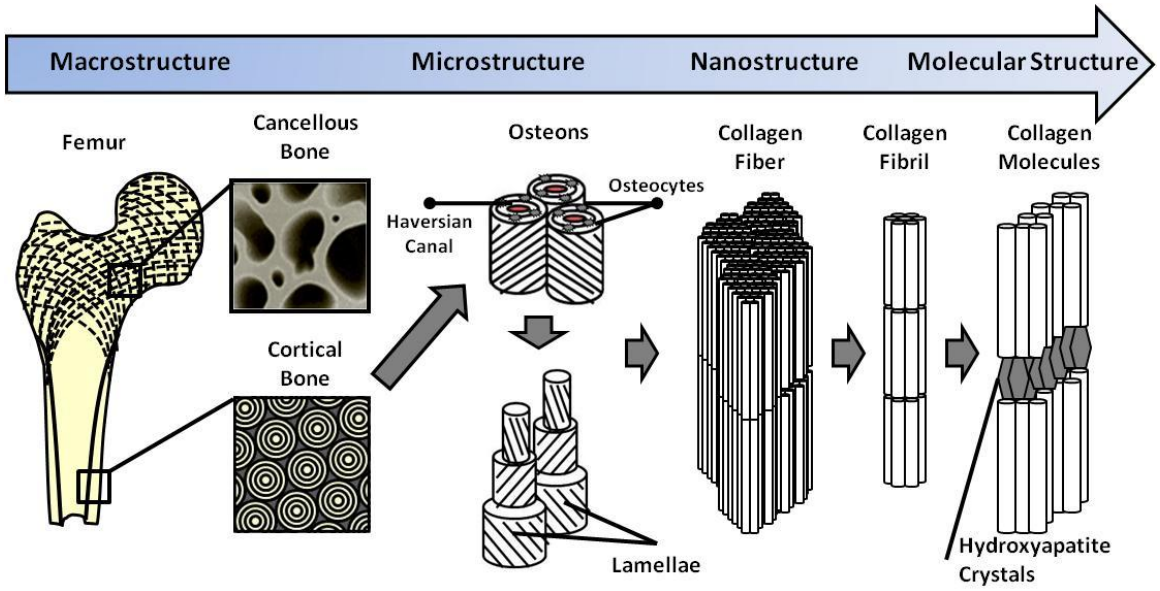

Figure 1-1: Schematic demonstrating the hierarchical nature of bone from the macroscale to the nanoscale [9].

In immature bone, such as found in early development or in a fracture callous, collagen fibers are randomly oriented to form what is called woven bone. In mature bone, such as found in both cortical or trabecular bone, collagen fibers align to form into 3-7 μm thick lamellae of uniform orientation [9]. Cortical bone is highly dense and the lamellae are very organized. Osteons are the major functional unit of cortical bone and are usually aligned along the length of long bones. Osteons are up to 500 μm in

diameter and contain multiple lamellae wrapped in layers around central a Haversian canal [6]. The alignment of fibers in adjacent lamellae is slightly offset; likely providing increased strength in torsion. The Haversian canal contains blood vessels or nerves that support osteocytes embedded within the osteons. These cells are critical in maintaining mature bone and providing sensory information to surrounding cells.

At the molecular level, bone is composed primarily of collagen I and hydroxyapatite, although a number of bone specific proteins are involved in bone matrix organization and the nucleation of hydroxyapatite crystals [6, 9]. Hydroxyapatite crystals form in nanoscale sheets within specific spaces of the collagen fibrils. This nanocrystalline organization increases strength and toughness and reduces the potential for crack propagation. The collagen fibrils and the c-axis (strongest axis) of the hydroxyapatite crystals both align along the direction of maximum stress. These collagen fibrils are arranged in to the larger fibers that make up woven and lamellar bone. Overall, the complex organization of bone at different length scales makes it an extremely efficient structure and also gives bone its ability to detect and continuously repair microdamage without compromising its overall structural integrity.

Bone Remodeling

Bone turnover is a highly regulated process that enables bone to regenerate itself, adapt to changing stress environments, and mobilize calcium to meet metabolic needs [6]. This process is described below and shown in Figure 1-2. Old or damaged bone is resorbed by osteoclasts via a process called bone resorption. Osteoclasts are large multinucleated cells of hematopoietic lineage derived from the fusion of monocytes and macrophages. Osteoclasts are activated and recruited to sites of microfracture by factors such as macrophage colony stimulating factor (M-CSF) and receptor activator of nuclear factor κβ ligand (RANKL) [11]. Active osteoclasts can be identified be their

ruffled cell borders, which seal and degrade the underlying bone in the resorption pit. Osteoclasts resorb bone through the release of hydrogen ions, matrix metalloproteases, and multiple hydrolytic enzymes.

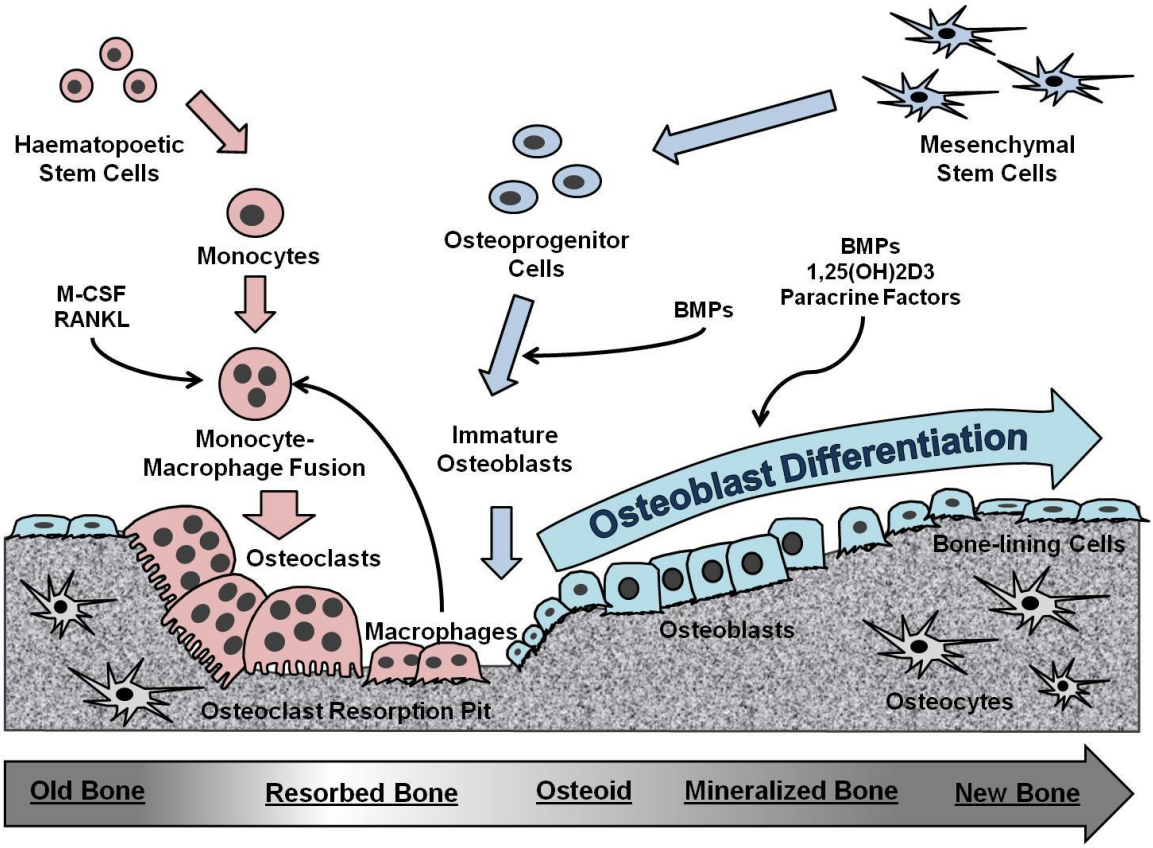

Figure 1-2: Bone remodeling process [6, 8]. Old bone is resorbed by osteoclasts. New bone is formed by osteoblasts, which eventually terminally differentiate into osteocytes.

New bone is formed by osteoblasts, which are cells of mesenchymal lineage derived from osteoprogenitor cells located in the periosteum or bone marrow. Osteoprogenitors differentiate into osteoblasts, a process that will be discussed extensively in section 1.5. Osteoblasts form new bone matrix, called osteoid, which is later mineralized as osteoblasts mature. As osteoblasts become surrounded by mineralized matrix, they become osteocytes. Osteocytes are terminally differentiated cells that are important in maintenance of deposited bone, mechanosensation, and

calcium homeostasis. Osteocytes rest in fluid-filled spaces called lacuna and communicate with surrounding cells via extensions called canniculae. Eventually, bone suffers microdamage and osteocytes undergo apoptosis, upon which time osteoclasts are recruited and the renewal of bone continues.

1.2. Total Joint Replacements

Total joint replacement has been an invaluable tool for relieving joint pain and restoring basic function for hundreds of thousands of patients each year suffering from traumatic injuries or from debilitating diseases such as late stage osteoarthritis, rheumatoid arthritis, or avascular necrosis [10]. Osteoarthritis is a painful degenerative disease in which the articular cartilage and subchondral bone are progressively damaged and worn, eventually necessitating surgical intervention. Osteoarthritis affects more than 60% of people over the age of 65 and is the primary cause of more than 39 million physician visits in the U.S. each year [12, 13]. Osteoarthritis is typically treated with non-steroidal anti-inflammatory drugs (NSAIDs), changes in diet and exercise, corticosteroids, arthroscopic surgery, and in severe cases total joint replacement [14]. Osteoarthritis accounts for half of NSAID prescriptions [12] and roughly 90% of the 285,000 hip implants and 523,000 knee implants each year in the U.S (2005 data) [13, 15]. Aging population trends, increasing obesity rates, and the treatment of younger patients is projected to increase the number of hip implants and knee implants in the U.S. per year to 572,000 and 3,480,000, respectively, by 2030 [15, 16]. Moreover, patients today expect implants to last their lifetime and to restore an active lifestyle. Such changing demographics and performance requirements are putting tremendous pressure on implant manufactures to deliver more innovative implant designs.

Current orthopaedic implant design is being driven by increased demand for longer lasting implants, for minimally invasive surgery, and for use in younger, more

active patients. Orthopaedic implants currently have an expected lifetime of more than 15 years in 85-90% of patients [7]. Such survival rates are a testament to the success of advances in biomaterials, implant design and manufacturing, and surgical techniques; however, increased life expectancies, lifestyle changes, and treatment of younger patients means many more patients will require revision surgeries over their lifetime [15]. Revision surgeries are difficult, expensive, dangerous to the patient, and statistically are less successful than primary surgeries [7]. Young patients present a unique problem because the increased activity puts more stress and wear on the implant. Even recent studies using advanced ceramic bearing surfaces have only shown 15-year implant survival rates of only 72% in patients fewer than 30 years old [17]. In addition, there is increasing pressure to treat more patients with osteoporosis or other comorbidities that affect bone ingrowth around an implant [3]. Such problems require technological improvements that further improve osteointegration and reduce long-term wear.

Implant Technology: A Focus on the Hip Implant

The total hip implant provides an illustrative example of the challenges facing engineers in designing better implants. A hip implant must be engineered to carry loads in excess of 1400 pounds, to survive years of fatigue loading, to be highly resistant to wear and corrosion, to be highly biocompatible, and to establish good long-term fixation with the host bone [1-3, 18]. The design of the modern hip implant still resembles the original design of Charnley from the 1960's, although the underlying materials have advanced [18]. A modern hip implant, shown in Figure 1-3, consists of three major components: the acetabular cup, the femoral head, and the femoral neck and stem. The femoral head and the acetabular cup of the implant replace the ball and socket portion of the natural hip joint. The metallic back of the acetabular cup is fixated to the pelvis, while the femoral component is fixated into the femur. The metallic components of

modern implants are usually made of fatigue resistant alloys of titanium (Ti-6Al-4V) or cobalt-chromium (CoCr). The acetabular cup has traditionally contained a plastic insert made of ultrahigh molecular weight polyethylene (UHMWPE); although companies have begun to market metal-on-metal and ceramic-ceramic wear systems. Wear rates for UHMWPE systems are generally about 0.1mm per year compared to 0.01mm per year or less for metal-on-metal (CoCr) or ceramic-on-ceramic (zirconia or alumina based) systems [18]; however, long-term clinical data has not yet proven which systems yield the highest long-term survival rates. While improved wear surfaces are certainly crucial to improving implant performance, the present thesis is focused more on the potential for improvements in bone-bonding surfaces and the osteointegration of titanium implants.

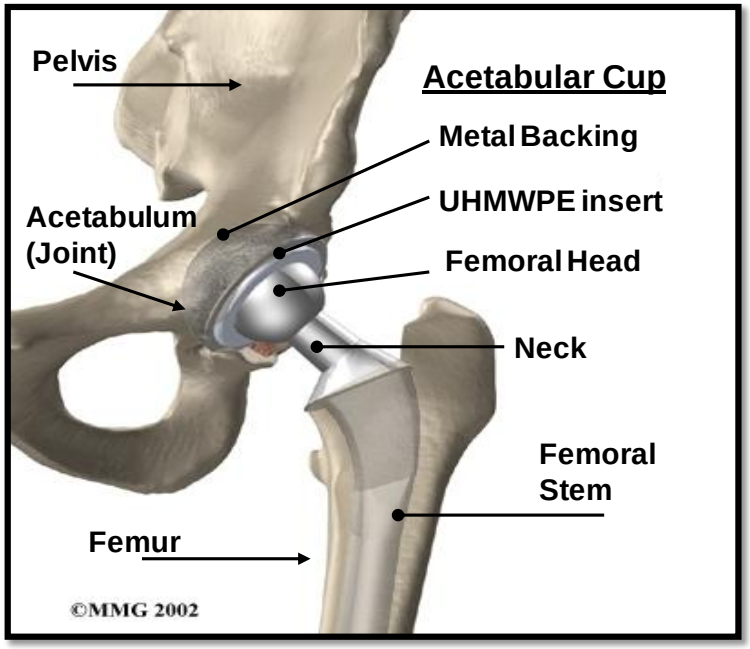

Figure 1-3: Model of a hip implant. Modified from the Medical Multimedia Group [19].

Titanium in Orthopaedic and Dental Implant Design

Titanium and its alloys are frequently used in orthopaedic and dental implants because of their biocompatibility, corrosion resistance, strength, fatigue resistance, and

ease of processing [20]. Titanium atoms can be arranged in two different phases: the hexagonal close packed (hcp) α phase or the body centered cubic β phase. Pure titanium is stable in the α phase at room temperature. The Ti-6Al-4V alloy is an α+β alloy where the aluminum atoms stabilize the α phase and the vanadium atoms stabilize the β phase. All alloys of titanium form a thin, passivating layer of oxide (primarily TiO_2) that is responsible for its resistance to corrosion and its good biocompatibility.

The most common metals used in orthopaedic implants are cpTi, Ti-6Al-4V, and CoCr [20]. Commercially pure titanium is used predominantly in dental implants since wear is not an issue. The properties and characteristics of these metals and other materials used in implants are shown below in Table 1 [1, 7]. Clear tradeoffs exist in the use of cpTi, Ti-6Al-4V, and CoCr for different components in implant design. Ti-6Al-4V is

Table 1: Relevant properties of materials used in orthopaedic and dental implants.

Material	Elastic Modulus (GPa)	Tensile Strength (MPa)	Advantages	Disadvantages	Uses
cpTi	110	400	Biocompatibility, osteointegration, resists corrosion	Fatigue and wear resistance	Orthopaedic & dental implants
Ti-6Al-4V	124	940	Biocompatibility, corrosion & fatigue resistance	Wear resistance (fretting)	Orthopaedic implants
316L Stainless Steel	193	540	Cost, availability	Biocompatibility corrosion	Some trauma hardware
CoCr	214	480	Wear & corrosion resistance fatigue strength	Biocompatibility stress shielding	Orthopaedic implants
PMMA	3	35-50	Rapid fixation	Fatigue, cracking, 3rd body wear	Bone cements
Bone	10-30	70-150	-	-	-

generally preferred over cpTi in high load bearing applications because it has higher strength, wear resistance, and fatigue resistance; however, cpTi has superior biocompatibility to Ti-6Al-4V because of potential host sensitivity to aluminum and

vanadium ions. Both forms of titanium are more biocompatible than either CoCr or stainless steel. Unfortunately, the relatively soft surface layer of titanium makes it susceptible to fretting corrosion and corrosion cracking under heavy wear. Because of problems with fretting wear of titanium, CoCr alloys are frequently used as a wear component of orthopaedic implants. CoCr alloys have excellent wear properties, corrosion resistance, and fatigue resistance, but they are less biocompatible than titanium alloys. CoCr alloys also have a higher elastic modulus than titanium, which can increase the risk of osteolysis and fracture due to stress shielding of bone surrounding the implant. Furthermore, many have or develop hypersensitivity to Co, Cr, or Ni [21]. The release of such metal ions and particles can cause metallosis, inflammation, and peri-implant osteolysis. For these reasons, titanium is the most preferred material for the components of implants that interface directly with bone and depend on osteointegration for function.

Long-term Failure of Orthopaedic Implants

Early problems with implants, such as infection and breakage, are largely avoided today because of improved surgical techniques, improved implant designs, more stringent manufacturing standards, and the use of strong alloys. Long-term failure of implants is most often attributed to implant loosening, which can cause severe pain, loss of joint function, and necessitate revision surgery [1]. Roughly 30-40% of hip implant patients show radiographic signs of femoral loosening by 10 years [22]. More than 10% of patients with orthopaedic implants will require a revision surgery within 15 years of their primary surgery [23]. The cascade of events leading to implant loosening is complex, although most these problems can be traced to two root causes: 1) bone resorption (osteolysis) due to cellular response to wear particles generated from the articulating surfaces, and 2) osteolysis due to poor long-term biocompatibility and/or loss

of fixation at the bone-biomaterial interface. These problems are inherently due to the materials selected for implantation and suboptimal engineering of the surfaces interfacing with the biological environment [23]. The development of a stable bone-material interface that promotes long-term fixation is essential to reducing implant loosening and extending implant lifetime.

1.3. Host Response to Orthopaedic Biomaterials

The interaction of a biomaterial with the biological environment is dependent on the composition and topography of the surface, the chemical nature of adsorbed proteins, and the physiological response of local host tissue [1]. This complex and dynamic process begins even before a device is implanted into the body. Metallic surfaces made of titanium or cobalt-chrome alloys quickly form an oxide layer after exposure to air. In addition, organic and inorganic particles from the air rapidly adsorb to the surface. This layer usually increases the material's hydrophobicity, changing the surface proteins and affecting protein adsorption [24]. Once a biomaterial is implanted, a protein monolayer adsorbs to the surface within a fraction of a second. Most proteins are amphiphilic and only partially soluble in an aqueous environment. Entropic forces drive adsorption of proteins to the surface in an effort to minimize energy [25]. The process of adsorption causes the proteins to partially unfold. The conformation a protein exhibits on a surface depends on the protein's primary amino acid sequence, which determines the secondary and tertiary structures through non-covalent binding; however, final structure of a protein is sensitive to the surrounding aqueous environment, the local pH, temperature, time of adsorption, and the interaction with nearby surfaces or other proteins, lipids, and ions. Moreover, the conformation, unfolding rate, and the degree of biological functionality of proteins vary by surface and depend on protein size, shape, and binding affinity for the surface. The first proteins to bind are those in high

concentration and those that diffuse quickly to the surface. Over time, the surface evolves as large, high affinity proteins replace proteins with less affinity according in a process called the Vroman effect. Serum proteins such as fibrinogen, albumin, vitronectin, fibronectin, and various immunoglobulins are among first proteins to attach and are crucial in initiating early clotting and inflammatory responses [26].

Peri-implant Healing Process

The first host response in peri-implant healing is the formation of a blood clot, or haematoma at the implant site [27, 28]. Thus, the first cells to come in contact with the implant are not predominantly osteoprogenitor cells, but are platelets, erythrocytes, neutrophils, leukocytes, and other cells present in the blood. The clot typically lasts a few days and is accompanied by acute inflammation of the injured tissue. Neutrophils are present at the injury site for the first few days. These first responders are largely responsible for identifying and destroying invading pathogens. Neutrophils are subsequently replaced by cells characteristic of chronic inflammation including monocytes, macrophages, and lymphocytes. These leukocytes fight infection, degrade damaged tissue, and control the healing response based on the release of various mitogens and cytokines. The formation of granulation tissue occurs within a few days of implantation and can last for several weeks. Granulation tissue is highly vascular and contains a high concentration of macrophages, leukocytes, and fibroblasts. Growth factors such as platelet derived growth factor (PDGF) and transforming growth factor β1 (TGF-β1) are important mitogens for recruiting fibroblasts, which produce the provisional extracellular matrix in granulation tissue. Angiogenic factors like vascular endothelial growth factor (VEGF) and fibroblast growth factor 2 (FGF2) initiate new blood vessel formation necessary for wound healing and the formation of bone.

In materials with poor biocompatibility, undesired host response can lead toward foreign body reaction and fibrosis of the implant. Foreign body reaction is characterized by chronic inflammation and the appearance of foreign body giant cells, which are large, multinucleated cells created by the fusion of macrophages for the purpose of surrounding and degrading the implanted biomaterial. Persistent foreign body reaction ultimately leads to fibrous encapsulation of the implant. Fibrosis occurs when the body forms a dense layer of fibroconnective tissue around the implant. Unfortunately, the strength of the bond between this scar tissue and the implant is not strong. The clinical result of a fibrous response is implant loosening, likely necessitating surgical revision.

Ideally, direct bone apposition, or osteointegration, occurs at bone-implant interface and creates lasting long-term fixation. In peri-implant healing, osteoprogenitor cells are primarily derived from the marrow because of the presence of newly vascularized granulation tissue [27]. Osteoprogenitors may be recruited to the surface by growth factors such as PDGF, FGF-2, or bone morphogenic proteins released by cells at the implant surface [27, 29]. The formation of bone requires recruitment and proliferation of osteoprogenitor cells as well as differentiation of these cells into mature osteoblasts. Mature osteoblasts secrete osteoid and mineralize it to form newly woven bone similar to new bone seen in fracture healing. Osteointegration occurs through the osteoconduction of these cells along the surface and through appositional bone growth [27]. Remodeling occurs continuously over the subsequent weeks and months to further strengthen the implant-bone interface. The level of bone-to-implant contact, a histological measure of osteointegration, is strongly affected by implant surface chemistry and topography [30, 31]. The following sections will discuss the direct interactions of osteoblasts with implant surfaces, how surface engineering can enhance osteointegration, and how steroid hormones modulate cell response to surfaces.

1.4. Osteoblast Interactions with Surfaces

Osteoblast proliferation, morphology, and phenotypic expression, along with intercellular signaling and recruitment, are indirectly affected by implant surface properties via the adsorbed protein layer [24]. As discussed in the previous section, surface properties affect biological response by controlling not only which proteins adsorb to the surfaces, but how these proteins are presented to cells.

Integrins

Cells interact with the extracellular matrix via receptors called integrins [32]. Integrins are heterodimeric glycoproteins consisting of a pair of α and β membrane-spanning subunits. There are currently known to be 18 different α subunits and 8 different β subunits that can be assembled into at least 24 different αβ dimer combinations [33], each of which may have unique binding specificity and sets of downstream signaling events. This vast array of combinations means that different tissues generally express different sets of integrins. For instance, osteoblasts have been shown to express the integrins $\alpha_1\beta_1$, $\alpha_2\beta_1$ $\alpha_3\beta_1$, $\alpha_4\beta_1$, $\alpha_5\beta_1$ $\alpha_6\beta_1$, $\alpha_8\beta_1$, $\alpha_V\beta_3$, $\alpha_V\beta_5$, [34], although reports in the literature vary on the relative expression levels of these integrins in bone cells [35-38]. Expression of integrins can also vary according to the composition of the surrounding ECM and to the state of maturation of the cell. In addition, standard tissue culture on tissue culture polystyrene surfaces and the culture of cells on surfaces of varying chemistry and topography can alter integrin expression [38, 39]. For instance, increasing the roughness of titanium surfaces leads to higher expression of $\alpha_2\beta_1$ and lower expression of $\alpha_5\beta_1$ [40]. These results correlate with higher levels of osteocalcin, an indicator of osteoblastic differentiation. Moreover, $\alpha_2\beta_1$ has been shown to regulate differentiation of MG63 cells in response to increasing surface roughness [41]. These results together suggest that integrins can affect cell

differentiation, and vice versa, that cell differentiation can affect integrin expression or activity.

Integrins bind to specific recognition sequences in proteins, such as the RGD (arginine, glycine, aspartic acid) binding domain of fibronectin or the GFOGER (glycine-phenylalanine-hydroxyproline-glycine-glutamine-arginine) binding domain of collagen I; although binding site accessibility and binding affinity are most certainly affected by secondary and tertiary protein structure [42]. Many integrins also require secondary binding of 'synergy sites' to initiate maximum signaling effectiveness [43]. Binding of individual integrins to the ECM is relatively weak, but ligand binding initiates clustering of multiple integrins to form a larger signaling complex. The cytoplasmic tails of clustered integrins bind to a multitude of adapter proteins that can connect integrins to the cytoskeleton, protein kinases and lipases, various growth factor receptors, and even caveolin-1 [44]. Clusters of integrins further arrange into larger focal adhesion complexes that are critical to cell attachment. Focal adhesions are points of attachment between the cell and the substrate that are often located at the end of cell extensions called filopodia. Such complexes maximize the cell-substrate binding strength. Furthermore, these complexes act as signaling nexuses that allow interaction between integrins, growth factor receptors, caveolae, and many other signaling pathways [44].

Integrin Signaling

Integrin signaling can activate a variety of different pathways to affect cell motility, survival, cytoskeletal organization, cell cycle progression, growth factor signaling, and cell differentiation [44]. Signaling is mediated by numerous adapter proteins and protein kinases as described in the text below and in Figure 1-4. Proteins such as focal adhesion kinase (FAK), integrin linked kinase (ILK), src-family kinases, talin, vinculin, α-actinin, and paxillin are important in early integrin signaling and the

formation of the focal adhesion complex [44, 45]. In addition, these factors promote actin polymerization and the formation of stress fibers. Cytoskeletal rearrangement and change in cell shape can be spatially controlled by integrins via Rac, Rho, and cdc42 dependent mechanisms [44]. Binding of some integrins promotes cell survival through phosphorylation of phosphoinositol-3-kinase (PI3K) and Akt and the inhibition of pro-apoptotic proteins such as Bcl-2 associated death protein (BAD) or caspase-9 [44, 46]. In osteoblasts, binding of the $\alpha_5\beta_1$ integrin to fibronectin increases activity of PI3K, Akt, and Bcl-2, which in turn reduces caspase activity and promotes cell survival [47, 48]. Integrin signaling can also directly affect cell cycle progression to promote proliferation of cells. In osteoblasts, the $\alpha_5\beta_1$ integrin has been shown to act through JNK and MAP kinase-mediated pathways to phosphorylate c-Jun and c-Fos, which form the activator protein 1 (AP-1) heterodimer, a transcription factor complex that promotes cell proliferation and also induces expression of several osteogenic target genes [44, 49]. Integrins signaling can also directly target pathways that affect cell differentiation. Several integrins can act through protein kinase C (PKC) and extracellular related kinases 1 and 2 (ERK1/2) mediated pathways, which have been shown to increase RunX2 transcriptional activity and increase osteoblastic differentiation [44, 50]. Interestingly, many membrane associated receptors, including the membrane $1,25(OH)_2D_3$ receptor Pdia3, also use JNK-mediated or ERK 1/2-mediated signaling pathways to affect cell proliferation and differentiation [44, 51]. The existence of such overlapping systems means that integrin signaling can modulate growth factor signaling, or vice versa, at many points in this pathway [52]. Integrin binding can directly increase growth factor receptor activity through conformational changes, or it can increase activity of Raf, MEK, and ERK 1/2 via phosphorylation by p21-activated kinase (PAK) or PKC. In fact, signaling of many growth factors is anchorage dependent, meaning that integrin binding is required for activation of growth factor signaling pathways. Treatment of

attached cells with various growth factors leads to sustained activation of FAK or ERK 1/2; however, treatment of suspended cells results in only transient and weak activation of ERK 1/2 [52, 53]. Conversely, growth factors are often required to sustain ERK 1/2 activation by integrins. Thus, integrins, growth factors, and steroid hormones often act synergistically to enhance signals essential for regulating osteoblast phenotype.

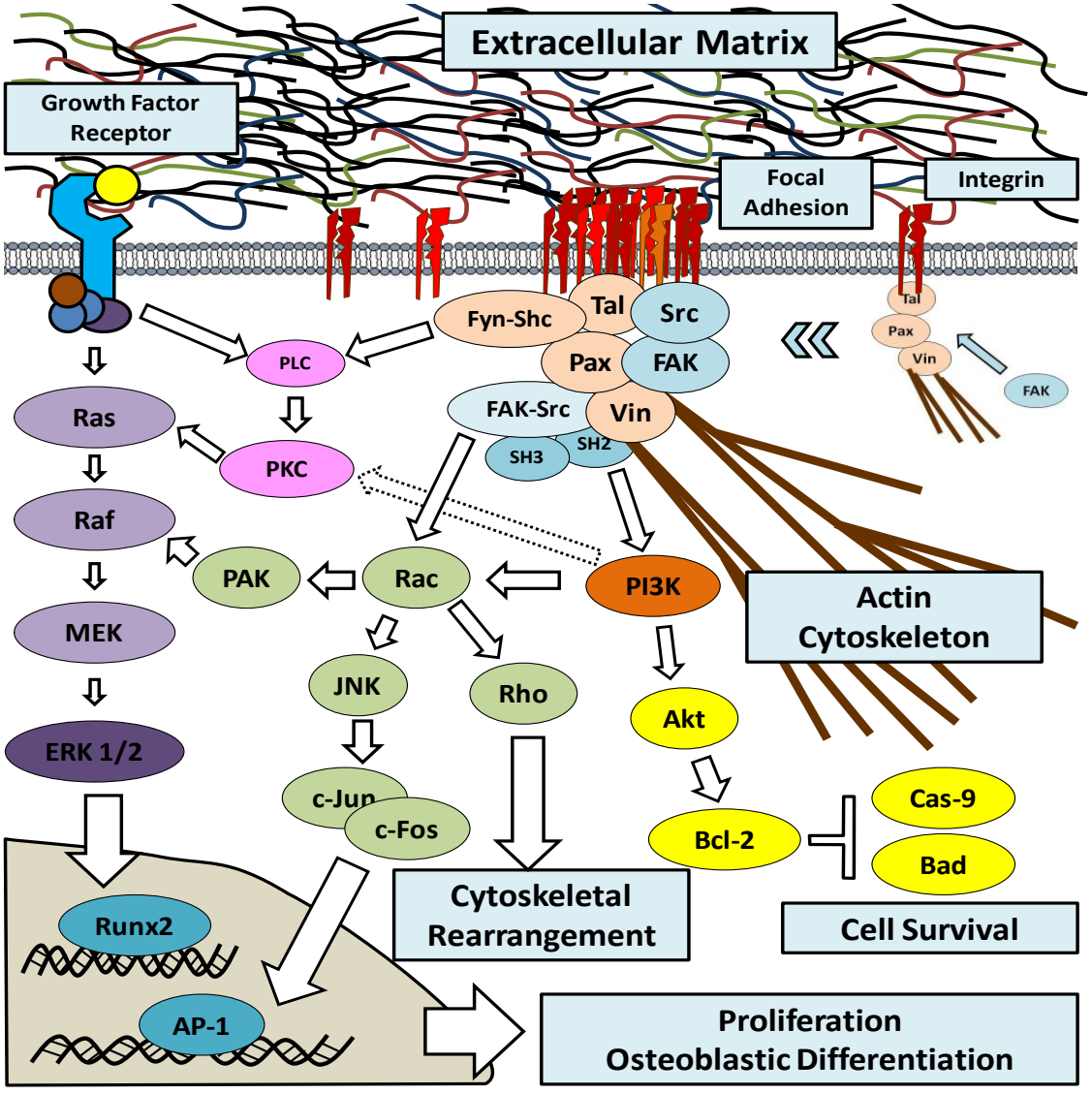

Figure 1-4: Major integrin signaling pathways affecting cell motility, survival, cytoskeletal organization, cell cycle progression, growth factor signaling, and cell differentiation.

1.5. Regulation of Osteoblast Differentiation

Osteoblast differentiation is a highly complex process that is regulated by extracellular matrix cues, growth factors, hormones, and mechanical forces. Runx2, a protein in the Runt-related family of transcription factors, is a master regulator of osteoblast function [54]. Runx2 appears in early osteochondral progenitor cells, well before the appearance of osteocalcin or other osteoblastic genes. Target genes of Runx2 include many bone proteins including osteocalcin, osteopontin, osterix, and bone sialoprotein [55]. Expression of Runx2 in non-bone cells is sufficient to induce production of bone specific proteins and to induce mineralization in some cell types; however, optimal mineralized bone matrix formation requires coordination with multiple other bone proteins [56, 57]. Because of the strong actions of Runx2, its expression levels and transcriptional activity are kept under tight control by various inhibitors or cofactors at different points in osteoblastic maturation. Immature osteoblasts produce a number of RunX2 inhibitors including TWIST1, Stat1, and Schnurri 3 [54]. Some inhibitors ensure proper closure of craniofacial joints by delaying osteoblastic differentiation, while others, potentially Schnurri 3, may be important in regulating adult bone mass [54, 58]. Osteoblast differentiation occurs in several distinct stages and is described briefly in the text below and in Figure 1-5 on the following page.

Commitment of mesenchymal stem cells into osteoprogenitor cells requires upregulation of the transcription factors Runx2 and Msx2, and downregulation of transcription factors for adipocyte, myoblast, or chondrocyte commitment. Osteoprogenitor cells have a high proliferative potential, which is important for achieving sufficient osteoblast population at a fracture site. The transition of osteoprogenitors to mature osteoblasts requires expression of osterix, a transcription factor upregulated strongly by BMPs, but also by Runx2 [54, 59]. Osterix is required for activation of many Runx2 target genes. Early markers for osteoblast differentiation include alkaline

phosphatase, bone sialoprotein, and collagen 1. Osteocalcin is a late marker for differentiation and is produced at an increasing rate leading up to mineralization. Osteoblasts also have diminishing proliferative potential as they mature. Mature osteoblasts express the transcription factor activating transcription factor 4 (ATF-4), which is important in late stage differentiation of osteoblasts. Osteoblasts terminally differentiate into osteocytes and bone-lining cells; however, 60-80% of the osteoblasts originally present in the resorption pit cannot be found, and presumably have undergone apoptosis [60]. Osteocytes are largely responsible for mechanical sensation and the maintenance of formed bone. Osteocytes are post-mitotic and can undergo apoptosis in the absence of mechanical loading or in the presence of microdamage. It is likely that osteocyte apoptosis and the various signaling molecules released concomitantly are essential in alerting surrounding cells to begin the bone remodeling process again.

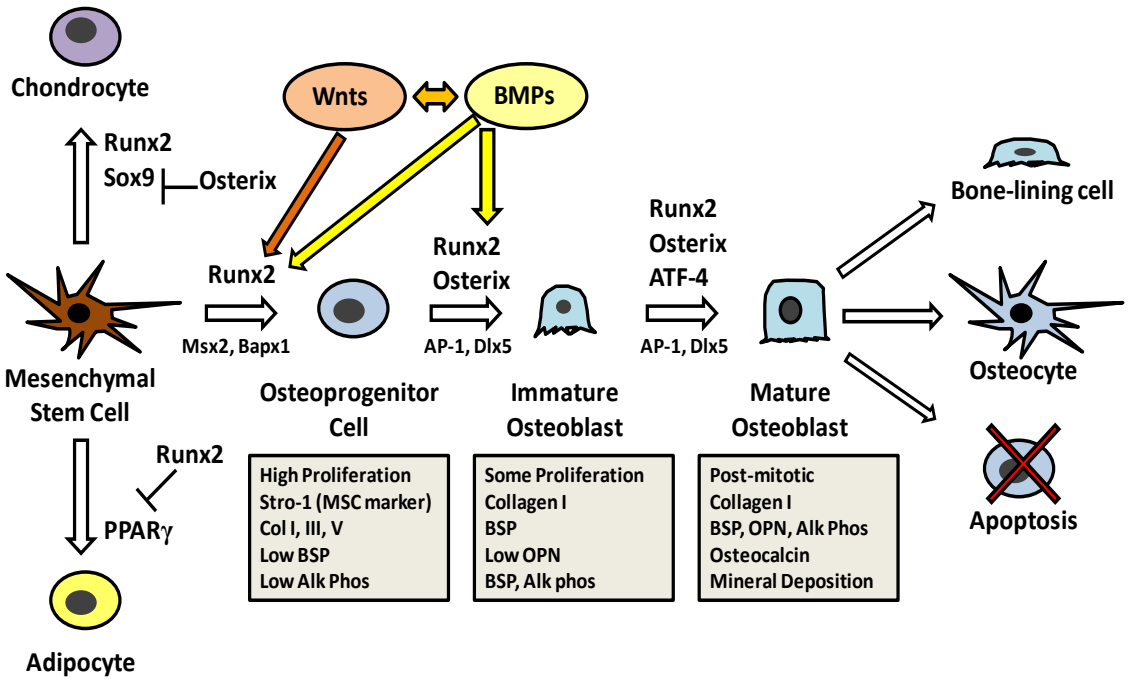

Figure 1-5: Osteoblast differentiation pathway and factors regulating differentiation.

The Effect of Growth Factors on Osteoblast Differentiation

Osteoblast phenotype can be modulated by numerous growth factors that are able to either promote or inhibit differentiation at different stages of osteoblast maturity. Osteoblast differentiation can be modulated through autocrine, paracrine, or endocrine signaling. Both canonical and non-canonical WNT/β-catenin signaling pathways are critical to bone development and regulation of osteoblast phenotype, particularly at early stages of differentiation [61]. Moreover, cell interaction with implant surfaces involves Wnt signaling. Mesenchymal stem cells grown on SLA and modSLA surfaces have increased levels of WNT5a, a powerful promoter of osteogenic commitment and differentiation via non-canonical signaling [62]. Members of the TGF-β superfamily, including TGF-β1 and BMPs, can also have potent effects on osteoblasts. BMP-2, BMP-4, and BMP-7 strongly promote osteoblastogenesis and osteogenic differentiation [63]. Other BMPs can either promote or inhibit osteogenesis. BMPs act through smads that can complex to Runx2 or other transcription factors to target osteogenic genes such as Dlx5 or osterix [64]. BMPs can also act through ERK 1/2 or JNK dependent pathways, which can lead to crosstalk between BMP and integrin signaling. In fact, activation of BMP-2 signaling requires integrin mediated activation of FAK [65]. BMPs also can affect osteoblast interaction with implant surfaces. BMP-2 treatment has been shown to alter $\alpha_5\beta_1$ integrin localization and increase FAK expression on osteoblasts grown on Ti-6Al-4V surfaces [66]. Moreover, rough cpTi surfaces enhance BMP-2 expression in macrophages, perhaps indicating an important role of surface roughness induced BMP expression in the recruitment of osteoprogenitor cells [67]. Osteoblast differentiation is also affected by the actions of endocrine signals such as parathyroid hormone (PTH) and $1\alpha,25(OH)_2D_3$, which will be extensively discussed in section 1.7. In summary, osteoblast differentiation is tightly regulated by a complex interplay between integrin,

growth factor, and endocrine signaling pathways that ensures proper spatial and temporal control of the bone formation processes.

1.6. Engineering Surfaces for Orthopaedic and Dental Implants

Orthopaedic and dental implant designers have been chemically and mechanically modifying the surfaces of implants for several decades now in an effort to improve osteointegration of implants. Commonly used techniques for surface modification include chemical treatment (etching), surface roughening, surface coating, thin-film deposition, and biological modification through the use of protein adsorption or and self assembled monolayers (SAMs) [1, 5]. These techniques will be briefly reviewed in the text below and are summarized in Figure 1-6.

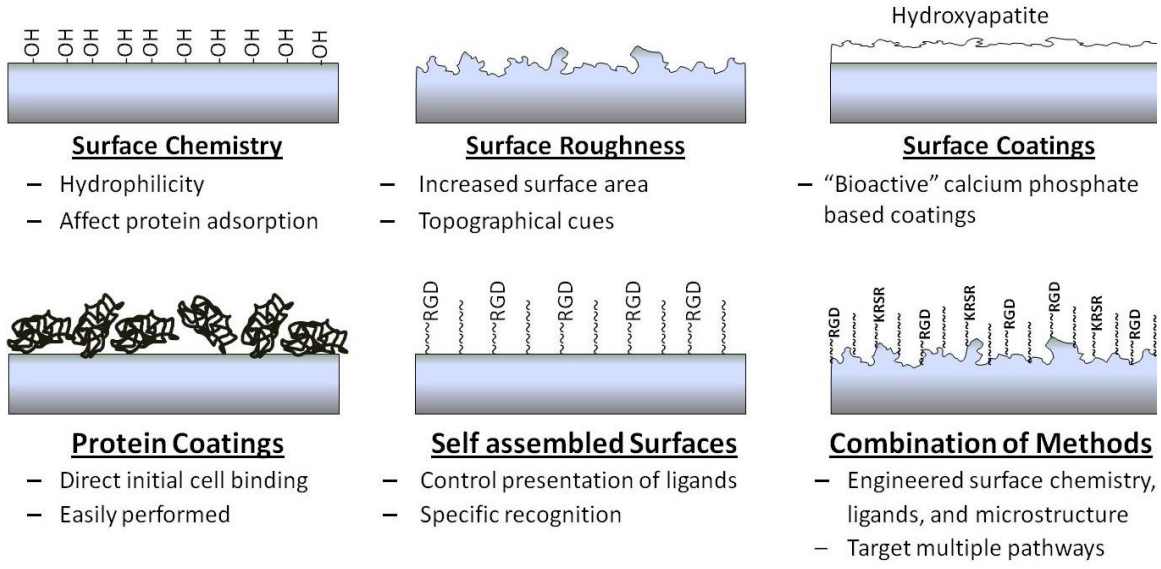

Figure 1-6: Commonly used methods for modifying implant surface properties.

Surface Topography

Clinical experience and research studies over the past few decades have demonstrated that roughening of the bone-bonding components of titanium implants increases osteointegration and long-term fixation [31, 68, 69]. *In vivo* studies have

shown that titanium implants with rough surfaces have higher pullout strengths and higher bone-to-implant contact area than implants with smooth surfaces [31, 68]. This improvement in performance is due in part to increased mechanical interlock, but it is also due to the direct effects of microtopography on osteoblast phenotype. *In vitro* studies have shown that titanium surfaces with rough microtopographies enhance phenotypic maturation of osteoblasts, as indicated by increased production of local regulatory factors such as prostaglandin E_2 (PGE_2), TGF-β1, and osteoprotegerin [70]. Osteoblast cultured on rough surfaces also exhibit a cuboidal morphology indicative of osteoblastic differentiation, whereas osteoblasts cultured on smooth surfaces exhibit a flattened, more fibroblastic phenotype [71]. In addition, rough surfaces enhance the response to $1\alpha,25(OH)_2D_3$ in a synergistic way. The mechanisms controlling the response of osteoblasts to surface roughness are not fully elucidated; however it is likely that integrins mediate these effects in conjunction with the actions of autocrine and paracrine signals. This topic will be discussed in Chapters 3 and 4.

Surface roughening can be created using a variety of techniques, each of which yields differing micro- and nanoscale features. Methods commonly used include titanium plasma spraying or grit blasting, which produce microscale features, and acid-etching or anodization, which produce nanoscale features [68]. Details regarding the production and characterization of the titanium discs used in this thesis are discussed in Chapter 2. Efforts have been made to unravel the response of osteoblasts to topographical features of specific sizes [72-74]. Interestingly, upregulation of PGE_2, active TGF-β1, and osteocalcin required the presence of both micro- and nanoscale topographical features created through photolithography and acid-etching, respectively [72]. The sand-blasted, acid etched (SLA) surfaces used throughout this thesis have such micro- and nano-scale features, and have been shown to increase osteoblast differentiation versus smooth surfaces. Interestingly, the SLA topography visually

mimics native osteoclast resorption pits (see Figure 2-1), although the exact mechanisms of osteoblast response to implant surface topography are being unraveled.

Surface Chemistry and Surface Energy

Modification of the surface chemistry and surface energy of titanium substrates has been shown to have profound effects on osteoblast proliferation and differentiation. Engineers have long looked at the hydrophobicity of a surface and its effect on the protein adsorption, protein conformation, cell attachment, and cell phenotype [1]. In general, hydrophobic surfaces, or low energy surfaces, bind proteins strongly, causing them to unfold and perhaps denature. Hydrophilic surfaces, or high energy surfaces, affect protein folding to a lesser degree, which may yield more biologically active conformations of adsorbed proteins. Bone formation and osteoblast response is enhanced on hydrophilic versus hydrophobic implant surfaces [75, 76]. However, cell response to surfaces is not simply a function of hydrophobicity. It is related to chemical nature of molecules exposed at the surface. For instance, osteoblasts grown on SAM-surfaces terminated with hydroxyl and amine groups have increased levels of alkaline phosphatase, BSP, and osteocalcin and increased mineralization versus osteoblasts grown on surfaces terminated with methyl or carboxyl groups [77]. These differences in surface chemistry affect fibronectin adsorption and conformation, which directly leads to changes in integrin binding and osteoblast response [78]. The titanium oxide layer of pure titanium is composed primarily of TiO_2, but also has free –OH and $–O^{2-}$ groups that can interact with water molecules to make the surface very hydrophilic. However, such high energy surfaces can rapidly adsorb hydrocarbons and other contaminants from the atmosphere to make the surface very hydrophobic. Immersion of freshly etched titanium into an isotonic solution can maintain hydrophilic properties. Dental implants made with hydrophilic modified SLA (modSLA or SLActive^{TM}) surfaces have been shown to

enhance osteoblastic differentiation *in vitro* and increase bone-to-implant contact *in vivo* compared to standard SLA surfaces [76, 79].

Surfaces Coatings and Thin Films

Coatings have been an attractive option for biomaterials design because of the opportunity to use bioactive surfaces without compromising the mechanical properties of the underlying bulk material. Plasma sprayed coatings of hydroxyapatite (HA) and other calcium phosphates are highly osteoconductive and have been shown to promote the closure of large (~1mm) bone gaps [80]. Unfortunately, concerns with the use of HA coatings have limited their clinical use. These problems include 1) rapid dissolution of HA and breakdown of the bone-implant interface, 2) mechanical failure of the coating-substrate interface, and 3) the release of wear-inducing particles. Despite these perceived problems, modern HA-coated implants have statistically comparable long-term survival rates to uncoated titanium implants [68, 81].

Biologically Modified Surfaces

Many researchers believe that the next generation of orthopaedic and dental implants will be biologically modified to elicit controlled cell response at the tissue-implant interface [5]. Surfaces functionalized with specific proteins or peptides can aid osteointegration of implants by favoring adherence of osteoprogenitor cells and subsequently promoting osteoblastic differentiation. For instance, titanium surfaces coated with fibronectin or collagen I enhance osteoblast attachment, proliferation, and differentiation [36, 82, 83]. However, reports are mixed on whether adsorbed fibronectin and collagen I affect bone formation *in vivo* [83-85]. Passive adsorption results in random protein conformations, which can reduce biological activity of the coating and possibly induce immunogenicity. In addition, the adsorbed protein layer is quickly

remodeled *in vivo* [5]. Because of these shortcomings, researchers have investigated using short peptides and methods to link them to the surface of the implant. Various peptides (respective full-length protein) have been shown to affect osteoblast attachment including RGD (fibronectin, multiple others), GFOGER (collagen I), FHRRIKA (bone sialoprotein), PHSRN (fibronectin), and DGEA (collagen I). *In vivo*, RGD has been shown reported to increase osteointegration in some studies [86-88], but not others [89, 90]. The biological activity of RGD is less potent than that of native fibronectin or the fibronectin fragment FNIII7-10 [42, 91]. Single peptides have certainly shown promising results in promoting osteointegration; however, such peptides lack the biological activity of full-length proteins. For instance, the biological activity of RGD is far less potent than that of native fibronectin or the fibronectin fragment FNIII7-10, which has the PHSRN synergy site [42, 91]. Furthermore, surfaces that contain multiple ligands may target distinct signaling pathways that act synergistically to enhance early osteoblast proliferation and later differentiation. The effectiveness of one such multifunctional peptide coating of RGD and KRSR will be explored in Chapter 4.

Proteins or peptides can be attached to surfaces using complex chemistries that present ligands in specific orientation, density, and spatial distribution. Ligand presentation can directly affect integrin binding, presumably by controlling access to binding sites. The density and spatial distribution of ligands can also alter integrin binding, especially when synergy sites are involved [42]. Moreover, ligand density and distribution can affect focal adhesion assembly, which can enhance attachment strength and downstream integrin signaling [92]. The most promising of these techniques is the use of SAM surfaces, which include assembling chemistries based on alkanethiols, silanes, alkanephosphonates, interpenetrating polymer networks, or poly-L-lysine grafted polyethylene glycol (PLL-*g*-PEG) [93]. SAM surfaces are often used because they limit non-specific protein adsorption, which means cells initially interact specifically with the

biological groups attached to the SAM surface. For example, protein adsorption on PLL-*g*-PEG coated titanium is significantly reduced compared to uncoated titanium [94]. Osteoblast attachment and proliferation are also reduced on PLL-*g*-PEG coated titanium surfaces compared to control titanium surfaces; however, ligation of RGD to the PLL-*g*-PEG surface significantly increases osteoblast attachment and proliferation compared to PLL-*g*-PEG and uncoated controls [95]. Overall, such biologically modified and self-assembled systems have promise in orthopaedic implant applications because of their cost, ease of use, controlled ligand presentation, and relative stability.

1.7. Vitamin D

The previous sections have focused on the role of the implant surface in affecting osteoblast phenotype and ultimately the degree of osteointegration of the implant. The systemic host environment can also play a crucial role in long-term performance of an implant. Hormones such as estrogen, parathyroid hormone (PTH), or vitamin D have profound effects on bone formation and turnover. Vitamin D deficiency (serum 25-hydroxyvitamin D < 50 nmol/L) is associated with lower bone mineral density, increased risk of fracture, and increased risk of osteoporosis [96]. Moreover, dietary supplementation of calcium and vitamin D_3 can increase bone mineral density and reduce the risks of falls and fractures in compliant patients [97, 98]. Vitamin D deficiency has also been shown in rats to reduce bone-to-implant contact and push-in force, which are measures for osteointegration and implant fixation, respectively [99]. At this time there does not appear to be sufficient evidence in humans as to whether calcium and vitamin D supplementation has an effect on osteointegration of dental or orthopaedic implants; however, $1\alpha,25(OH)_2D_3$ does have direct effects on promoting osteoblast differentiation *in vivo* [8, 100]. Furthermore, osteoblasts plated on surfaces with rough microtopography exhibit synergistic increases in osteocalcin and PGE_2 when they are

treated with 1α,25$(OH)_2D_3$ [69]. The following section will explore vitamin D physiology, VDR dependent and independent signaling, and the influence of surface properties on integrin and vitamin D signaling.

Vitamin D Physiology

Vitamin D is a steroid hormone that plays a major role in the regulation of calcium and phosphate levels and in the maintenance of bone mineral homeostasis. Vitamin D is critical to the development and maintenance of the skeleton, and chronic lack of vitamin D causes a disease called rickets in children and osteomalacia in adults, both of which are characterized by severe hypocalcemia and skeletal defects [8, 10]. The most biologically active metabolite of vitamin D, 1α,25$(OH)_2D_3$, is converted from the prohormone Vitamin D_3 by 25-hydroxylase in the liver and then by 1α-hydroxylase in the kidney. 1α,25$(OH)_2D_3$ exerts its effects on a variety of tissues in the body, including the intestines, kidney, bone, and parathyroid gland. Feedback loops tightly regulate levels of 1α,25$(OH)_2D_3$, 24,25R$(OH)_2D_3$, PTH, calcium, and phosphorus. The effects of vitamin D on bone are complex and are the compilation of direct effects on bone cells and indirect effects via mineral ion regulation [101]. 1α,25$(OH)_2D_3$ acts on the intestines and kidneys to increase calcium and phosphate levels, which increase mineralization by increasing the calcium-phosphate ion product. In osteoblasts, treatment with 1α,25$(OH)_2D_3$ causes an increase in levels of alkaline phosphatase activity and levels of osteocalcin, PGE_2, and TGF-β1, indicating that vitamin D stimulates osteoblast differentiation and the creation of an osteogenic environment [102]. *In vivo*, 1α,25$(OH)_2D_3$ increases osteoblast differentiation and the formation of osteoid, which is quickly mineralized at elevated blood Ca^{++} levels [8, 100]. However, 1α,25$(OH)_2D_3$ also upregulates M-CSF and RANKL in osteoblasts, which lead to an increase in osteoclastogenesis and bone turnover [8, 103]. The direct effect of 1α,25$(OH)_2D_3$ on

bone appears to be an increase in bone turnover because of the increase in both osteoblast and osteoclast activity, but the overall action of $1\alpha,25(OH)_2D_3$ on bone is to increase net bone mineralization because of elevated blood calcium and phosphate. Still, some debate remains whether $1\alpha,25(OH)_2D_3$ has an overall positive or negative effect on peri-implant bone formation and osteointegration.

Traditional $1\alpha,25(OH)_2D_3$ Signaling

The molecular actions of $1\alpha,25(OH)_2D_3$ are regulated through two receptors, the classic nuclear vitamin D receptor (VDR) and the recently discovered membrane vitamin D receptor known as protein disulfide isomerase, family A, member 3 (Pdia3). Pdia3 is also known as endoplasmic reticulum protein 60 (ERp60) and membrane-associated-rapid response, steroid-binding ($1,25D_3$-MARRS) protein. The classical effects of $1\alpha,25(OH)_2D_3$ through the VDR have been widely studied and reviewed [100, 103, 104], and are also illustrated in Figure 1-7 on the following page. Briefly, binding of $1\alpha,25(OH)_2D_3$ to cytosolic VDR causes a conformational change in VDR and dissociation of co-repressor proteins. This 1,25-bound VDR then heterodimerizes to the retinoid X receptor (RXR) and translocates to the nucleus where this complex binds to vitamin D response elements (VDREs) in the genome to alter gene expression and cell phenotype. Target genes include alkaline phosphatase, osteocalcin, osteopontin, Runx2, LRP5, collagen XIII, p21, 17β-hydroxysteroid dehydrogenase, 24-hydroxylase, FGF23, and RANKL [105-108]. These genes have tissue-specific actions on PTH and vitamin D metabolism, mineral ion homeostasis, cell cycle regulation, osteoblast differentiation, and osteoclastogenesis [101].

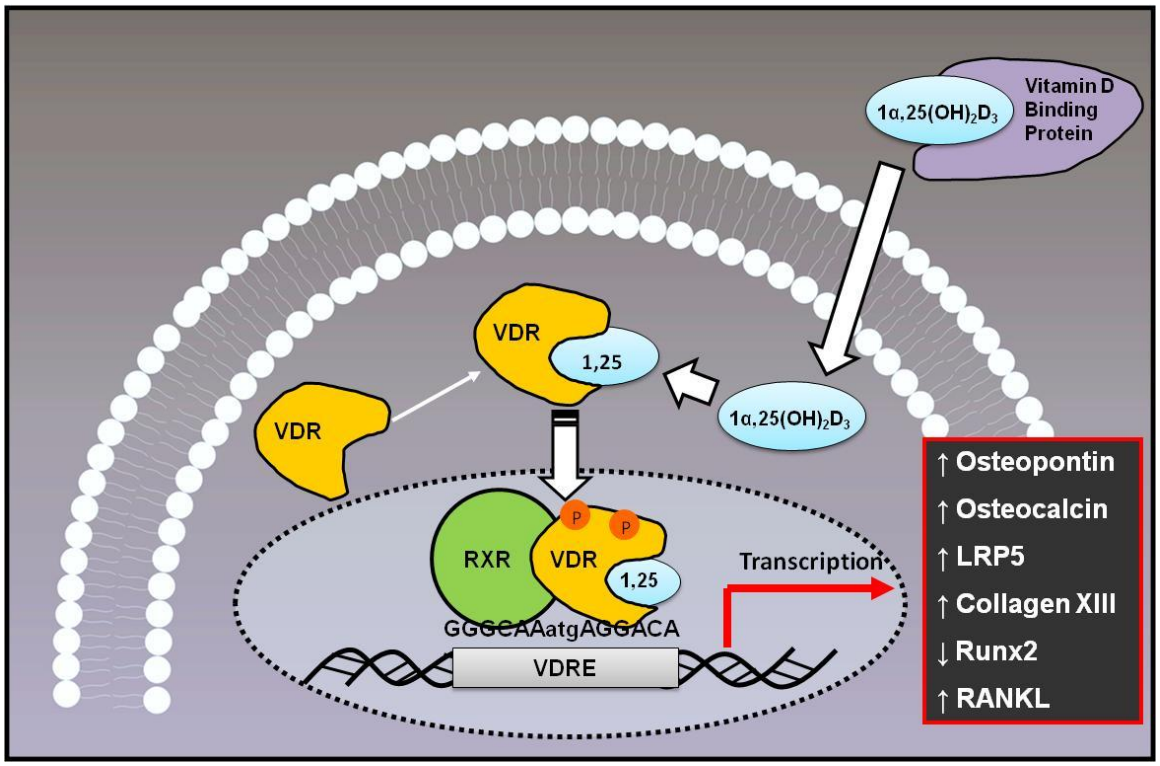

Figure 1-7: Genomic actions of 1α,25(OH)$_2$D$_3$ regulated through the VDR and VDREs.

Rapid 1α,25(OH)$_2$D$_3$ Signaling

While studies have shown that VDR plays a critical role in the genomic response to 1α,25(OH)$_2$D$_3$, multiple groups have reported rapid, non-genomic activation of PKC and release of intracellular calcium that cannot be accounted for by traditional VDR signaling [109-111]. Furthermore, osteoblasts from VDR-deficient mice exhibit rapid activation of PKC and release of intracellular calcium when treated with 1α,25(OH)$_2$D$_3$ [112]. These findings clearly demonstrate that rapid, non-genomic events of 1α,25(OH)$_2$D$_3$ occur independently of the VDR. It is now widely believed that Pdia3 is the membrane receptor for 1α,25(OH)$_2$D$_3$ [113, 114]. Studies first demonstrated that a polyclonal blocking antibody (Ab99) targeting Pdia3 blocked downstream activation of PKC by 1α,25(OH)$_2$D$_3$ in chondrocytes [115]. Moreover, rybozyme knockdown of Pdia3

in chick intestinal epithelial cells eliminated 1α,25$(OH)_2D_3$-mediated rapid release of intracellular calcium [116].

There are still many questions regarding the exact membrane 1α,25$(OH)_2D_3$ signaling pathway and its downstream targets. The hypothesized signaling pathway is described below and is illustrated in Figure 1-8 on the following page. The rapid 1α,25$(OH)_2D_3$ signaling cascade likely begins as 1α,25$(OH)_2D_3$ binds to Pdia3 present in caveolae. Recent studies have shown that Pdia3 localizes to caveolae, and that mice deficient in caveolin-1 and caveolae lack increased PKC activity normally associated with treatment of 1α,25$(OH)_2D_3$ [117]. The mechanism could act through unknown protein intermediaries or G-protein coupled receptors to activate phospholipase A2 (PLA_2) and phospholipase C (PLC) [118, 119]. These lipases cause phosphatidylinositol to be cleaved into diacylglycerol (DAG) and inisitol triphosphate (IP_3). IP_3 stimulates rapid release of intracellular calcium from the endoplasmic reticulum, which is a co-factor for activation of PKCα by DAG [117]. DAG is converted to arachidonic acid, which is released by PLA_2 and can lead to the production prostaglandins such as PGE_2 via the action of cyclooxygenases [118]. ERK1/2 and other MAP kinases are activated downstream of these events and could lead to changes in gene transcription and cell phenotype [120].

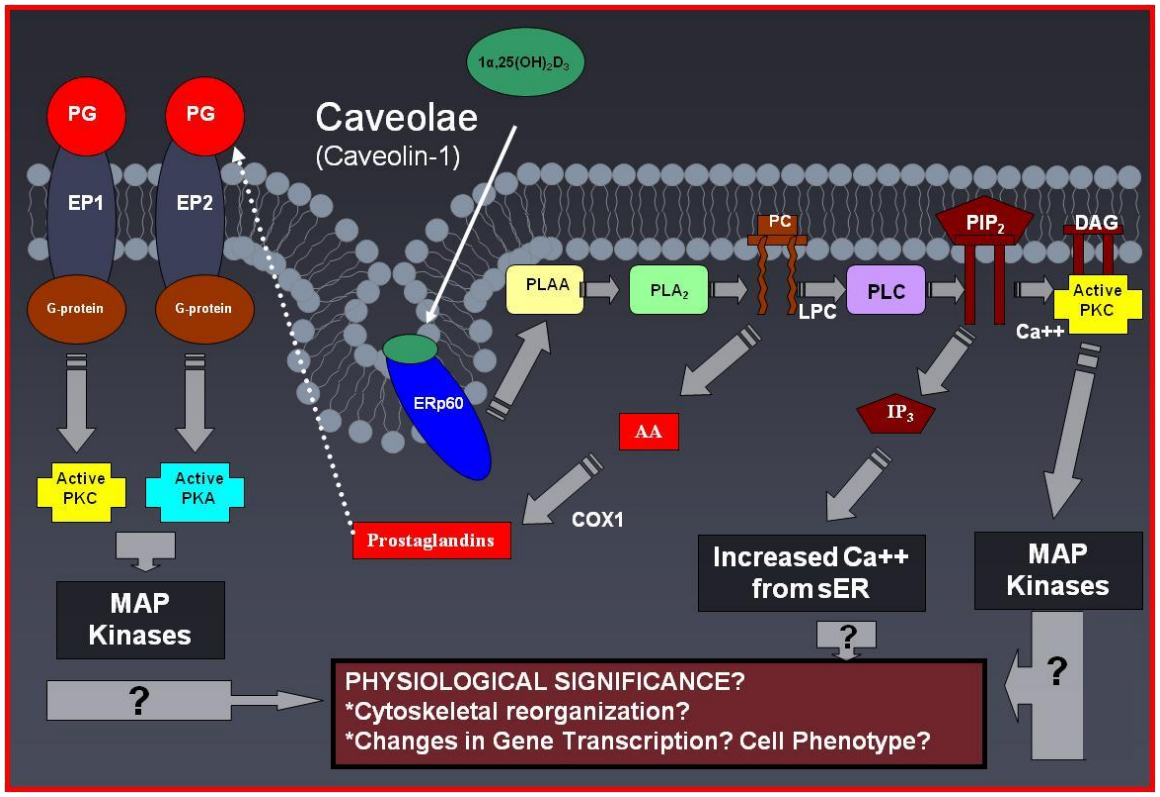

Figure 1-8: Proposed membrane 1α,25(OH)$_2$D$_3$ signaling pathway.

Despite this knowledge about signaling events following 1α,25(OH)$_2$D$_3$ binding to Pdia3, the effects of Pdia3-mediated signaling on bone cell phenotype are still largely unknown. It is likely that Pdia3-mediated signaling of 1α,25(OH)$_2$D$_3$ could be important in rapid calcium and phosphate uptake in intestinal cells [113], but genomic signaling via VDR also appears to be critical [121]. Pdia3 may also be critical to the 1α,25(OH)$_2$D$_3$-stimulated release of calcium, phosphate, matrix metalloproteinases, and growth factors from matrix vesicles, which lack traditional VDR-mediated genomic signaling [122]. This role of Pdia3 may be very important in matrix mineralization.

Pdia3-mediated signaling of 1α,25(OH)$_2$D$_3$ could also directly interact with traditional VDR-mediated pathways, although no direct link has yet been established. Various studies have shown that VDR transcriptional activity and its interactions with transactivators can be modulated by phosphorylation by PKC-β, PKA, casein kinase II,

MAPK, and $Ca2^{++}$/calmodulin-dependent kinase IV (CaMKIV) [123-126]. Moreover, 1α,25$(OH)_2D_3$ treatment has been demonstrated to increase PKC-β translocation to the nucleus [127], where it may phosphorylate VDR at serine 51 and decrease binding to VDREs [123]. In contrast, phosphorylation of VDR by CaMKIV, which could be activated by the 1α,25$(OH)_2D_3$-induced increase in intracellular calcium levels, has been shown to significantly enhance VDR transcriptional activity [126, 128]. It is not clear whether Pdia3-mediated rapid 1α,25$(OH)_2D_3$ signaling enhances, represses, or selectively modulates VDR transcriptional activity, or whether these effects are dependent on the cell type and state of differentiation of the cell. Moreover, it is possible that Pdia3-mediated rapid 1α,25$(OH)_2D_3$ signaling could affect the phosphorylation and activty of other transcription factors. This possibility leads to the question of whether Pdia3-mediated rapid 1α,25$(OH)_2D_3$ signaling has physiological effects independent of the VDR. This topic will be explored using VDR deficient osteoblasts in Chapter 6.

1.8. Caveolae

Caveolae are a specialized form of cholesterol-enriched lipid rafts that are characterized by 60-80 nm flask-shaped invaginations in the cell membrane [129]. Caveolae are stabilized by caveolin-1, a small, 22kD protein that forms oligimeric scaffolds critical to stabilizing lipid domains and maintaining the cave-like shape of caveolae in non-muscle tissues [130]. Caveolin-3 is the critical to the structure of caveolae in muscle cells. Caveolin-2 is co-localized with caveolin-1 and is critical to proper pulmonary function, but its role in bone remains undefined [131]. Caveolae are involved in endocytosis, lipid and cholesterol regulation, and a wide variety of cellular signaling pathways. Caveolae serve as a nexus for many glycosylphosphatidylinositol (GPI)-anchored proteins, membrane associated receptors, and secondary messenger

proteins. Close proximity of these signaling molecules may enhance crosstalk or provide a mechanism for quickly up- or downregulating multiple signaling cascades [132]. Moreover, caveolae may interact with integrins and focal adhesions to spatially and temporally control signaling. In bone cells, caveolae have been shown to be involved in the modulation of extracellular matrix and integrin interactions, mechanical stress transduction, BMP signaling, and $1\alpha,25(OH)_2D_3$ signaling [129, 131-133]. In addition, caveolae may play a direct role in mineralization via their potential involvement with matrix vesicle biogenesis [134].

Despite the abundance of caveolae and the direct involvement of caveolae in a wide variety of signaling pathways, Caveolin-1 deficient [Cav-1(-/-)] mice show surprisingly few defects, suggesting that compensatory mechanisms exist to overcome the loss of certain signaling pathways in the absence of caveolae [135]. Cav-1(-/-) mice are relatively healthy and grow to full size, although some cardiovascular and pulmonary problems do develop later in life. Although the effects of caveolae deficiency are not manifested by gross bone abnormalities, recent studies have shown that Cav-1(-/-) mice do exhibit an altered bone phenotype [136]. The growth plates of Cav-1(-/-) mice are widened and have abnormally high numbers of hypertrophic cells [117]. The femurs of Cav-1(-/-) mice show a significant increase in the elastic modulus, cortical bone thickness, stiffness, and overall yield strength compared to wild-type bones [137]. In addition, osteoblasts in Cav-1(-/-) mice display increased mineral apposition rates and bone formation rates compared to osteoblasts in Cav-1(+/+) mice. Moreover, previous studies have shown that knockdown of Cav-1 in stromal cells leads to increased levels of Runx2 and osterix. Taken together, these studies suggest that caveolae may serve to suppress signals for osteoblastic differentiation, thus slowing the rate of bone formation.

The mechanism by which loss of caveolae increases the rate of bone formation is unknown; however, caveolae have been shown to be involved in matrix vesicle

biogenesis [134], mechanotransduction [129], integrin trafficking and signaling [138], BMP signaling [133], and rapid vitamin D signaling [117]. It is unlikely that the role of caveolae is simply to delay differentiation as some reports have suggested [136]. Because of the wide involvement of caveolae in multiple signaling pathways, it is more likely that caveolae acts to suppress, enhance, or in other ways modulate different osteogenic signals depending on extracellular cues or the state of differentiation of the cell. Interestingly, caveolin-1 has been shown to either enhance or inhibit BMP receptor function depending on which isoform of caveolin-1 binds to BMP receptors I or II. Cav-1β appears to inhibit BMP signaling, whereas Cav-1α appears to promote it [133]. In addition, caveolae may sequester β-catenin, which suppresses canonical Wnt/β-catenin signaling important in early osteoblasts [139]. Caveolae may also act in concert with Pdia3 to modulate VDR activity through phosphorylation by PKC-β, CaMKIV, or casein kinase II mechanisms discussed in the previous section. Finally, caveolae may affect mineralization directly by mediating matrix vesicle biogenesis. This theory is supported by evidence that caveolin-1 is present both in caveolae and matrix vesicles in chondrocytes and osteoblasts [134]. Furthermore, overexpression of caveolin-1 leads to a large increase in osteoblast matrix mineralization. Interestingly, studies using chondrocytes have shown that $1\alpha,25(OH)_2D_3$ acts through Pdia3 to release lysophospholipids that destabilize matrix vesicles [122]. It is theorized that these vesicles could then release stored calcium, phosphate, matrix metelloproteinases, and a myriad of proteins involved in matrix mineralization [122]. In summary, evidence is building that caveolae appear to suppress early osteoblast differentiation through regulation of BMP, Wnt, or VDR signaling, but later promote mineralization via matrix vesicle biogenesis or other mechanisms. However, the role of caveolae is wide-ranging and complex, and their role in bone is only now being unraveled.

Caveolae Mediated Interactions Between Integrins and 1α,25(OH)$_2$D$_3$ Signaling

Rough surface microtopography and 1α,25(OH)$_2$D$_3$ treatment cause a synergistic increase in markers for osteoblastic differentiation, including alkaline phosphatase activity, and levels of osteocalcin, osteoprotegerin, and PGE_2 [69]. Caveolae likely are involved in this synergy, since separate studies have shown that integrins can traffic through caveolae [140] and that both VDR and Pdia3 are present in caveolae [117, 141]. Integrin signaling could enhance cell responsiveness to 1α,25(OH)$_2$D$_3$, or vice versa, 1α,25(OH)$_2$D$_3$ could enhance integrin function through inside-out signaling or by crosstalk with downstream signal mediators. Such crosstalk could be the basis for the observation that osteoblasts grown on surface roughness and treated with 1α,25(OH)$_2$D$_3$ exhibit synergistic increases in markers for osteoblast differentiation.

Interestingly, caveolae may be directly involved in integrin clustering and assembly of focal adhesions. Studies have shown that knockdown of caveolin-1 expression decreases the formation rate of focal adhesions and decreases integrin signaling [44, 142]. Cav-1 has also been shown to be important in association of src-family kinases with β1 integrins [142]. Caveolin-1 deficient cells show impaired directional migration, spatial recognition, and the establishment of cell polarity due to disruption of proper src kinase and RhoGTPase signaling [143]. It is hypothesized that such loss of polarity and control of attachment dependent signaling may lead to changes in how osteoblasts interpret changes in surface roughness or chemistry (see Chapter 6). In addition, integrins $\alpha_2\beta_1$ and $\alpha_5\beta_1$, which are highly expressed in osteoblasts, have been shown to traffic through caveolae. In summary, loss of cav-1 has been shown to decrease the stability and number of focal adhesions [144], alter Ras/Erk, PI3K/Akt and Rac/Pak signaling [138], alter growth factor and steroid hormone signaling [117, 138], and disrupt cell polarization and migration [143]. These roles of caveolae point to the

possibility that caveolae might be important in integrating osteoblast responses to changing surface roughness and 1α,25$(OH)_2D_3$.

Integrin binding has also been shown to regulate caveolae internalization, which may enhance spatial and temporal sensing by regulating the activity of caveolae-dependent signaling pathways [138, 145]. Integrin activation at focal adhesions recruits and sequesters phosphorylated (tyrosine 14) caveolin-1 (pY14Cav-1) to the focal adhesion complex. Loss of cell attachment causes translocation of pY14Cav-1 to caveolae, which in turn triggers dynamin-2 mediated endocytosis of caveolae. As caveolae are internalized, signaling pathways including Ras/Erk, PI3K/Akt and Rac/Pak are rapidly shut down; however, these pathways remain in an active state in caveolin-1 deficient cells unable to internalize caveolae-associated lipid rafts [138]. Caveolin-1 deficient cells have increased rates of proliferation. In fact, many metastatic cancer cell lines have mutations in caveolin-1 that increase proliferation, increase migration, and enable anchorage independent growth. Furthermore, membrane 1α,25$(OH)_2D_3$ requires caveolae. Signaling of 1α,25$(OH)_2D_3$ could be affected through attachment mediated control over pY14Cav-1 sequestration. Conversely, signaling molecules could modulate focal adhesion disassembly through cAMP-mediated dephosphoylation of pY14Cav-1 [138], thus providing a mechanism for growth factor mediated effects on attachment. In summary, evidence supports the theory that caveolae and lipid rafts interact with integrins and focal adhesions to modulate signaling, thus providing rapid mechanisms for integrin mediated regulation of growth factor signaling, or vice versa, allowing growth factors to mediate integrin signaling and focal adhesion assembly.

1.9. Summary and Thesis Objective

Roughened surfaces used on orthopaedic and dental implants today are known to promote osteogenic differentiation *in vitro* and bone formation *in vivo*, although

relatively little is known about the molecular mechanisms through which osteoblasts actually sense differences in surface topography and chemistry. Moreover, these initial signaling events fundamentally alter osteoblast response to growth factors or steroid hormones, which lead to further enhancement of osteogenic phenotype. The previous sections have explored the roles of integrins, 1α,25$(OH)_2D_3$ receptors, and caveolae in mediating osteoblast response to surface properties and 1α,25$(OH)_2D_3$; however, many questions regarding these signaling pathways still remain unanswered. Understanding these cellular mechanisms could enable biomedical engineers to design surfaces or combination therapies that actively promote osteoprogenitor attachment and osteoblast differentiation, thus potentially leading to increased bone formation and better long-term implant fixation. The development of such advanced biomaterials and combination therapies in orthopaedics requires 1) an understanding of the cellular signaling processes guiding cell and tissue response to biomaterials, 2) advances in surface engineering and biomolecular technology that specifically target these osteogenic pathways, and 3) the translation of these biologically inspired designs into actual medical products.

The purpose of the present thesis is to explore how integrins mediate osteoblast response to changes in surface chemistry and topography, and whether titanium surfaces functionalized with the specific ligands RGD and KRSR can enhance osteoblast proliferation and differentiation. In addition, the purpose of this thesis is to determine whether the synergistic effects of surface topography and 1α,25$(OH)_2D_3$ require caveolae to mediate the interaction between integrin and VDR-independent pathways. To address these questions, several studies were undertaken to investigate the role of the $\alpha_5\beta_1$ integrin, VDR, and caveolae in response to changing surface topography and 1α,25$(OH)_2D_3$ treatment.

The first aim of the thesis uses shRNA techniques separately targeting the β_1 (Chapter 3) and α_5 (Chapter 4) integrin subunits to determine whether loss of these integrins disrupts osteoblast response to changes in surface energy and surface topography and reduces osteoblast sensitivity to $1\alpha,25(OH)_2D_3$ treatment. The results show that the β_1 integrin is required for mediating the response of osteoblast-like MG63 to surface roughness and topography, and that the response to $1\alpha,25(OH)_2D_3$ is also abrogated. Silencing of the α_5 subunit did not appear to alter the response of MG63 cells to surface properties and $1\alpha,25(OH)_2D_3$, although this finding may be dependent on the cell type or the state of differentiation [146]. The results suggest that specific integrins are critical in mediating osteoblast phenotypic maturation in response to different surface cues.

The second aim of the thesis (Chapter 5) uses titanium surfaces functionalized with the ligands RGD, KRSR, and K<u>S</u>SR to determine whether multi-functional PLL-*g*-PEG based surfaces can distinctly target integrin and heparin sulfate binding to increase both osteoblast proliferation and differentiation. The results show that RGD increased osteoblast proliferation and reduced differentiation, KRSR had no effect on osteoblast phenotype, and K<u>S</u>SR increased osteoblast differentiation. The results from this aim suggest that RGD/K<u>S</u>SR functionalized PLL-*g*-PEG coated SLA surfaces should be further investigated for use as osteointegrative surfaces.

The third and final aim of the thesis uses osteoblasts derived from VDR (Chapter 6) and Cav-1 (Chapter 7) knockout mice to determine whether $1\alpha,25(OH)_2D_3$ signaling pathways require VDR and Cav-1 to promote osteoblast differentiation, and whether loss of these genes alters osteoblast response to surface energy and topography. The results in VDR deficient osteoblasts demonstrate that VDR is required for the effects of $1\alpha,25(OH)_2D_3$ on all markers for osteoblastic phenotype. VDR-independent effects on osteoblast phenotype were not demonstrated. In caveolae deficient osteoblasts,

1α,25$(OH)_2D_3$ affected cell number, alkaline phosphatase activity, and TGF-β1 levels, although levels of osteocalcin and PGE_2 were not affected. These results are consistent with the hypothesis that VDR is required for the actions of 1α,25$(OH)_2D_3$, but that caveolae-dependent membrane 1α,25$(OH)_2D_3$ signaling modulates traditional VDR signaling.

The results in this thesis demonstrate that integrins, VDR, and caveolae play important roles in mediating osteoblast response to surface properties and 1α,25$(OH)_2D_3$. However, the results also raise many more questions regarding the interaction between nuclear and membrane 1α,25$(OH)_2D_3$ and how these pathways are modulated by integrin binding. Overall, the results are important in better understanding how cells interact with implant surfaces via integrins to affect osteoblast phenotype and responsiveness to 1α,25$(OH)_2D_3$.

CHAPTER 2: General Methodology

2.1. Implant Surface Models

One problem limiting direct comparison between many biomaterial studies in the scientific literature is the wide variability in processing techniques used to create substrates being studied. Such differences inherently create variability in terms of surface roughness, surface morphology, grain size, surface chemistry, and surface energy. While surfaces can be generally compared using measurable parameters such as average peak to valley roughness (Ra), any single measurement does not take into account changes in other surface properties that may also be influencing cell behavior. Thus, it is not only critical to minimize processing variability among surfaces used within a particular study, but it is also useful to limit differences in surface characteristics when making comparisons between studies.

In an effort to specifically control surface roughness and surface energy throughout these experiments, model titanium disks were created with consistent size, surface roughness, morphology, surface energy, grain size, and chemical composition. Institut Straumann AG (Basel, Switzerland) provided commercially pure titanium (cpTi) discs of differing surface roughness and surface energy. These surfaces, in order of increasing surface roughness, include pre-treatment (PT) cpTi, sand blasted acid etched (SLA) cpTi, modified high surface energy SLA (modSLA) cpTi, and titanium plasma sprayed (TPS) cpTi. The production and characteristics of these discs are described in detail below and are summarized in Figure 2-1 on the following page. In addition, tissue culture treated polystyrene (TCPS) surfaces were used as controls because of their widespread use in cell culture and their transparency, which enables easy monitoring of cell confluence under traditional light microscopy.

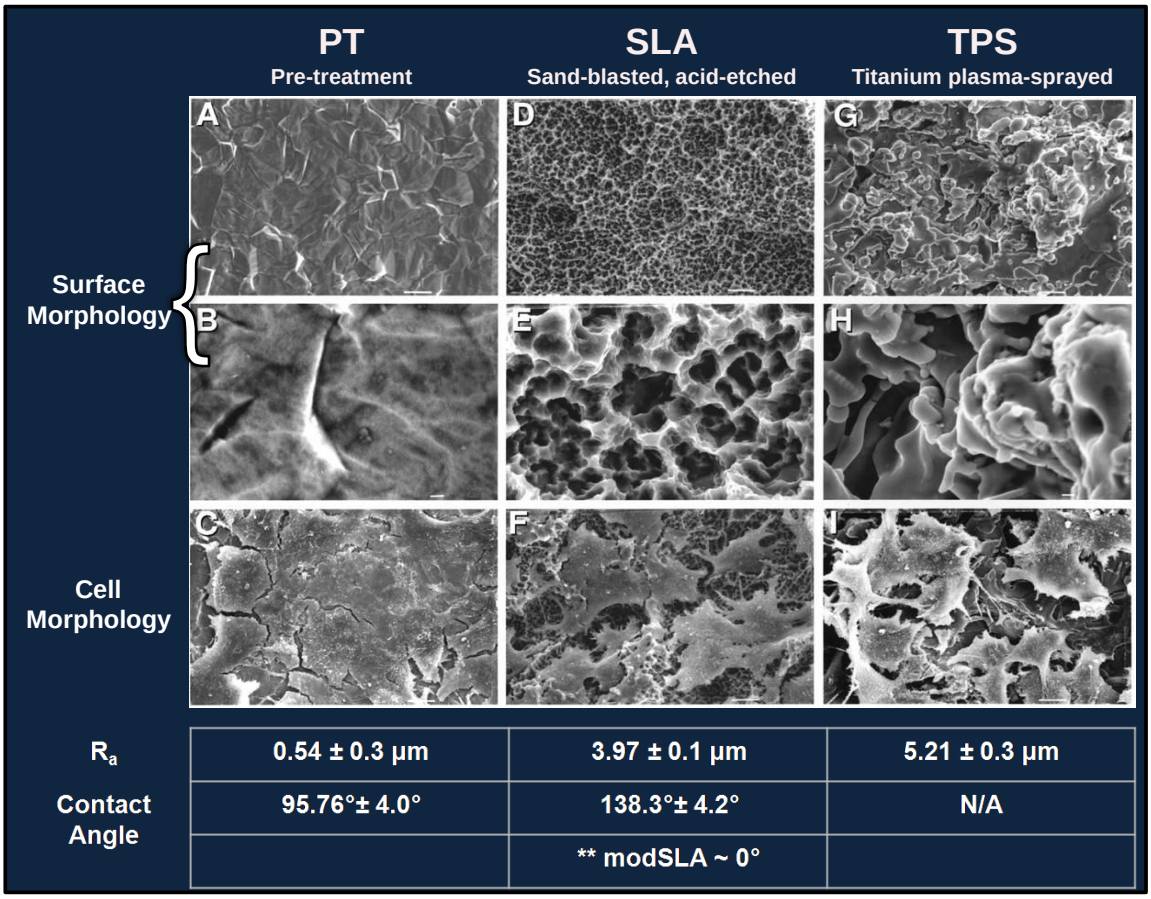

Figure 2-1: Morphology of PT, SLA, and TPS titanium surfaces viewed using scanning electron electron microscopy. Adapted from Zhao [147]. Note: modSLA surfaces have identical surface morphology to SLA surfaces. The table shows values for average peak to valley height (roughness; R_a) and advancing contact angles measurements [76].

The production of PT, SLA, modSLA, and TPS discs was performed by Institute Straumann AG under stringent protocols similar to those methods used in the production of dental implants [148]. Briefly, cpTi discs were cut from 1 mm-thick sheets of grade 2 commercially pure titanium (ASTM F67) to a diameter of 15 mm to match the size of wells in a standard 24-well tissue culture plate. The discs were then cleaned in acetone and briefly etched using 2% ammonium fluoride/2% hydrofluoric acid/10% nitric acid solution for 30 seconds at 55°C to produce PT surfaces. SLA and modSLA discs were sandblasted with alumina (corundum, Al_2O_3) particles averaging 250 µm in diameter at a pressure of 5 bar (low impact energy) to produce a rough microtopography. SLA and

modSLA discs were degreased in acetone and subsequently etched using a proprietary process involving a mixture of hot $HCl/H_2SO_4/H_2O$ at ratio of 1:8:1 [148]. This two-step process creates a complex morphology consisting of craters 20-50 μm in diameter (from sandblasting) overlaid with micropits between 0.5 and 2 μm in diameter (from etching), such that the overall topography mimics that of osteoclast resorption pits as shown in Figure 2-2 [149].

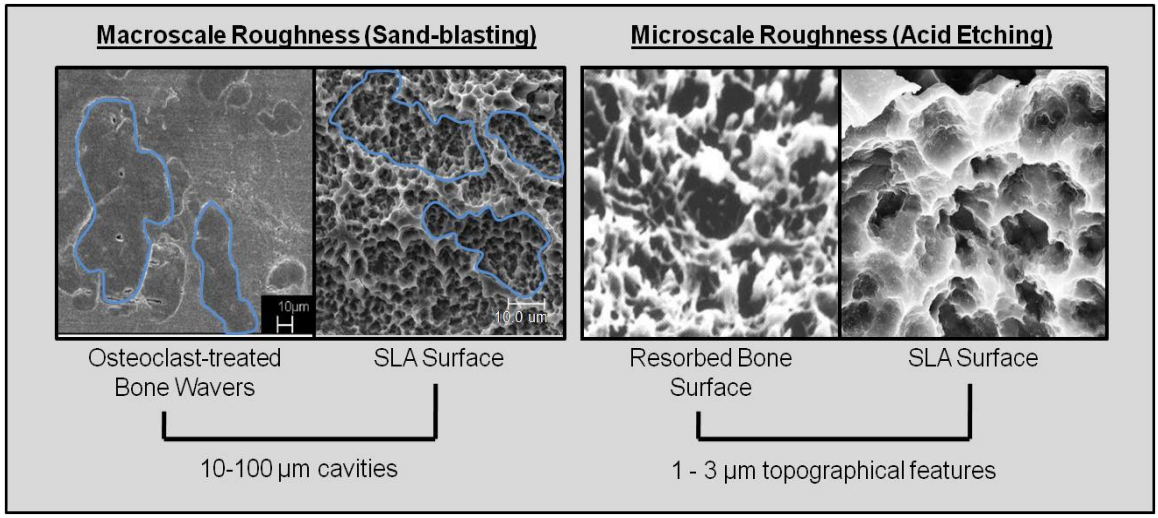

Figure 2-2: Comparison of SLA to bone wafers treated with osteoclasts. SLA surfaces have similar macroscale features as osteoclast resorption pits (left) and similar microscale features as the resorbed surface of bone (right). Adapted from Zhao, Davies, and Boyan [27, 147, 150].

TPS discs have the roughest surface morphology of the discs tested. TPS discs were first sandblasted with alumina particles in a similar manner to SLA and modSLA discs as described above. The surfaces were subsequently coated with titanium (and TiO_2) using a plasma spray process [151]. Briefly, a high temperature (15,000 – 20,000 ºF) plasma jet was created by applying a direct current (DC) arc discharge to an Argon carrier gas as it flowed through a high velocity nozzle. Titanium hydride powder was introduced into the plasma and the titanium particles were rapidly heated and accelerated to high velocity (3,000 m/s) before impacting the titanium substrate. These

molten particles quickly cooled upon impinging the substrate, leaving a highly adherent coating of roughened titanium approximately 30μm thick [68]. In preparation for cell culture, all PT, SLA, and TPS disks were sterilized by steam autoclaving at 121°C for 15 minutes. The sealed modSLA discs were sterilized by gamma irradiation at 25 kGy overnight by Institut Straumann AG.

Titanium PT, SLA, modSLA, and TPS surfaces have been characterized to assess surface roughness, surface energy, and surface chemical composition, all of which are known to influence osteoblast phenotype. Surface profilometry has shown that PT surfaces have an average peak to valley roughness (R_a) of 0.54 ± 0.3 μm, SLA and modSLA surfaces have an R_a of 3.97 ± 0.1 μm, and TPS surfaces have an R_a of 5.21 ± 0.3 μm [147]. Roughness is only one aspect of surface morphology that can be easily measured and understood. Surface morphologies for PT, SLA, and TPS surfaces have been observed using scanning electron microscopy as shown previously in Figure 2-1. Surface contact angle measurements showed varying surface energy between PT, SLA, and TPS surfaces. PT and SLA surfaces are fairly hydrophobic (low surface energy). Advancing contact angles of water droplets are 95.76°± 4.0° for PT and 138.3°± 4.2° for SLA [76]. The advancing contact angle for modSLA is indistinguishable from 0°, which indicates that modSLA surfaces are extremely hydrophilic (high surface energy). All surfaces have a 10-30nm thick oxide layer (primarily TiO_2), but other elements present vary between surfaces. X-ray electron spectroscopy has shown that carbon concentration is 29.2% ± 1.5%, 34.2% ± 2.0%, and 14.9% ± 0.9%, titanium concentration is 17.9% ± 1.0%, 14.3% ± 1.4%, and 23.0% ± 1.1%, and oxygen concentration is 47.6% ± 1.2%, 50.2% ± 2.6%, and 60.1% ± 0.7%, on PT, SLA, and modSLA surfaces, respectively [147]. These results demonstrate that modSLA surfaces have significantly less hydrocarbon contamination than PT or SLA surfaces. The

difference in surface energy between SLA and modSLA surfaces is directly related to this reduction in hydrocarbon contamination.

2.2. *In Vitro* Osteoblast Models

Several different osteoblast cell types were used within this thesis depending on the objective of the particular study. MG63 cells were used for the β_1 and α_2 knockdown studies in chapters 3 and 4. MG63 cells were also used for the RGD/KRSR study in chapter 5. Cavarial osteoblasts derived from VDR knockout and Cav-1 knockout mice were used in the studies described in Chapters 6 and 7. These cell lines are briefly described below:

MG63 Cells

MG63 cells were obtained from the American Type Culture Collection (ATCC, Rockville, MD). MG63 cells are an osteoblast-like cell line derived from human osteosarcoma cells originally isolated from a 14-year old Caucasian male. MG63 cells have been well characterized previously and show numerous traits of immature osteoblasts [69]. MG63 cells show enhanced differentiation in response to increasing surface roughness and $1\alpha,25(OH)_2D_3$, as determined by increases in alkaline phosphatase activity, osteocalcin levels, and other osteoblastic markers. MG63 cells display a flattened, fibroblast-like morphology when cultured on TCPS surfaces, but display a more cuboidal, osteoblast-like morphology on rough surfaces. These cells do not normally mineralize their matrix except under certain culture conditions [150]. MG63 cells were chosen for implant surface studies because they model an immature osteoblast that might contact an implant surface *in vivo*. These cells were chosen for integrin silencing so that a permanent cell line could be established.

Vitamin D Receptor Deficient Osteoblasts

A colony of VDR deficient mice was established at the Georgia Institute of Technology after a generous donation of mice from Marie DeMay of Massachusetts General Hospital. VDR(-/-) mice are completely deficient in functional VDR as demonstrated in previous studies [121]. A heterozygous breeding colony was maintained in a parasite-free animal facility. All mouse studies were performed under Georgia Tech IACUC approval and procedures. Mice were kept on a 12 hour light/dark cycle and fed a "non-rescue" 1:1 mix of Labdiet^{TM} 5001 rodent and 5015 mouse chow containing 0.88% calcium, 0.58% phosphorous, and 3.9 IU/gram of vitamin D_3. To collect DNA for genotyping, tail snips were performed under light anesthesia using isofluorane. DNA was extracted using a Buccal Amp DNA extraction kit (Epicentre Biotechnologies). VDR(-/-) mice were identified with PCR by the presence of the inserted neomycin resistance gene using the following primers: 5'-GCT GCT CTG ATG CCG CCG TGT TC-3' and 5'-GCA CTT CGC CCA ATA GCA GCC AG-3'. VDR(+/+) mice were identified using the primers 5'-CTG CCC TGC TCC ACA GTC CTT-3' and 5'-GCA GAC TCT CCA ATC TGA AGC-3', which are specific to the missing exon 2 section of the mouse VDR gene. VDR(+/+) and VDR(-/-) mice were euthanized by CO_2 at eight weeks old. Osteoblasts derived from VDR(-/-) mice were the experimental group and those from homozygous VDR(+/+) were used as wild-type littermate controls.

Osteoblasts were immediately isolated from the calvaria of 6-8 mice of each group. The calvaria was scraped to remove soft tissue and then diced into pieces smaller than 1-2mm. Calvaria pieces were then enzymatically digested using collagenase I and dispase for three 20 minute periods. Cells from the first digestion were discarded, but cells from the remaining two digestions were collected and seeded onto T-25 flasks for culture and expansion. Osteoblasts were cultured in DMEM plus 10%

FBS and 1% Penicillin/Streptomycin and were expanded through two passages before passage onto experimental surfaces.

Caveolin-1 Deficient Osteoblasts

Caveolin-1 deficient mice were obtained through collaboration with Dr. Hanjoong Jo of Emory University. A heterozygous mouse colony was maintained at the Emory University Medical School transgenic mouse facility. All mouse studies were performed under Emory University IACUC approval and procedures. Caveolin-1 deficient mice were euthanized by CO_2 at eight weeks old. Osteoblasts derived from Cav-1(-/-) mice were the experimental group and those from homozygous Cav-1(+/+) were used as wild-type littermate controls. Osteoblasts were immediately isolated from the calvaria of 6-8 mice of each group. Calvarial osteoblasts were harvested in an identical manner as VDR osteoblasts described previously. Osteoblasts were cultured in DMEM plus 10% FBS and 1% Penicillin/Streptomycin and were expanded through two passages before passage onto experimental surfaces.

2.3. Assessment of Osteoblast Phenotype

Osteoblasts phenotype was assessed through measures of osteoblast proliferation, differentiation, and local factor production. These tests are used throughout the thesis and are described in detail below:

Cell Number

Cell number measurements are affected by a combination of factors including cell seeding density, attachment, proliferation, and apoptosis. At cell harvest, which varied by experiment, media was collected and cells were washed twice with Dulbecco's Modified Eagle Medium (DMEM). Cells from each 24-well plate were then treated with

500 µL of 0.25% trypsin solution. Two 10 minute trypsin treatments were performed to detach cells from rough surfaces. Cells were centrifuged at 1500g and then resuspended in saline solution for counting. Cell number was determined using a Coulter automatic cell counter (Z1 cell and particle counter, Beckman Coulter, Fullerton, CA), which counts cells based on changes in electrical conductance as cells move through a microfluidic tube.

Total Protein:

After counting, cells were centrifuged and then lysed using 500 µL per well of 0.05% Triton X-100 followed by three consecutive freeze-thaw cycles. The cell lysate was used to measure total protein levels and alkaline phosphatase activity. Total protein was measured using a commercially available kit (Micro/Macro BCA, Pierce Chemical Co., Rockford, IL) and a fluorescence microplate reader at 570nm. Protein levels are used to normalize cellular alkaline phosphatase activity.

Alkaline Phosphatase Specific Activity

Alkaline phosphatase is a hydrolase that removes phosphates from many different molecules and proteins. Alkaline phosphatase is critical in matrix mineralization and is an early marker for osteoblastic differentiation. Alkaline phosphatase specific activity (orthophosphoric monoester phosphohydrolase, alkaline; E.C. 3.1.3.1) was assessed by measuring the release of *p*-nitrophenol from *p*-nitrophenylphosphate at pH 10.2. Activity was assessed using a fluorescence microplate reader at 415nm. This activity was normalized by total protein levels and by the total reaction time in minutes.

Osteocalcin Levels

Osteocalcin is a bone and dentin specific protein that is believed to act as a negative regulator of bone formation. Despite its abundance in bone, osteocalcin deficient mice actually exhibit increased bone mass [152]. Osteocalcin is considered to be a late marker for differentiation that is expressed just prior to mineralization. Osteocalcin was measured in the conditioned media using a commercially available radioimmunoassay kit (Human Osteocalcin RIA Kit, Biomedical Technologies, Stoughton, MA). Osteocalcin levels were normalized to total cell number.

Active and Latent TGF-β1:

TGF-β1 is a member of the TGF-β superfamily that has autocrine and paracrine effects on cell proliferation and differentiation. Bone extracellular matrix contains high levels of latent TGF-β1. The role of TGF-β1 in bone is complex, but increases in TGF-β1 expression are associated with increased osteoblastic differentiation. TGF-β1 was measured using an enzyme-linked immunoassay (ELISA) kit specific for human TGF-β1 (TGF-β1 $E_{max}^{®}$ Immunoassay System, Promega Corp., Madison, WI). Latent TGF-β1 was measured prior to acidification of the conditioned media. Total TGF-β1 was measured by acidification of the media with HCl for 10 minutes at room temperature followed by neutralization with NaOH. The amount of latent TGF-β1 was calculated by subtracting the amount of active TGF-β1 from the total TGF-β1. Latent and active TGF-β1 levels were normalized according to cell number.

Prostaglandin E_2

Prostaglandin E_2 is another autocrine and paracrine factor secreted by osteoblasts. At low levels PGE_2 may promote osteoblastic differentiation, but at high

levels it promotes osteoclastogenesis [153]. Increasing PGE_2 secretion is generally associated with increasing osteoblastic differentiation. PGE_2 was measured using a commercially available competitive binding radioimmunoassay kit (Prostaglandin E_2 RIA Kit, Perkin Elmer, Wellesley, MA). PGE_2 levels were normalized to cell number.

Osteoprotegerin

Osteoprotegerin is a secreted protein that inhibits osteoclastogenesis by binding directly to RANKL and preventing RANK/RANKL signaling. Affirming this role, OPG deficient mice develop osteoporosis at an early age [154]. Secretion of OPG by osteoblasts indicates the creation to a microenvironment promoting bone formation over resorption. Osteoprotegerin was measured using a commercially available enzyme-linked immunoassay (ELISA) kit specific for human osteoprotegerin (DY805, R&D systems, Minneapolis, MN). Osteoprotegerin levels were normalized to cell number.

CHAPTER 3:

The Role of Integrin β_1 in Osteoblast Response to Surface Microtopography and $1\alpha,25(OH)_2D_3$

3.1. Introduction

The chemical composition and topography of the surface are important in regulating adsorption of proteins and adhesion of cells, which affect cell phenotype, response to local and systemic regulatory factors, and the overall biological response to the implant [1, 155-157]. *In vitro* studies show that Ti surface microtopography is capable of promoting osteogenic maturation in both osteoblast-like MG63 cells and normal human osteoblasts (NHOst cells) [71, 158], as indicated by increases in levels of osteocalcin, TGF-β1, PGE_2, and OPG [69]. Moreover, increasing surface roughness and surface energy enhances the response of osteoblasts to bone anabolic agents such as $1\alpha,25(OH)_2D_3$ in a synergistic manner [159]. These studies suggest that the increased pull-out strength and bone-to-implant contact observed when implants with rough surfaces are used *in vivo* is due in part to the production of local osteogenic factors [31, 68]. By understanding the mechanisms involved with cell response to surface properties, materials can be designed to better promote osteointegration and long-term implant fixation.

Osteoblasts interact with their substrate initially via integrin binding to proteins adsorbed on the surface of a biomaterial as discuss in detail in section 1.4. Osteoblasts have been shown to express the integrins $\alpha_1\beta_1$, $\alpha_2\beta_1$ $\alpha_3\beta_1$, $\alpha_4\beta_1$, $\alpha_5\beta_1$, $\alpha_6\beta_1$, $\alpha_8\beta_1$, $\alpha_V\beta_3$, $\alpha_V\beta_5$, [34], but the integrins $\alpha_2\beta_1$ and $\alpha_5\beta_1$ have been shown to be particularly important in bone. The $\alpha_2\beta_1$ integrin binds to type I collagen [14], which is the dominant bone matrix protein, and $\alpha_2\beta_1$-mediated binding to extracellular matrix has been reported to

regulate osteoblastic differentiation [160, 161]. The integrin pair $\alpha_5\beta_1$ is selective for fibronectin; $\alpha_5\beta_1$ binding has been shown to be necessary for bone-like nodule formation *in vitro* when osteoprogenitor cells are grown on tissue culture plastic [162, 163].

Integrin expression is sensitive to substrate chemistry [164], raising the possibility that integrin requirements for osteoblast differentiation may also vary with surface chemistry. Expression of the β_1 integrin, which partners with α_2 and α_5, is increased in osteoblast-like MG63 cells cultured on titanium in comparison with tissue culture plastic [40]. When these cells are grown on titanium surfaces with rough microtopographies, expression of the β_1 integrin is further increased. In contrast, α_2 expression is increased and α_5 expression is decreased. These results correlate with higher levels of osteocalcin, indicating that changing integrin expression might be important in osteoblast differentiation. Integrin β_1 mRNA is also regulated by $1\alpha,25(OH)_2D_3$ in a dose-, time-, and surface roughness-dependent manner, but it is regulated independently of either α_2 or α_5 mRNA. However, it is not known if this increase in β_1 expression is responsible for increase in differentiation in response to surface roughness and $1\alpha,25(OH)_2D_3$, or whether these events are simply associated.

In the present paper, we investigated whether the synergistic effects of surface roughness and $1\alpha,25(OH)_2D_3$ on osteoblast differentiation are mediated by the β_1 integrin. In order to determine the specific roles of an integrin in the attachment, proliferation and differentiation of osteoblasts, many investigators have relied on the use of antibodies to block integrin binding [165, 166]. Integrins are also expressed on non-binding surfaces of the cell [167, 168]; thus some of the effect of the antibodies may be via integrins not involved in cell/substrate interactions, particularly if antibodies are added to the culture after initial attachment has occurred. To overcome this potential for artifact, the present study uses RNA interference (RNAi) technology to specifically suppress levels of β_1 expression. RNAi reduces the production of an individual protein

by post-transcriptionally inhibiting or degrading the mRNA for that protein via the introduction of a double stranded short hairpin RNA (shRNA) [169]. To test the hypothesis that the β_1 integrin mediates the response of osteoblasts to the microarchitecture of their substrate, MG63 cells were stably transfected with shRNA targeting the β_1 integrin mRNA. Control and β_1-silenced MG63 cells were plated on Ti substrates with different surface microtopographies and treated with $1\alpha,25(OH)_2D_3$ to determine whether loss of the β_1 integrin altered osteoblast proliferation or differentiation in response to these stimuli.

3.2. Materials and Methods

Titanium Surfaces

Institut Straumann AG (Basel, Switzerland) supplied the PT, SLA, and TPS titanium disks used in this study. Surfaces were manufactured and characterized as described in chapter 2.

Construction of DNA Vector-based shRNA Plasmids

The selection of coding sequences was determined empirically and was analyzed by blast search to avoid significant sequence homologies with other genes. Briefly, the β_1 integrin shRNA designed by Dr. Liping Wang targets 21 bases starting from the base 647 of the ITGB1 gene (NM_002211). Sequences of sense and antisense oligonucleotide strands constituting β_1 shRNA are 5'-tcg agg agg att act tcg gac ttc agg aat tcg tga agt ccg aag taa tcc tcc ttt tt-3' and 5'-cta gaa aaa gga gga tta ctt cgg act tca cga att cct gaa gtc cga agt aat cct cc-3', respectively. In addition, oligonucleotides that had scrambled β_1 sequences were used as a negative control. After annealing the oligonucleotides, the fragments were cloned into a pSuppressorNeo vector containing a

U6 promoter with a GeneSupressorTM system (IMGENEX Corp., San Diego, CA) according to manufacturer protocols [170].

Transfection and Selection of β1-silenced MG63 cells

MG63 cells were used as a model in this study and are described in chapter 2. Cells were cultured in DMEM containing 10% fetal bovine serum (FBS) and 0.5% antibiotics (diluted from a stock solution containing 5000U/mL penicillin and 5000U/mL streptomycin; GIBCO, Grand Island, NY) and in an atmosphere of 100% humidity and 5% CO_2. The media were changed at 24 h and then at 48 h intervals. At confluence, cells were subcultured in a 6-well plate at a plating density of 2 x 10^5 cells in 0.5 ml of growth medium without antibiotics.

When cells were 90–95% confluent, they were transfected using Lipofectamine 2000 (Invitrogen, Carlsbad, CA) with either the pSuppressorNeo/ U6 plasmid containing the β_1 shRNA or the control plasmids according to the manufacturer's instructions. Briefly, plasmids were incubated with Lipofectamine 2000^{TM} in OPTI-MEM^{TM} reduced serum medium (GIBCO) for 20 minutes at room temperature before transfection. Then, the plasmid-Lipofectamine complexes were added to individual wells, each of which contained cells and growth medium, and incubated for 48 h at 37ºC. The effectiveness of the β_1-shRNA silencing was determined by quantitative reverse transcription polymerase chain reaction (qRT-PCR). To select for cells containing plasmid, following the transfection, the growth media were replaced with media containing DMEM, 10% FBS, and 400 mg/ml of the antibiotic G418 (Invitrogen). Surviving cells were cultured until they reached confluence and then subcultured into T-75 flasks. Confluent cultures were subpassaged onto the experimental surfaces. In addition, aliquots of these cells were stored at -80ºC for subsequent experiments. G418 was included in the growth medium until cells reached confluence on the test substrates. Two cell lines were

selected for these studies. β_1-shRNA MG63 cells exhibited a consistent 65% reduction in β_1 integrin mRNA. β_1S scrambled MG63 cells contained the scrambled shRNA plasmid and exhibited the same β_1 mRNA levels as non-transfected MG63 cells.

Real-time PCR Measurement of Integrin β_1 mRNA

The presence of β_1 integrin mRNA in the cells was verified by RT-PCR and qRT-PCR. Total RNA was isolated using the TRIZOL reagent (Invitrogen) from wild-type MG63 cells as well as from cells treated with Lipofectamine alone, Lipofectamine plus empty plasmid, Lipofectamine plus β_1 shRNA, and plasmid containing the scrambled shRNA template (N=1 per group). One mg of RNA was reversed transcribed with 200 ng each of human β_1 integrin sense and antisense primers in a 15 ml volume using the Amersham-Pharmacia-Biotech RT kit (Amersham Biosciences, Piscataway, NJ). Optimal oligonucleotide primers were designed using Beacon Designer 2.0 software (MWG Biotech, High Point, NC). The primers used to amplify human integrin β_1 were synthesized according to the following sequences: 5'-caacgaggtcatggttcatgtt-3' (antisense) and 5'-caacgaggtcatggttcatgtt-3' (sense). Quantitative RT-PCR was performed on an i-cycler^{TM} (Bio-Rad Laboratories, Hercules, CA) using software i-cycler iQ^{TM}, version 3.0a. PCRs were carried out in a total volume of 25 µl in PCR master mix containing 12.5 µl SYBR® green, 200 ng each of sense and antisense primer, 25mM $MgCl_2$, and 3 µl of the reverse transcription product. The volume was adjusted with diethylpyrocarbonate (DEPC)-treated water. The amplifications were performed in duplicate for each sample and the optimal PCR conditions for integrin β1 were 61ºC for 40 cycles; and for the GapDH, they were 54ºC for 40 cycles.

To normalize the content of cDNA samples, we used the comparative threshold (Ct) cycle method, which consists of the normalization of the number of target gene copies versus the endogenous reference gene GAPDH. The Ct is defined as the

fractional cycle number at which the fluorescence generated by cleavage of the probe passes a set threshold baseline when amplification of the PCR product is first detected. Through this method, a single sample, represented in our experiments by cells without any treatment, was designed as a calibrator and used for comparison of gene expression level of any unknown samples.

Physiological Responses of Osteoblasts MG63 Cells

Wild type, β_1-silenced, and β_1-scrambled-transfectants were grown to confluence on tissue culture plastic and then subcultured into 24-well plates on six discs each of TCPS, PT, SLA, or TPS surfaces. When the cells reached confluence on tissue culture plastic, media in all wells were replaced with experimental media containing ethanol vehicle or 10^8 M 1α,25$(OH)_2D_3$. Cells were cultured an additional 24 hours. At that time, cells were harvested and conditioned media were collected. Osteoblast phenotype was assessed by measuring cell number, alkaline phosphatase activity, and levels of osteocalcin, TGF-β1, OPG, and PEG_2 according to protocols discussed in chapter 2. Soluble RANKL was also measured in this study using a commercially available ELISA kit (ALPCO Diagnostics, Windham, NH), but levels were undetectable in any of the cells.

Statistical Analysis

The data presented are from one of two separate sets of experiments, both of which yielded comparable results. Each data point represents the mean ± standard error of the mean (SEM) of six independent cultures. Data were analyzed by analysis of variance and statistical significance between groups was determined using Bonferroni's modification of Student's t-test. $p<0.05$ was considered to be significant.

3.3. Results

RT-PCR demonstrated that integrin β_1 mRNA was present in normal cells as well as in the cells treated with Lipofectamine 2000 reagent and control plasmids (Figure 3-1). β_1 shRNA caused about a 65% decrease in the β_1 mRNA of MG63 cells compared to wild-type cells or cells transfected with the control plasmids.

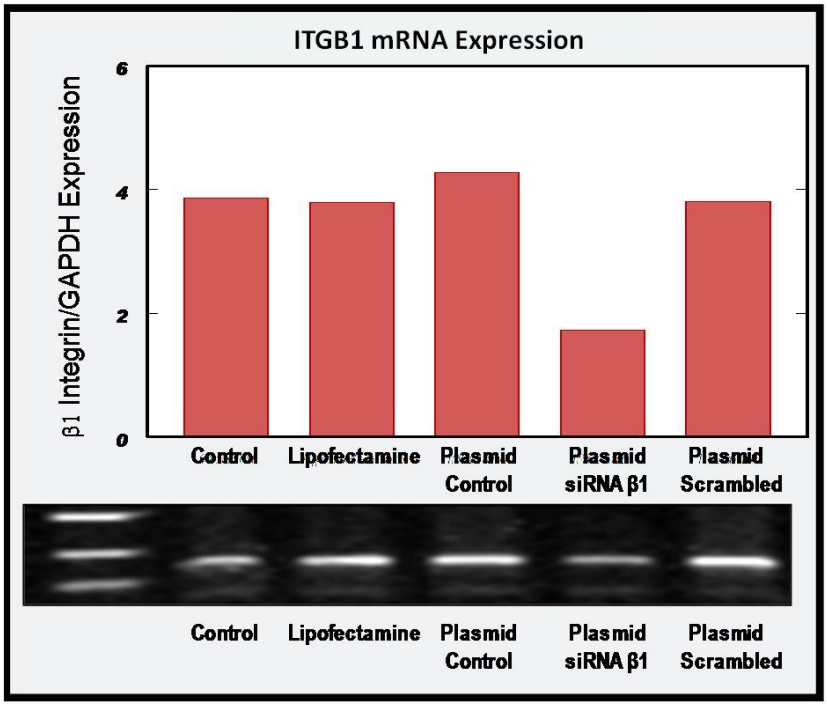

Figure 3-1: RT-PCR and qRT-PCR demonstrating a 65% reduction in β_1 integrin mRNA.

Cell number, alkaline phosphatase activity, and osteocalcin levels were similar in wild-type MG63 and β_1 scrambled MG63 cells, indicating that plasmid transfection by itself does not alter osteoblast phenotype. This comparison was completed by Liping Wang and is reported in the published study [102]. The comparisons presented in this thesis are between wild-type MG63 and β_1-silenced MG63 cells in response to surface roughness and $1\alpha,25(OH)_2D_3$.

Increasing surface roughness decreased the number of wild-type MG63 cells as shown in Figure 3-2. β_1 silencing reduced cell number compared to wild-type MG63

cells by approximately 40% on all surfaces. The effect of $1\alpha,25(OH)_2D_3$ on wild-type cells was to reduce cell number to the level seen in β_1-silenced cells. $1\alpha,25(OH)_2D_3$ also decreased the number of β_1-silenced cells, but the effect was less robust than on wild-type MG63 cells.

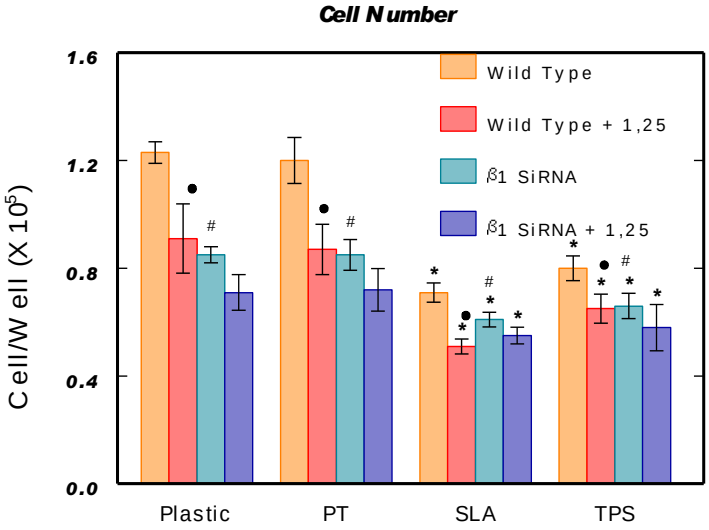

Figure 3-2: Effect of surface roughness and $1\alpha,25(OH)_2D_3$ on cell number in wild-type MG63 and β_1 silenced cells. * Ti surface vs. Plastic (TCPS); • 1,25 vs. vehicle control; # β1 siRNA vs. control

Alkaline phosphatase activity was increased in wild-type cells on rough SLA and TPS surfaces and with treatment of $1\alpha,25(OH)_2D_3$ (Figure 3-3). The effects of β_1-silencing on osteoblast differentiation were surface dependent. β_1-silencing reduced alkaline phosphatase specific activity on all titanium surfaces, but the percent reduction was greater on the rougher surfaces. $1\alpha,25(OH)_2D_3$ stimulated alkaline phosphatase activity in wild-type and β_1-silenced cells. Osteocalcin levels varied in the same manner as alkaline phosphatase activity. β_1-silencing caused a small reduction in osteocalcin production in cells grown on TCPS and PT surfaces, but caused a large reduction on SLA and TPS surfaces (Figure 3-4). Osteocalcin levels were similar in all β_1-silenced cells regardless of surface, although a small surface-dependent increase was seen on

the SLA surface. $1\alpha,25(OH)_2D_3$ had a stimulatory effect on osteocalcin levels in all cells but this effect was attenuated significantly in the β_1-silenced cells.

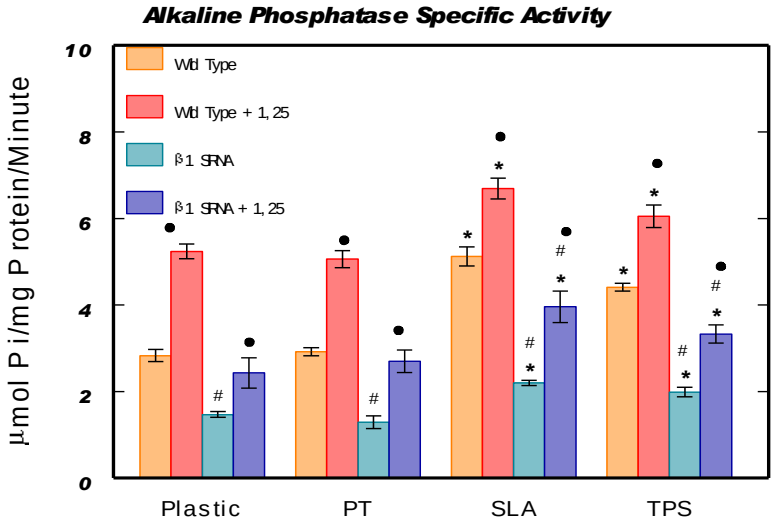

Figure 3-3: Effect of surface roughness and $1\alpha,25(OH)_2D_3$ on alkaline phosphatase activity in wild-type MG63 and β_1 silenced cells. * Ti surface vs. Plastic (TCPS); • 1,25 vs. vehicle control; # β1 siRNA vs. control

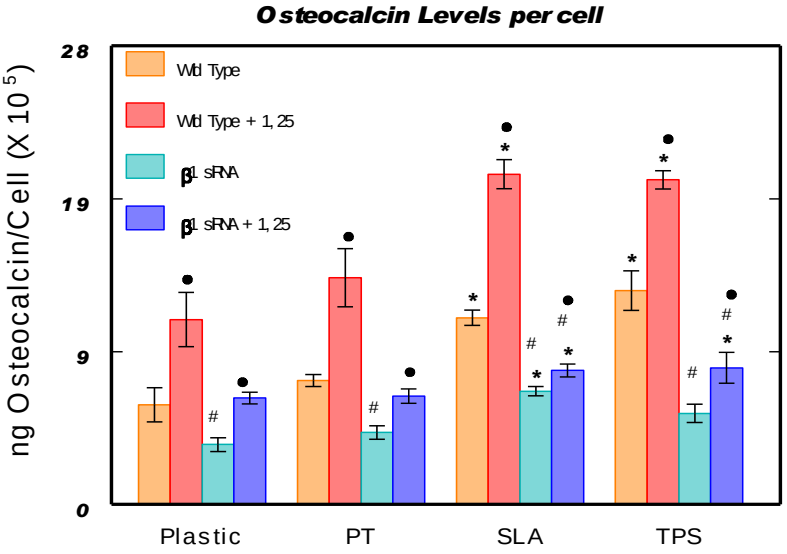

Figure 3-4: Effect of surface roughness and $1\alpha,25(OH)_2D_3$ on osteocalcin levels in wild-type MG63 and β_1 silenced cells. * Ti surface vs. Plastic (TCPS); • 1,25 vs. vehicle control; # β1 siRNA vs. control

Production of local regulatory factors was also sensitive to β_1-silencing but the consequence of β_1-silencing was specific to each of the factors examined. OPG levels

were reduced by approximately 50% in the β_1-silenced cells, regardless of surface, although β_1-silencing did not prevent the surface-dependent increase in OPG production (Figure 3-5). $1\alpha,25(OH)_2D_3$ increased OPG in all cultures, regardless of surface. The relative stimulatory effect of the hormone was less robust in wild-type MG63 cells than β_1-silenced cells. In the β_1-silenced cells, $1\alpha,25(OH)_2D_3$ caused a 100% increase in OPG levels compared to vehicle control treatment on all surfaces. Despite these increases, the levels of OPG in the β_1-silenced cells grown on SLA and TPS were still not as great as those seen in wild-type cultures.

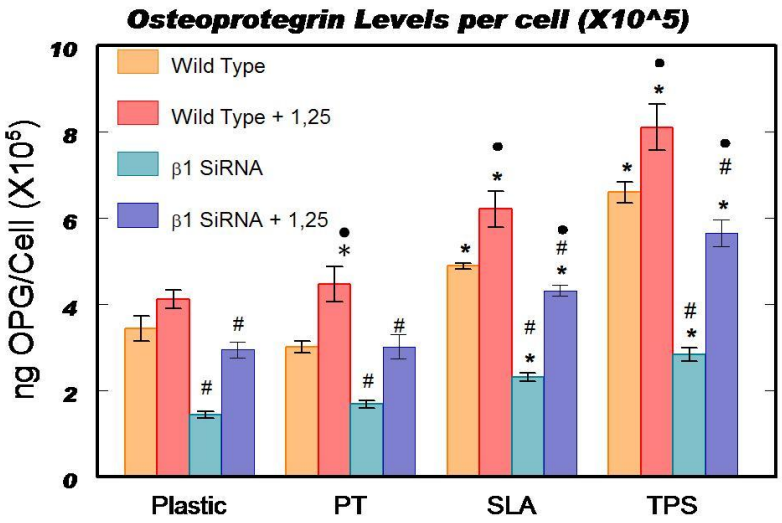

Figure 3-5: Effect of surface roughness and $1\alpha,25(OH)_2D_3$ on osteoprotegerin levels in wild-type MG63 and β_1 silenced cells. * Ti surface vs. Plastic (TCPS); • 1,25 vs. vehicle control; # β1 siRNA vs. control

PGE_2 production was reduced in β_1-silenced cells on all surfaces but the effect of silencing on this parameter was relatively small (Figure 3-6). $1\alpha,25(OH)_2D_3$ had no discernable effect on PGE_2 production by wild-type MG63 cells grown on plastic or PT; however, $1\alpha,25(OH)_2D_3$ did have a stimulatory effect on PGE_2 levels on SLA and TPS surfaces. The effect of $1\alpha,25(OH)_2D_3$ was slightly less robust in the β_1-silenced cells. Total levels of TGF-β1 varied with surface roughness in wild type and β_1-silenced cells (Figure 3-7). Cells transfected with the β_1 shRNA produced 40–50% less TGF-β1 on

each surface. $1\alpha,25(OH)_2D_3$ increased TGF-β1 slightly in the wild-type cells, but it had no significant effects in β_1-silenced cells.

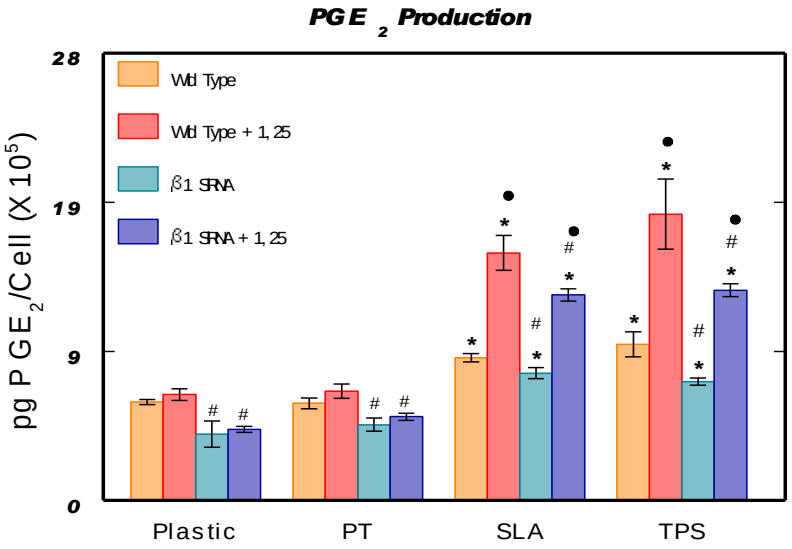

Figure 3-6: Effect of surface roughness and $1\alpha,25(OH)_2D_3$ on PGE_2 levels in wild-type MG63 and β_1 silenced cells. * Ti surface vs. Plastic (TCPS); • 1,25 vs. vehicle control; # β1 siRNA vs. control

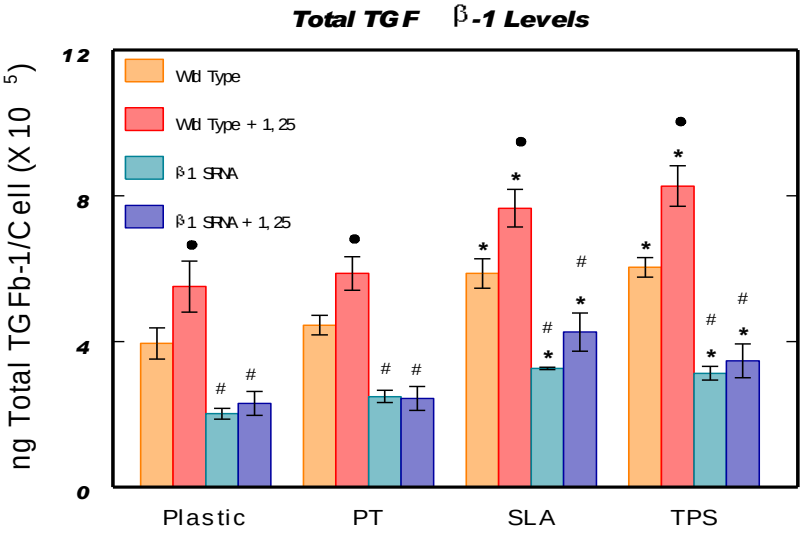

Figure 3-7: Effect of surface roughness and $1\alpha,25(OH)_2D_3$ on TGF-β1 levels in wild-type MG63 and β_1 silenced cells. * Ti surface vs. Plastic (TCPS); • 1,25 vs. vehicle control; # β1 siRNA vs. control

3.4. Discussion

The results in this study provide definitive evidence that the effects of surface microarchitecture on osteoblast differentiation and the response to 1α,25$(OH)_2D_3$ are mediated in part through the β_1 integrin. Silencing of the β_1 integrin resulted in reduced cell numbers as well as in reductions in alkaline phosphatase specific activity and levels of osteocalcin, OPG, PGE_2, and TGF-β1. Moreover, it inhibited the effects of surface roughness on these parameters. These results are consistent with the hypothesis that β_1 and its heterodimeric partners, particularly $\alpha_2\beta_1$ and $\alpha_5\beta_1$, are critical in mediating extracellular matrix cues for osteoblast attachment, proliferation, and differentiation.

Inhibition of osteoblast proliferation is often associated with enhancement of differentiation [171], and it has been shown to occur on titanium surfaces with rough microtopographies [158]. However, in the present study the β_1-silenced cells had a reduced capacity for both proliferation and differentiation. Attachment of many cell types, including osteoblasts, is critical to anchorage dependent signals regulating cell cycle control and survival. For example, multiple groups have shown that the initial attachment of osteoblasts or osteoprogenitor cells to Ti surfaces is via $\alpha_5\beta_1$ [37, 146]. Binding of the $\alpha_5\beta_1$ integrin to fibronectin can act through PI3K and Akt pathways to promote cell survival [47, 48], or through JNK and MAP kinase-mediated pathways to promote cell proliferation and early differentiation [44, 49]. How the β1 integrin is involved in mature osteoblast differentiation is unclear, but it is known be involved in numerous signaling pathways. For example, many integrins activate PKC and ERK1/2 mediated pathways shown to increase Runx2 transcriptional activity and increase osteoblastic differentiation [44, 50]. Moreover, many growth factors, including BMP or membrane 1α,25$(OH)_2D_3$ receptors present in caveolae, require integrin binding for proper signaling [138]. For this reason, it is not surprising that β_1-silenced cells have both decreased proliferation and differentiation.

The β_1 integrin partners with α_2 and α_5 in MG63 cells [172], but is not known if one or both heterodimers was affected differentially by the silencing. It is likely that both heterodimers were involved. Raz et al. previously showed that both α_2 and β_1 increase as a function of time in culture in MG63 cells grown on titanium whereas α_5 is reduced [40], suggesting that enhanced differentiation mediated by integrins on these substrates is dependent on the $\alpha_2\beta_1$ heterodimer. $\alpha_2\beta_1$ binds to type I collagen in the bone extracellular matrix , and therefore, might be more important for differentiation once the cells become established on their substrate. Subsequent work since this study has shown that knockdown of the $\alpha_2\beta_1$ integrin inhibits differentiation of MG63 cells in response to surface topography and $1\alpha,25(OH)_2D_3$ [41]. Some studies suggest that $\alpha_5\beta_1$ mediates attachment and differentiation of osteoprogenitors and possibly early osteoblast, but that the $\alpha_2\beta_1$ integrin is required for osteoblast differentiation [146].

Integrin β_1 deficiency may also affect osteoblast differentiation via changes in local factor production. Our results showed that the levels of OPG, PGE_2 and TGF-β1 in the conditioned media of the MG63 cells were reduced in the β_1-silenced cells. OPG, PGE_2 and TGF-β1 are all associated with osteogenesis and previous studies show that all are increased in MG63 cultures grown on SLA and TPS surfaces [69]. β_1 silencing blocked most of the stimulatory effects of surface microroughness on each of these parameters. It has been shown previously that inhibition of prostaglandin production blocks the stimulatory effect of surface microarchitecture on osteoblastic differentiation [173]. This supports the possibility that a reduction in PGE_2 production mediated the reduction in differentiation observed in the β_1-shRNA treated cells.

OPG is produced by osteoblasts as a decoy receptor for RANKL, thereby suppressing the differentiation of osteoclasts and inducing their apoptosis [154, 174]. Soluble RANKL is produced by osteoblasts to deplete local levels of OPG, thereby reducing the inhibitory effect of OPG on osteoclast formation and activity. Soluble

RANKL was not detectable in the cultures, either in cultures of wild-type cells or in cultures of the transfectants. Others have shown that integrin β_1 upregulates RANKL expression on osteoblasts [165], while this study showed that β_1 may be involved in increasing OPG secretion. The fact that β_1 appears to play such dual roles hints at complex feedback loops with other receptors.

$1\alpha,25(OH)_2D_3$ is a bone anabolic agent that regulates the differentiation of osteoblasts by increasing alkaline phosphatase expression and activity, expression of osteocalcin, and production of local factors including OPG, PGE_2, and TGF-β_1 [69, 175]. Growth on surfaces with rough microtopography modifies the response of osteoblasts to $1\alpha,25(OH)_2D_3$ and effects of microtopography per cell are synergistic with those of $1\alpha,25(OH)_2D_3$. β_1 silencing reduced the effects of $1\alpha,25(OH)_2D_3$ on alkaline phosphatase activity and osteocalcin production. While alkaline phosphatase and osteocalcin are both regulated by $1\alpha,25(OH)_2D_3$, the mechanisms involved are not identical [176], suggesting that β_1 mediates its effects via multiple pathways shared in common with $1\alpha,25(OH)_2D_3$ and integrin signaling. Previous studies demonstrated that surface roughness exerts its effects on TGF-β1 via PKC signaling while the PKA pathway was involved in mediating the effects of surface roughness on PGE_2 production [175]. $1\alpha,25(OH)_2D_3$ modulates osteoblast differentiation via these pathways as well as through traditional nuclear vitamin D receptor mechanisms [176, 177]. In addition, the β_1 integrin could modulate these pathways via interactions with caveolae since receptors for both $1\alpha,25(OH)_2D_3$ and TGF-β1 have been reported in caveolae. While it is tempting to try to explain the actions of the β_1 integrin through one single pathway, such as PKC, silencing of the β_1 has likely disrupted multiple signaling pathways, making it clear that future studies need to investigate the role of individual αβ partners.

5.5. Conclusion

The results indicate that both osteoblast proliferation and differentiation depend on β_1 integrin signaling. Moreover, osteoblast response to the effects of increasing surface roughness is diminished, and osteoblasts appear to be less responsive to some of the effects of $1\alpha,25(OH)_2D_3$. These results suggest that complex interplay exists between integrin and $1\alpha,25(OH)_2D_3$ signaling pathways. Given the broad importance of the β_1 integrin demonstrated herein this study, it is now critical to investigate the role of specific integrin pairs, such as $\alpha_2\beta_1$ and $\alpha_5\beta_1$, to determine how these integrins regulate osteoblast attachment, proliferation, and differentiation in response to implant surface properties and $1\alpha,25(OH)_2D_3$ at different stages of osteoblast maturity.

CHAPTER 4:

Role of the $\alpha_5\beta_1$ Integrin in Mediating the Response to Surface Energy and Microtopography

4.1. Introduction

The previous chapter demonstrated that the β_1 integrin subunit is involved in osteoblast response to surface microtopography. However, osteoblasts possess multiple heterodimers of the β_1 integrin that play disparate roles in affecting osteoblast proliferation and differentiation at different points in osteoblast maturation. As discussed in the previous section, osteoblasts express the integrins $\alpha_1\beta_1$, $\alpha_2\beta_1$ $\alpha_3\beta_1$, $\alpha_4\beta_1$, $\alpha_5\beta_1$, $\alpha_6\beta_1$, $\alpha_8\beta_1$, $\alpha_V\beta_3$, $\alpha_V\beta_5$ [34]. The integrins $\alpha_2\beta_1$ and $\alpha_5\beta_1$ have been shown to be particularly important in osteoblast maturation and bone development. The $\alpha_2\beta_1$ integrin binds to type I collagen [14], which is the dominant bone matrix protein, and $\alpha_2\beta_1$-mediated binding to the extracellular matrix has been reported to regulate osteoblastic differentiation [160, 161]. The $\alpha_2\beta_1$ integrin has also been shown to be critical for osteoblast response to surface energy and microtopography, since previous reports have shown that silencing of the $\alpha_2\beta_1$ integrin inhibits osteoblast differentiation induced by increasing surface roughness [41]. The integrin $\alpha_5\beta_1$ is selective for fibronectin and is known to be important in early attachment and differentiation of osteoblast and osteoprogenitor cells. Reports have shown that $\alpha_5\beta_1$ is necessary for bone-like nodule formation in osteoprogenitor cells grown on TCPS [162, 163]. Moreover, a recent study claims that $\alpha_5\beta_1$ silencing in bone marrow stromal cells reduces cell attachment, proliferation, and osteogenic differentiation [146]. Overall, evidence suggests that the $\alpha_5\beta_1$ integrin may be involved in early osteoblastic differentiation, but its role in mediating the response of osteoblasts to surface microtopography in osteoblasts in unclear.

Surface chemistry and topography are well known to effect integrin expression, which in turn directs cell response. Previous studies have shown in MG63 cells grown on titanium that both α_2 and β_1 increase as a function of time in culture and increasing surface roughness, whereas α_5 is reduced [40]. This change in integrin expression was correlated with changes in osteocalcin expression, suggesting a shift from $\alpha_5\beta_1$ to $\alpha_2\beta_1$ expression as osteoblasts mature. In addition, integrin β_1 mRNA is regulated by $1\alpha,25(OH)_2D_3$ in a dose-, time-, and surface roughness-dependent manner, but it is regulated independently of either α_2 or α_5 expression. Previous studies in MG63 cells showed an increase in $\alpha_5\beta_1$ binding and FAK activity on TPS and SLA surfaces versus PT surfaces [178]. Using blocking antibodies against $\alpha_5\beta_1$ resulted in a decrease in proliferation ([^{3}H]-thymidine incorporation) on all surfaces and an increase in alkaline phosphatase activity at 7 days post-seeding. These findings suggest a strong role of $\alpha_5\beta_1$ in controlling proliferation, and also suggest $\alpha_5\beta_1$-mediated control of differentiation at some time points. However, no studies have examined the effect of $\alpha_5\beta_1$ silencing on production of late markers for differentiation in osteoblasts.

Multiple groups have shown that the initial attachment of osteoblasts or osteoprogenitor cells to titanium surfaces is via $\alpha_5\beta_1$ [37, 146]. In osteoblasts, binding of the $\alpha_5\beta_1$ integrin to fibronectin increases activity of PI3K, Akt, and Bcl-2, which in turn reduces caspase activity and promotes cell survival [47, 48]. In addition, the $\alpha_5\beta_1$ integrin can act through JNK and MAP kinase-mediated pathways to phosphorylate c-Jun and c-Fos, which form activator protein 1 (AP-1), a transcription factor complex that promotes cell proliferation and also induces expression of several early osteogenic target genes [44, 49]. These studies suggest that the $\alpha_5\beta_1$ integrin signals through a wide variety of signaling pathways to promote cell survival, proliferation, and early osteoblast differentiation.

The present study aims to determine whether the $\alpha_5\beta_1$ integrin mediates the synergistic effects of surface roughness and 1α,25$(OH)_2D_3$ on osteoblast proliferation and differentiation. To determine the role of the $\alpha_5\beta_1$ integrin, osteoblast-like MG63 cells were transduced with lentiviral particles containing a plasmid with shRNA targeting the α_5 integrin subunit. Control and α_5-silenced MG63 cells were plated on titanium substrates with different surface chemistries and microtopographies to determine whether loss of the $\alpha_5\beta_1$ integrin altered osteoblast proliferation or differentiation.

4.2. Materials and Methods

Titanium Surfaces

Institut Straumann AG (Basel, Switzerland) supplied the PT, SLA, and modSLA titanium disks used in this study. Surfaces were manufactured and characterized as described in chapter 2. TCPS surfaces were also used as controls.

Lentiviral-based Transfection of MG63 Cells with α_5-shRNA

MG63 cells were used as a model in this study and are described in chapter 2. Sigma MISSION® shRNA Lentiviral Transduction Particles targeting the alpha 5 integrin gene (ITGA5, NM_002205) were purchased from Sigma-Aldrich (St. Louis, MO). Five different clones were purchased in order to maximize the chance for knockdown. The sequences of the clones were as follows:

TRCN0000029649

CCGGCCATGATGAGTTTGGCCGATT**ctcgag**AATCGGCCAAACTCATCATGGTTTT

TRCN0000029650

CCGGCCACAGATAACTTCACCCGAA**ctcgag**TTCGGGTGAAGTTATCTGTGGTTTTT

TRCN0000029651

CCGGCCACTGTGGATCATCATCCTA**ctcgag**TAGGATGATGATCCACAGTGGTTTTT

TRCN0000029652

CCGGCCTCAGGAACGAGTCAGAATT**ctcgag**AATTCTGACTCGTTCCTGAGGTTTTT

TRCN0000029653

CCGGCTCCTATATGTGACCAGAGTT**ctcgag**AACTCTGGTCACATATAGGAGTTTTT

In addition to these lentiviral vectors (clones 49, 50, 51, 52, 53), control vectors were also used including MISSION® pLKO.1-puro Control Transduction Particles. Control MG63 cells with and without selection media were also used as transduction controls. Transduction of MG63 cells was performed under biosafety level 2 safety precautions. Briefly, MG63 cells were plated in 24-well plates at a seeding density of 10,000 cells/cm^2 in DMEM + 10% FBS + 1% Penicillin/Streptomycin. Cells were transduced after reaching 60-70% confluence. On the day of transduction, media was changed to DMEM + 10% FBS and cells were transduced with lentiviral particles at a multiplicity of infection (MOI) of 30. Each vector was transduced into two wells of the 24-well plate. After 18 hours, media was discarded into bleach solution and was replaced by DMEM + 10% FBS + 1% Penicillin/Streptomycin. On the following day, 0.5 ug/mL of puromycin was added to every well except the control MG63 cells. Control cells and vectors not expressing puromycin resistance genes were killed. Clone 50 did not survive transduction. Transduced cells (pLKO.1-puro "vector" control; α_5-shRNA clones 49, 51, 52, and 53) containing the puromycin resistance gene survived and were passed

to T-25s at confluence. Puromycin selection was continued throughout passaging. Cells were then passed to T-75s for expansion.

Testing Silencing Efficiency: qRT-PCR and Western Blots

The effectiveness of the α_5-shRNA silencing was determined first by quantitative reverse transcription polymerase chain reaction (qRT-PCR). All five clones were screened using qRT-PCR to determine relative α_5 mRNA expression. Total RNA was isolated using the TRIZOL reagent (Invitrogen) from wild-type MG63 cells as well as from cells treated α_5-shRNA clones. Following RNA isolation, RNA was quantified using a Nanodrop™ spectrophotometer (Thermo Scientific, Wilmington, DE). All samples were normalized to 1ug RNA/uL with diethylpyrocarbonate (DEPC)-treated water. Reverse transcription was performed using Omniscript™ reverse transcriptase (Invitrogen) and random primers. qRT-PCR was performed was carried out in a total volume of 25 µl in PCR master mix containing 12.5 µl SYBR® green, 200 ng each of sense and antisense primer, 1uL 25mM $MgCl_2$, and RNAase free water. All reactions were carried out for 40 cycles on an i-cycler™ (Bio-Rad Laboratories, Hercules, CA) using software i-cycler iQ™, version 3.0a. The following primers and conditions were used for each gene:

- ITGA5 R 57ºC 5'-AAGTTCCCTGGGTGTCTG-3'
- ITGA5 F 57ºC 5'-ATCTGTGTGCCTGACCTG-3'
- GapDH R 54ºC 5'-GCTCTCCAGAACATCATCC-3'
- GapDH F 54ºC 5'-TGCTTCACCACCTTCTTG-3'

To normalize the content of cDNA samples, we used the comparative threshold (Ct) cycle method, which consists of the normalization of ITGA5 versus the endogenous reference gene GAPDH. Expression of the α_5 integrin gene (ITGA5) normalized to

GapDH was measured in Control MG63, vector control, and α_5-shRNA clones. Clone 50 did not survive puromycin selection. Clone 49/51 is transfected with both the clone 49 and 51 lentiviral particles. Expression of ITGA5 (Figure 4-1) demonstrates that clone 52 exhibits the highest level of suppression.

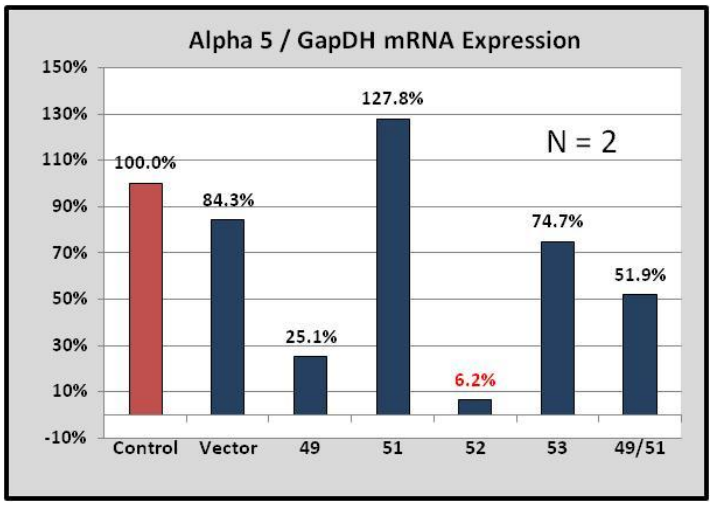

Figure 4-1: qRT-PCR of ITGA5/GapDH expression levels in Control MG63, vector control, and α_5-shRNA clones.

Knockdown efficiency was also measured using western blot analysis. Control cells and α_5-shRNA clones were grown in T-75 tissue culture flasks until confluence. Cells were harvested using RIPA lysis buffer and were scraped to collect protein. Westerns were run on 10% SDS-polyacrylamide gels and were stained with antibodies for integrin α_5 (H-104, Santa Cruz Biotechnology, Santa Cruz, CA) and GapDH (MAB374 Chemicon, Billerica, MA). Protein expression of integrin α_5 by western blot analysis (Figure 4-1) demonstrates that clone 52 exhibits the highest level of knockdown efficiency.

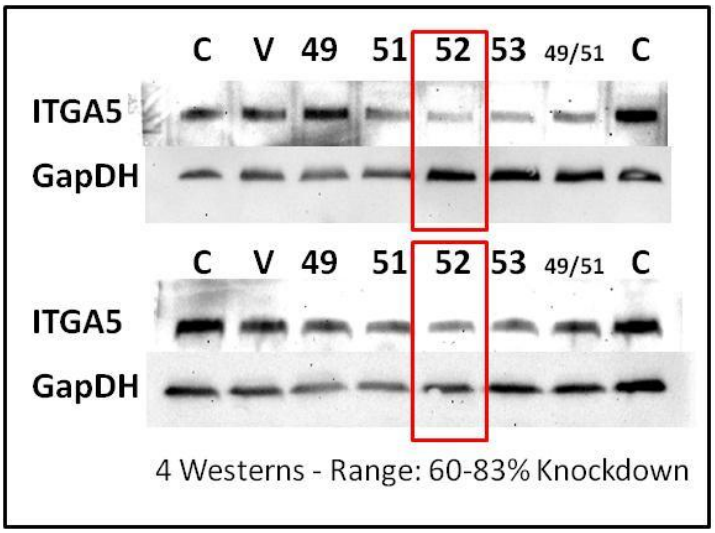

Figure 4-2: Two representative western blots for integrin α_5 and GapDH in Control MG63, vector control, and α_5-shRNA clones. Clone 52 was selected for silencing.

Functional Response of Osteoblast-like MG63 Cells

The functional ability of $\alpha_5\beta_1$ to mediate cell attachment was also measured in order to determine if α_5-silencing was effective. To measure attachment, 96-well plates were coated for one hour with 1% BSA solution, 10 µg/mL collagen I, or 10 µg/mL fibronectin. Following coating, plates were then blocked for an hour with 1% BSA solution. Wild type MG63 cells and two α_5-silenced clones (52 and 53) were incubated with a calcein solution for 30 minutes at 37ºC prior to plating. Each group of cells was then plated at 10,000 cells / cm^2 on the coated 96-well plates (N=7) and the bottom row was left blank. Cells were allowed to attach for 45 minutes at room temperature (21ºC). The plate was then centrifuged upside-down at 350g to detach weakly attached cells. Preliminary studies had identified 45 minutes and 350g as the time point and speed as optimal for the cell type and conditions described here. Cells were observed under a light microscope and calcein levels were measured using a microplate reader. Figure 4-3 on the following page shows that calcein intensity is reduced on fibronectin coated surfaces in both clones 52 and 53 compared to wild-type MG63 cells, thus indicating that

silencing of the α_5 integrin subunit impaired cell ability to attach to fibronectin. Clone 53 also demonstrated reduction in calcein intensity. Attachment to collagen I surfaces was also low in all cell types due to the relatively short attachment time.

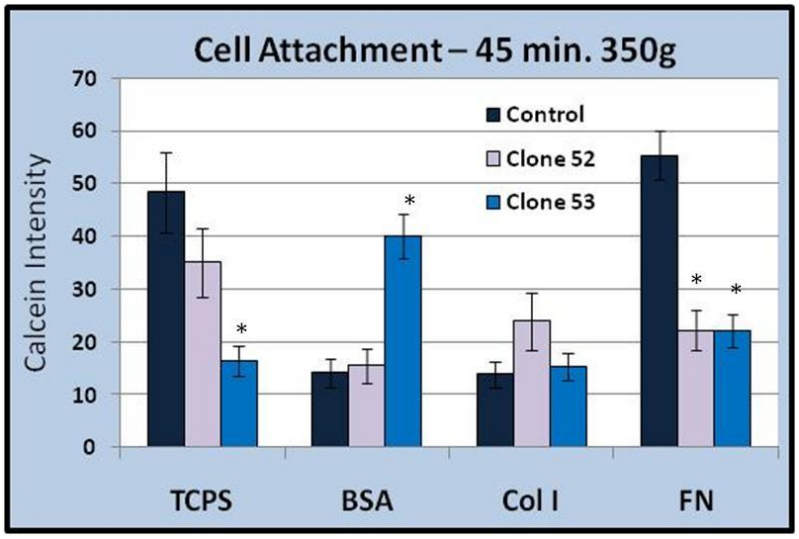

Figure 4-3: Attachment of control MG63 and α_5-shRNA clones 52 and 53 determined by measure of calcein intensity following centrifugation at 350g. The $\alpha_5\beta_1$ integrin binds primarily to fibronectin. Attachment was reduced in both α_5-shRNA clones on fibronectin. * α_5-shRNA clone vs. control.

Calcein readings were corroborated by images taken under light microscopy. Two representative images each for control cells and α_5-shRNA clones 52 and 53 are shown in Figure 4-4 on the following page. The α_5-shRNA clone 52 showed more reduction in attachment than clone 53 based on qualitative visual observation, but calcein intensity measurements were similar. Based on the combined results from qRT-PCR, western blots, and functional testing, α_5-shRNA clone 52 was chosen for use in flow cytometry and testing of the physiological response to surfaces.

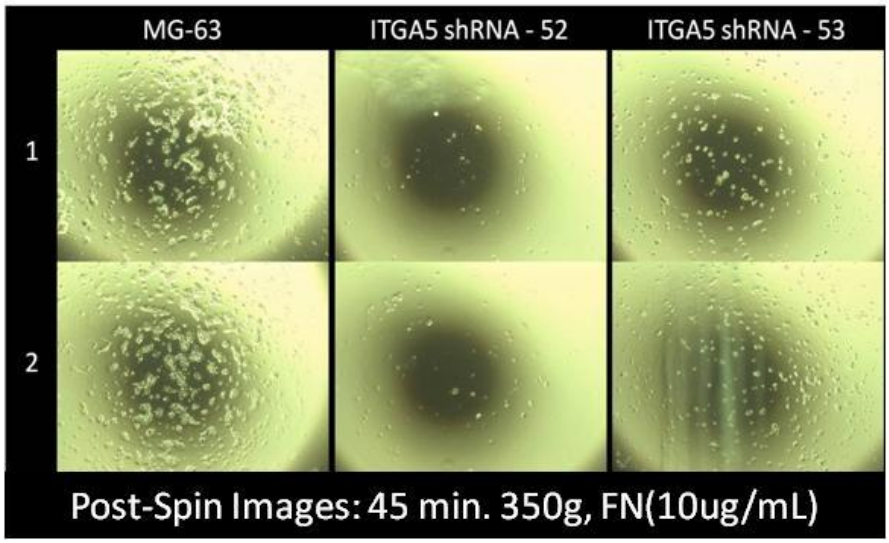

Figure 4-4: Visual images of control MG63 and α_5-shRNA clones 52 and 53 cells on fibronectin-coated surfaces following centrifugation at 350g. The α_5-shRNA clones 52 and 53 showed reduction in attachment based on visual observation, which was confirmed by calcein intensity readings in the previous figure.

Surface Protein Expression: Flow Cytometry

Surface protein expression of integrin α_5 in control MG63 and α_5-silenced cells (clone 52) was analyzed using flow cytometry. In addition, expression levels of other integrins were measured to determine if integrin α_5 silencing leads to increases in expression of other alpha subunits to compensate for loss of integrin α_5. Briefly, we purchased an alpha integrin blocking and IHC kit (Millipore, Temecula, CA) containing integrins α_1 (MAB1973Z-20), α_2 (MAB1950Z-20), α_3 (MAB1952Z-20), α_4 (MAB1698Z-20), α_6 (MAB-1378-20), and α_V (MAB1953Z-20). Secondary antibodies were FITC tagged and selected to bind to the respective IgG isotypes (anti-mouse IgG_1-FITC, anti-rat IgG-FITC, Santa Cruz Biotechnology) of the primary antibodies. IgG-FITC antibodies were used in the absence of primary antibodies as controls. The integrin α_5 antibody (NKI-SAM1-FITC, Santa Cruz Biotechnology) did not require a secondary antibody. Mouse IgG_{2b}-FITC (Santa Cruz Biotechnology) was used as a control for integrin α_5. Flow cytometry was performed on a Becton Dickinson LSR II flow cytometer. Histograms

were compiled from 5,000 counts within threshold side- and forward-scatter values. Positive expression is considered to be FITC values above the top 1% of FITC values in the control cell population. Histograms for the integrin α_5 expression are shown below in Figure 4-5. Integrin α_5 expression is low in both control and α_5-silenced cells. Silencing of α_5 only led to only a very small reduction in surface levels of the α_5 integrin.

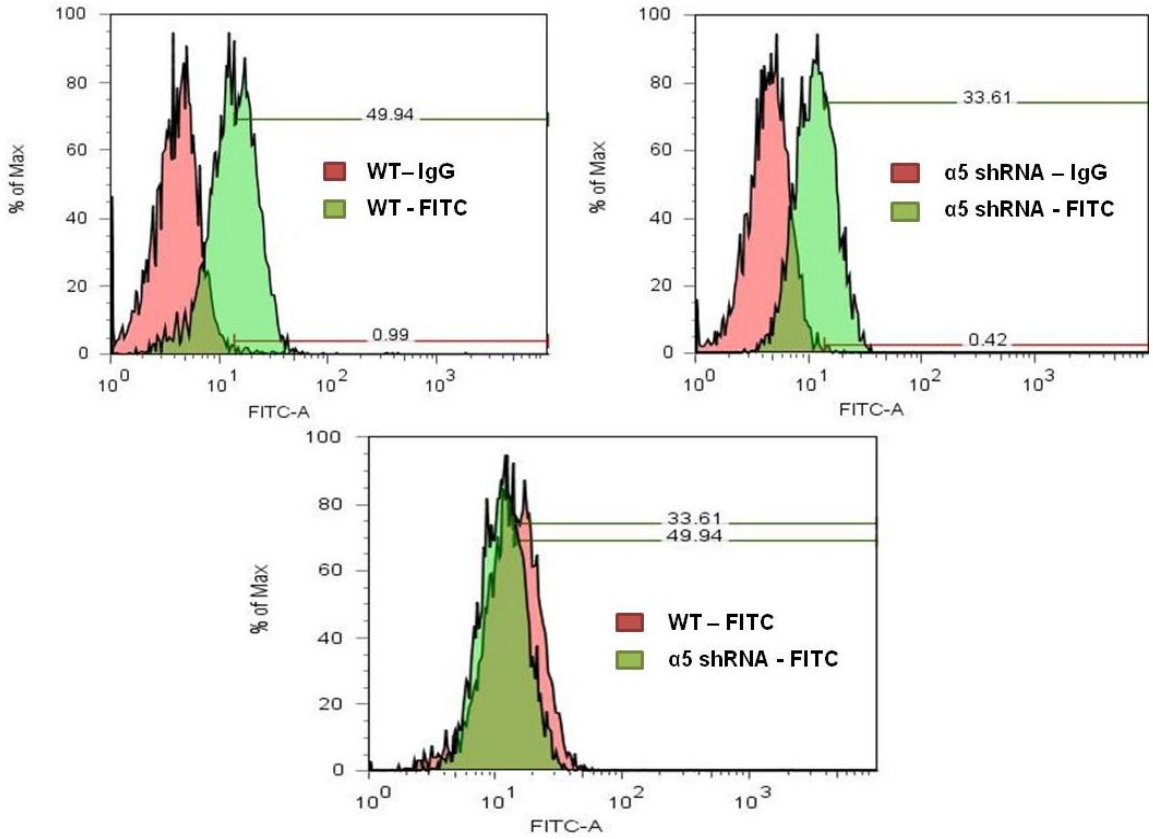

Figure 4-5: Flow cytometry of the α_5 integrin in MG63 and α_5-shRNA clones. Lines represent "percent positive" cells based on the top 1% of wild type IgG labeled cells.

Histograms of the expression of the α_1, α_2, α_3, α_4, α_6, and α_V integrins in MG63 and α_5-silenced cells are shown in Figure 4-6 on the next page. Slight increases in expression of integrins α_3 and α_4 were observed in α_5-silenced cells versus control cells. Integrin α_1 was not detected in either cell type. Integrin α_3 was the most strongly detected integrin in both cell types. Integrin α_2 and α_6 levels were not affected by α_5 silencing. Integrin α_V histograms were broader in wild-type cells than α_5-silenced cells.

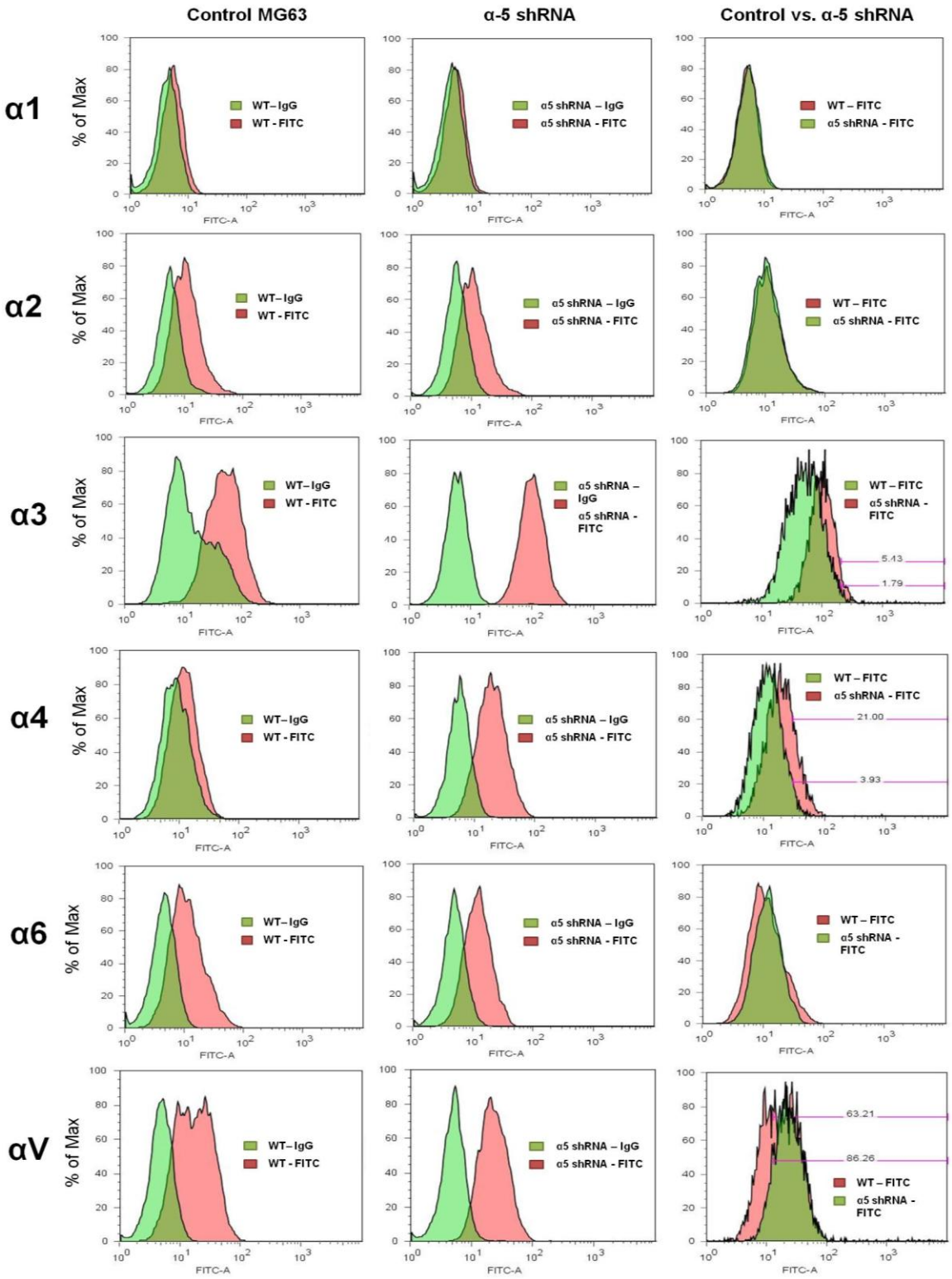

Figure 4-6: Alpha integrin expression in control MG63 and α_5-silenced MG63 cells. Lines represent "percent positive" cells based on the top 1% of wild type IgG labeled cells. Lines and unsmoothed histograms are displayed for α_3, α_4, and α_5 cells where clear differences exist between control and α_5-silenced cells.

Physiological Responses of Osteoblasts MG63 Cells

Wild type MG63 and α_5-silenced MG63 cells (clone 52) were grown to confluence in T-75 tissue culture flasks and then subcultured into 24-well plates on six discs each of TCPS, PT, SLA, or TPS surfaces. When the cells reached confluence on tissue culture plastic, media in all wells were replaced with experimental media containing ethanol vehicle or 10^{-8} M $1\alpha,25(OH)_2D_3$. Cells were cultured an additional 24 h. At that time, cells were harvested and conditioned media were collected. Osteoblast phenotype was assessed by measuring cell number, alkaline phosphatase activity, and levels of osteocalcin, TGF-β1, and OPG according to protocols discussed in chapter 2.

Statistical Analysis

The data presented are from one of two separate sets of experiments, both of which yielded comparable results for surface roughness effects. The effects of $1\alpha,25(OH)_2D_3$ were only tested in one experiment. Each data point represents the mean ± standard error of the mean (SEM) of six independent cultures. Data were analyzed by analysis of variance and statistical significance between groups was determined using Bonferroni's modification of Student's t-test. $p<0.05$ was considered to be significant.

4.3. Results

Assessment of α_5 silencing effectiveness presented in the previous section demonstrated that mRNA levels of α_5 were reduced by nearly 94% (Figure 4-1), protein levels of α_5 were reduced between 60-83% (Figure 4-2), and the functional ability of α_5 to mediate adhesion to fibronectin was reduced by roughly 60% (Figures 4-3 and 4-4) in α_5-silenced cells compared to control MG63 cells. Surface expression levels of integrin α_5 were only slightly reduced (49.9% positive vs. 33.6% positive) in α_5-silenced cells

(Figure 4-5). Expression of other alpha integrin subunits was altered (Figure 4-6), possibly to compensate for lower levels of α_5. Slight increase in expression of integrins α_3 and α_4 was observed in α_5-silenced cells versus control cells; however, expression of no other integrins appeared to be affected. The lack of silencing observed using flow cytometry raises significant concerns in comparing control to α_5-silenced cells.

The physiological response of α_5-silenced cells and control MG63 cells to surface roughness and surface chemistry was similar in both cell types. Treatment with 10^{-8} M $1\alpha,25(OH)_2D_3$ did not affect either control MG63 or α_5-silenced cells. These data are similar to untreated cells and so the $1\alpha,25(OH)_2D_3$ treated groups are not shown. Cell number decreased in both control MG63 and α_5-silenced cells as surface roughness was increased (Figure 4-7). Rough and high surface energy surfaces (modSLA) caused the most reduction in cell number. No differences were observed between control MG63 and α_5-silenced cells.

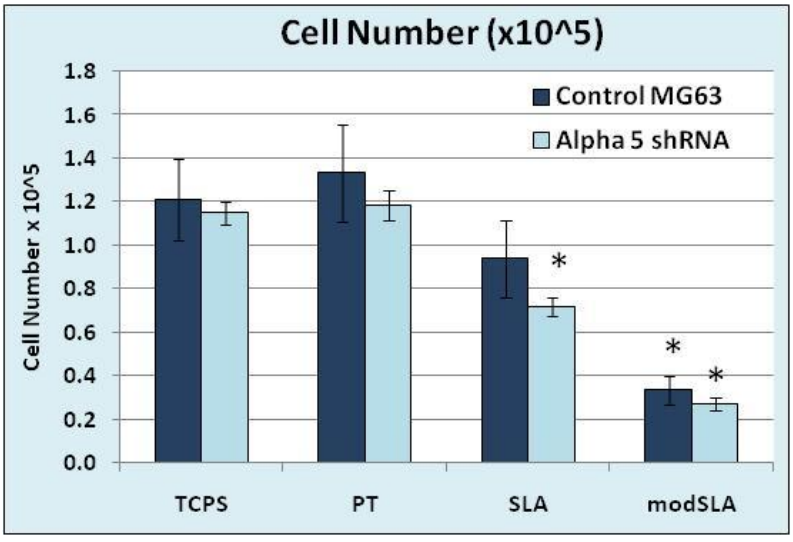

Figure 4-7: Effect of surface roughness on cell number in control MG63 and α_5-silenced cells. * Ti surface vs. Plastic (TCPS); • α_5 shRNA vs. control.

Markers for osteoblast differentiation were not affected by silencing of the α_5 integrin. Alkaline phosphatase activity was slightly increased in control cells on modSLA

surfaces compared to PT and TCPS (Figure 4-8). There was no surface effect in α_5-silenced cells, but alkaline phosphatase activity in α_5-silenced cells was not statistically different from control cells on any surfaces. Osteocalcin levels were also very similar in control MG63 and α_5-silenced cells. Increasing surface roughness and high surface energy increased osteocalcin levels in both control and α_5-silenced cells (Figure 4-9).

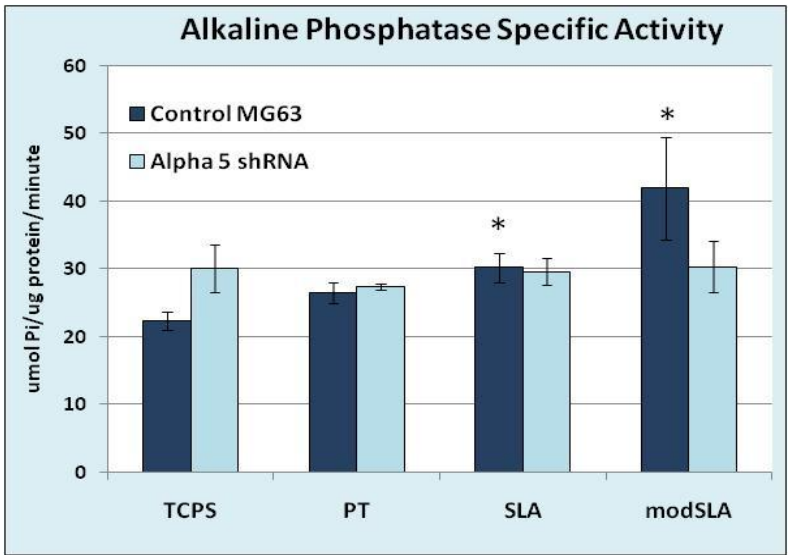

Figure 4-8: Effect of surface roughness on alkaline phosphatase activity in control MG63 and α_5-silenced cells. * Ti surface vs. Plastic (TCPS); • α_5 shRNA vs. control.

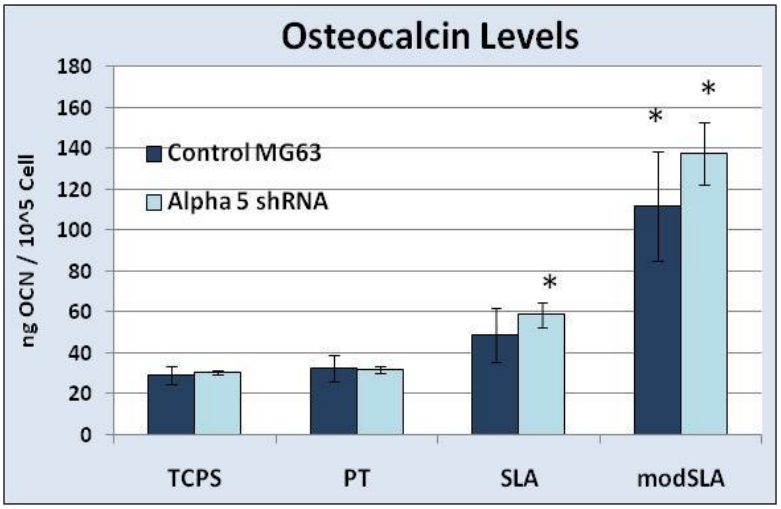

Figure 4-9: Effect of surface roughness and on osteocalcin levels in control MG63 and α_5-silenced cells. * Ti surface vs. Plastic (TCPS); • α_5 shRNA vs. control.

Local factor production was also examined. Active and total TGF-β1 were similar in α_5-silenced versus control MG63 cells. Both active and total TGF-β1 levels increased with increasing surface roughness in control MG63 and α_5-silenced cells (Figure 4-10).

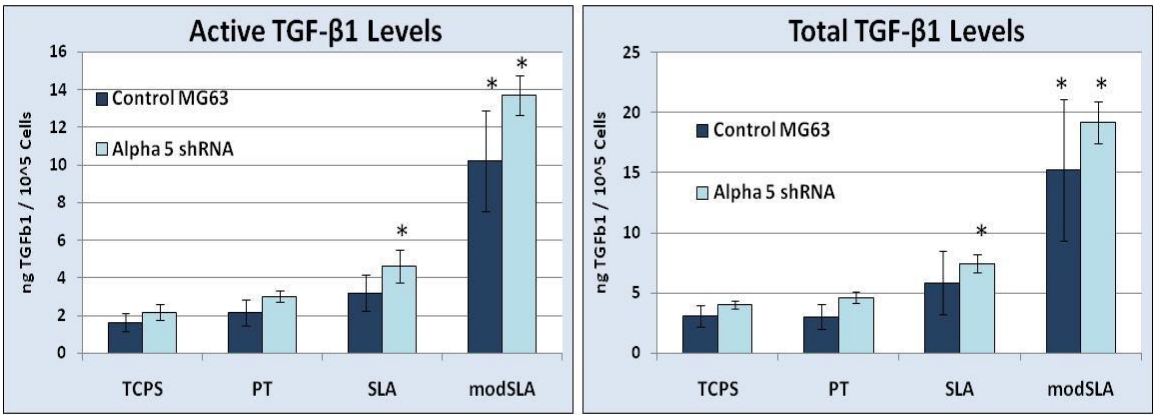

Figure 4-10: Effect of surface roughness on active and total TGF-β1 in control MG63 and α_5-silenced cells. * Ti surface vs. Plastic (TCPS); • α_5 shRNA vs. control.

Osteoprotegerin levels were also not affected by α_5-silencing. Increasing surface roughness and high surface energy increased osteoprotegerin levels in both control and α_5-silenced cells (Figure 4-11).

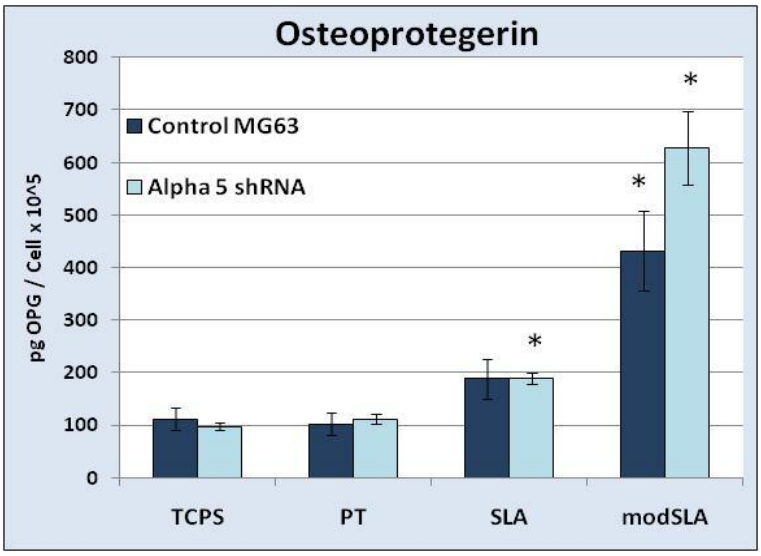

Figure 4-11: Effect of surface roughness on osteoprotegerin levels in control MG63 and α_5-silenced cells. * Ti surface vs. Plastic (TCPS); • α_5 shRNA vs. control.

4.4. Discussion

The results herein demonstrate that α_5-silencing did not lead to large changes in osteoblast response to surface chemistry or topography in MG63 cells; however, the lack of α_5-silencing at the cell surface level (flow cytometry) raises significant concerns regarding the validity of any conclusions made from this data. The α_5-silenced cells had altered TGF-β1 production in response to $1\alpha,25(OH)_2D_3$, but no other measures for osteoblast proliferation, differentiation, or local factor production were altered consistently in α_5-silenced cells. If the α_5 integrin was truly 'knocked down' in this study, then the results suggest that the α_5 integrin is not required in the response of MG63 cells to respond to changes in surface chemistry and surface topography. This result is somewhat surprising since various other studies have suggested that the α_5 integrin is important in promoting proliferation and early differentiation in osteoblasts [162, 163], and that the α_5 integrin is involved in initial attachment of osteoblasts and osteoprogenitor cells to titanium surfaces [37, 146]. Because of the limited silencing achieved at the cell surface level, future α_5-silencing studies will be necessary to confirm these findings.

Previous studies using blocking antibodies against $\alpha_5\beta_1$ showed that cells exhibited decreased proliferation ($[^3H]$-thymidine incorporation), that cell number was slightly decreased on TCPS and PT (but not SLA or TPS) surfaces seven days post-seeding, and that alkaline phosphatase activity was slightly decreased at 7 days post-seeding [178]. The results from the present study did not show differences in cell number, nor did the results show changes in alkaline phosphatase activity due to surface roughness or chemistry. Clear differences exist between the previous study and the current study. Although both studies used MG63 cells, the previous used blocking antibodies, which may be bind and affect integrins not on the surface side of the cell

[167, 168]. Cells also likely differed in the level of confluence since the previous experiment tested cells at particular day post-seeding while the present study used cells harvested at visual confluence of TCPS surfaces.

Since the observed effects of α_5-silencing were minimal in terms of altering osteoblast response to surface roughness and topography, it obviously raises concerns over silencing efficiency. Results showed that transduction of α_5-shRNA led to significantly decreases in α_5 mRNA levels and α_5 protein levels. Surface receptor expression measured by flow cytometry was only slightly reduced. The flow cytometry results are certainly concerning given that integrins function at the cell surface; however, the ability of α_5 to mediate attachment to fibronectin coated surfaces was demonstrated to be reduced in α_5-silenced cells. It is possible that α_5-silencing affects initial attachment in a more pronounced manner because high levels of $\alpha_5\beta_1$ would presumably be required to bind fibronectin coating surfaces. However, low levels of α_5 expression may be sufficient for later $\alpha_5\beta_1$ functions that affect osteoblast phenotype. Insufficient knockdown is often a limitation of shRNA-based studies, although the results here do suggest that α_5 mRNA and protein expression and $\alpha_5\beta_1$-mediated attachment were impaired.

Surface expression levels of integrin subunits α_3 and α_4 were slightly upregulated in α_5-silenced cells. The α_3 integrin subunit was highly expressed on surfaces of control MG63 and α_5-silenced cells. The $\alpha_3\beta_1$ integrin can bind to collagen, fibronectin, and laminin and has been shown to be highly expressed in osteoblasts synthesizing bone [38]. The $\alpha_4\beta_1$ integrin can bind an alternative splice variant of fibronectin. Studies have reported that $\alpha_4\beta_1$ is not found in osteoblasts in vivo [38], but that it is expressed on osteoblasts grown on titanium surfaces [37]. It is possible that MG63 cells may compensate for loss of $\alpha_5\beta_1$ integrins by upregulating expression of $\alpha_3\beta_1$ or $\alpha_4\beta_1$, but

relatively little is known if these integrins play a role in osteoblast function *in vivo* or osteoblast response to surface properties *in vitro*.

Overall, the results suggest that the $\alpha_5\beta_1$ does not regulate the response of MG63 cells to surface roughness and topography, although limited silencing of α_5 as measured by flow cytometry raises doubts onto the validity of this conclusion. Even if α_5-silencing was effective, there are also concerns regarding the use of a single cell line for this study. MG63 cells are an osteosarcoma cell that has characteristics of an immature osteoblast. It is possible that normal human osteoblasts might respond differently since MG63 cells are cancerous and have multiple mutations that affect cell cycle regulation and other functions likely targeted by $\alpha_5\beta_1$ signaling. In addition, other reports have suggested that the $\alpha_5\beta_1$ integrin is important in the differentiation of osteoprogenitor cells to osteoblasts [146, 162, 163]. Silencing of the $\alpha_5\beta_1$ integrin in osteoprogenitor models might alter cell response to surfaces, although that possibility was not tested here. In contrast, studies silencing the $\alpha_2\beta_1$ integrin have shown that it is critical in MG63 cell response to surfaces [102]. Perhaps the $\alpha_5\beta_1$ integrin regulates the attachment and proliferation of osteoprogenitors, but the $\alpha_2\beta_1$ integrin is critical in differentiation of osteoblasts. This possibility will have to be explored in future tests.

4.5. Conclusion

This study suggests that the $\alpha_5\beta_1$ integrin is not required for the response of osteoblast-like MG63 cells to changing surface topography and surface energy; however, limited α_5-silencing at the cell surface level (flow cytometry) makes it impossible to definitively make these conclusions. Markers for osteoblast proliferation, differentiation, and local factor production were similar in control and α_5-silenced MG63 cells on TCPS, PT, SLA, and modSLA surfaces. TGF-β1 levels were slightly increased in α_5-silenced cells treated with $1\alpha,25(OH)_2D_3$ versus control cells treated similarly, but

no other markers showed a consistent effect of α_5-silencing on osteoblast response to 1α,25$(OH)_2D_3$. Overall, these results and the results of β_1-silencing in previous chapter suggest that osteoblast response to surface roughness is not mediated by $\alpha_5\beta_1$, but by other αβ pairs including $\alpha_2\beta_1$. Because of low cell surface level silencing, future tests using α_5-silenced cells are necessary to confirm these results and make definitive conclusion regarding the role of $\alpha_5\beta_1$. In addition, silencing of other osteoblast cell lines is necessary to determine if $\alpha_5\beta_1$ affects differentiation at other stages of osteoblast maturation. Integrin expression certainly changes as osteoblasts mature, although the roles of different integrins as cells progress through differentiation are still being elucidated.

CHAPTER 5:

Osteoblast Response to Peptide Functionalized Implant Surfaces

5.1. Introduction

Recent efforts by bioengineers have focused on the development of biocompatible surfaces engineered to elicit specific biological responses and even mimic native tissue. Methods for controlling the surface chemistry and energy can affect protein adsorption on the surface of an implant; however, the surface in such cases does not interact directly with attached cells, nor is there controllability over the types of cells that attach or the types of signaling cues that are presented to attached cells. Because of these limitations, researchers have turned to the use of biologically modified surfaces using specific proteins, peptides, and attachment chemistries.

Many researchers believe that surfaces functionalized with specific proteins or peptides can aid in the osteointegration of implants by favoring attachment of osteoprogenitor cells and by promoting osteoblastic differentiation and the formation of mineralized bone matrix [5, 42, 179]. Moreover, functionalized surfaces could discourage early attachment of macrophages and fibroblasts that may be associated with chronic inflammation, fibrosis, and eventual implant failure. Peptide functionalization methods can be used in conjunction with rough implant surface topographies already known to enhance osteoblast differentiation *in vitro* and increase implant pull-out strength *in vivo* [5, 31, 69]. The combination of osteoblast-specific ligands with rough surface microtopographies would provide initial cues to enhance early

osteoblast attachment and differentiation, and would also provide a rough surface topography known to sustain long-term osteointegration and implant fixation.

Integrins are cell receptors involved with recognition and cell attachment to the extracellular matrix, and are often the target of bioengineered surfaces [32, 180]. The most common design approach is to attach short oligopeptides, which contain specific amino acid sequences that bind specific cell surface receptors. Oligopeptides are more cost-effective and less susceptible to degradation than full-length proteins [93]. In addition, oligopeptide conformation and presentation of binding domains are easier to control than for full-length proteins. One of the most commonly used oligopeptides is RGD, which is found in various extracellular matrix proteins, including fibronectin, vitronectin, and bone sialoprotein [181-183]. Depending on how it is presented in its native protein, it is recognized by multiple integrins including $\alpha_V\beta_3$. RGD is also recognized by the $\alpha_5\beta_1$ integrin, an integrin that is highly expressed in osteoblasts, although high affinity binding of $\alpha_5\beta_1$ to RGD requires the PHSRN synergy site to maximize activation of osteoblastic signaling pathways [184].

RGD has been extensively shown to enhance osteoblast attachment and proliferation [88, 181, 182] and several studies examining cell behavior on TCPS have shown that RGD enhances differentiation and bone matrix mineralization [42, 185]. However, when osteoblasts were grown on sand-blasted/acid etched titanium substrates (SLA) that were coated with RGD-functionalized PLL-*g*-PEG, osteoblast differentiation was reduced compared to PLL-*g*-PEG coated surfaces [95]. The effect of RGD was to block the stimulatory effect of the PLL-*g*-PEG coating on osteoblast differentiation. These studies suggest that osteoblast differentiation may be promoted by substrates fostering reduced spreading like microtextured titanium and PLL-*g*-PEG [69, 95].

In vivo, RGD has been shown reported to increase osteointegration in some studies [86-88], but not others [89, 90]. The biological activity of RGD is less potent than that of native fibronectin or the fibronectin fragment FNIII7-10 [42, 91]. This suggests that the linear RGD peptide alone may be insufficient for optimal interaction of the cell with its substrate or extracellular matrix. In addition, it is unlikely that any one mimetic is responsible for all responses of osteoblasts on a functionalized surface. It is likely that proliferation and differentiation are regulated through separate pathways, which would necessitate the use of multiple ligands providing different signaling cues. Other peptides have been found to affect osteoblast attachment and phenotype including KRSR (heparan sulfate-binding), GFOGER ($\alpha_2\beta_1$-binding), PHSRN ($\alpha_5\beta_1$-binding), and FHRRIKA (heparan sulfate-binding) [42, 186]. Several recent studies suggest that increased biological activity can be achieved through the combination of binding domains like RGD and GFOGER, RGD and FHRRIKA, or RGD and PHSRN [42, 186-188]. Taken together, these studies suggest that a combination of binding domains presented in the proper spatial configuration is necessary to maximize biological activity [42, 188-190]. These studies also suggest that surfaces can be functionalized with peptides from two or more proteins, thereby driving optimal attachment, proliferation, and differentiation through a combination of signaling cues.

The present study was based on the hypothesis that osteoblast attachment, proliferation and differentiation on a microstructured Ti surface could be enhanced by a biomimetic peptide coating that presented a combination of amino acid motifs that targeted two different signaling pathways: RGD to target integrin signaling and KRSR to target transmembrane proteoglycans. KRSR was designed based on its basic-basic-nonbasic-basic (BBXB) amino acid charge structure that was proposed by Cardin et al. to bind heparan sulfate, a component of transmembrane proteoglycans expressed by

osteoblasts [191]. BBXB patterns are also found in various bone adhesive proteins including fibronectin, vitronectin, bone sialoprotein, thrombospondin, and osteopontin [151, 192]. KRSR was shown to selectively increase osteoblast adhesion to TCPS relative to uncoated controls [192]. In contrast, KSSR, which has a basic-nonbasic-nonbasic-basic (BXXB) amino acid charge structure, did not support attachment. These two peptides differ in only one amino acid residue, demonstrating the specificity of the KRSR effect on attachment. Whether one or both peptides modulate osteoblast differentiation is not known, nor is it known if they have the potential to modify cell response to RGD.

Material surface chemistry affects how cells respond to surfaces via the differential adsorption of proteins and other serum components almost immediately following implantation [31, 193]. Surface chemistry also greatly affects the conformation and presentation of ligands at the surface, making it critical for scientists to consider not just the ligands chosen, but also the underlying surface chemistry and the desired peptide conformation [42]. Many studies have examined the effects of various ligands on polymer surfaces or thin metallic films [179], but these studies may not be relevant to rough titanium surfaces given differences in surface energy, surface charge, and effective surface area. Various methods exist for adsorbing or chemically attaching proteins or peptides directly to titanium surfaces, including direct adsorption or attachment of proteins to adlayers [42, 179]. While methods such as dip-coating peptides directly from solution are simple, peptides can assume denatured conformations on the surface or other adsorbed proteins may act to shield or displace engineered peptides [93, 95, 194]. The use of self-assembled monolayers, which include assembling chemistries based on alkanethiols, silanes, alkanephosphonates,

interpenetrating polymer networks, or PLL-*g*-PEG, can overcome many of these aforementioned limitations [93].

PLL-*g*-PEG was chosen in this study because of its advantages in terms of its ease of functionalization, ease of synthesis, stability on titanium surfaces, and ability to resist protein adsorption [93, 94]. PLL-*g*-PEG is a copolymer that forms a comb-like monolayer on titanium surfaces and acts to limit non-specific protein adsorption. PLL-*g*-PEG self-assembles on titanium as the positively charged PLL backbone adsorbs to the negatively charged titanium oxide surface layer, while the more hydrophilic PEG chains are presented at the surface. PEG has been shown to reduce protein adsorption to less than 5 ng/cm^2 as well as to greatly reduce cell adhesion [94]. The PEG chains can be functionalized at the terminal end, resulting in presentation of the biologically active ligand with minimal interference from adsorbed proteins or other sources [95]. Previous experiments showed that osteoblast attachment and proliferation are markedly reduced on PLL-*g*-PEG coated titanium surfaces compared to control titanium surfaces, although markers for differentiation are significantly increased [95]. PLL-*g*-PEG functionalized with RGD greatly increased osteoblast proliferation, but decreased differentiation compared to PLL-*g*-PEG controls. These results illustrate the need for attaching ligands that not only increase osteoblast attachment and proliferation, but also drive osteoblastic differentiation following the initial stages of implantation.

In the present study, rough titanium surfaces were coated with PLL-*g*-PEG with varying combinations of the peptides RGD and KRSR. It was hypothesized that RGD would support early attachment and proliferation via integrin signaling, and that KRSR would drive osteoblastic differentiation via interaction with transmembrane proteoglycans. These combinations of ligands were intended not just to balance cues for proliferation and differentiation, but also to potentially lead to synergistic effects on

osteoblastic phenotype. Finally, it was hypothesized that the combination of these ligands with rough titanium surfaces would provide a mixture of topographic and biologic cues that would enhance osteointegration.

5.2 Methods

Surfaces

SLA surfaces were manufactured as described extensively in chapter 2. Although SLA is normally hydrophobic with an advancing contact angle of 139.88° [74], the SLA substrates used in the present study were plasma cleaned prior to use and therefore, were hydrophilic.

Synthesis of PLL-g-PEG/PEG-peptide

Unfunctionalized PLL-*g*-PEG was synthesized according to protocols by Huang et al. and Pasche et al. [195, 196]. Briefly, poly(L-lysine) hydrobromide (PLL-HBr; Sigma-Aldrich, Buchs, CH) was dissolved in sodium borate buffer and sterilized with a 0.22 *μ*m filter. Succinimide propionate methoxy-PEG (mPEG-SPA; Nektar Therapeutics, Bradford, UK) at a molecular ratio corresponding to a grafting ratio *g*=3.5 was added and the reaction was allowed to proceed for 6 hours at room temperature. Dialysis was done first against phosphate buffered saline (PBS, pH 7.4) and then deionized water each for 24 hours before the product was freeze-dried and stored at -20 ◦C.

PLL-*g*-PEG/PEG-peptide polymers were synthesized by Martin Schuler according to techniques developed in the Laboratory for Surface Science and Technology at ETH Zurich [151]. Briefly, peptides and N-hydroxysuccinimide polyethylene glycol vinylsulfone (NHS-PEG-VS, Nektar Therapeutics, Bradford, UK)

were reacted for 5 minutes in a salt buffer solution containing 10 mM N-(2-hydroxyethyl)-piperazine-N'-2-ethanesulfonic acid (HEPES; Sigma-Aldrich, Buchs, CH) at pH 8.4. PLL hydrobromide was dissolved in HEPES and added to the reaction. After one hour mPEG-SPA was dissolved in HEPES and added to the final mixture that was stirred for 24 hours at room temperature. 50 µl of *β*-mercaptoethanol (Fluka, Buchs, CH) was used for quenching. Prior to freeze-drying, the mixture was dialyzed against deionized water for 48 hours. Deionized water was changed twice a day. Polymers resulted in a white powder and were kept frozen at -20 ◦C before use. The peptide sequences used were N-acetyl-GCRGYG**RGD**SPG-NH_2, N-acetyl-GCRGYG**KRSR**G-NH_2, and N-acetyl-GCRGYG**K<u>S</u>SR**G-NH_2 (all purchased from JPT Peptide Technologies, GmbH, Berlin, Germany). The Gly-Cys-Arg (GCR) sequence of the linker is critical because reaction occurs between the vinylsulfone group of PEG-VS and the thiol group of the cysteine. The Gly-Tyr-Gly (GYG) sequence is primarily used as a spacer, but is also used to measure grafting efficiency based on the specific hydrogen nuclear magnetic resonance (H-NMR) signal of the tyrosine. Neither peptide alone or in sequence has been reported to have biological activity in osteoblasts.

Several quality control steps were taken to ensure appropriate synthesis and functionalization of each batch of polymer [93, 94]. The grafting ratio *g* and degree of peptide functionalization were measured using H-NMR and polymer adsorption was measured using optical waveguide lightmode spectroscopy (OWLS) [196]. The surface peptide densities were calculated by Dr. Martin Schuler as published elsewhere and are shown in Table 5-1 on the following page [88, 94]. Competitive binding was examined in earlier studies and showed no preferential binding between different PLL-*g*-PEG/PEG-peptide combinations [95]. OWLS was also used to confirm resistance to protein

adsorption of all PLL-*g*-PEG polymer surfaces in full serum, which was estimated at less than 5 ng/cm^2 [94].

Table 5-1: Molecular weight, grafting ratio, peptide functionalization, polymer/protein adsorption and peptide surface density for all polymers and peptides used in creating ligand functionalized surfaces [88, 94].

	PEG	RGD	KRSR	KSSR
Molecular weight PLL [kDa]	15.9	15.9	15.9	15.9
Molecular weight lysine unit [kDa]	0.128	0.128	0.128	0.128
Molecular weight peptide [kDa]	-	1.222	1.197	1.128
Molecular weight entire polymer [kDa]	99.1	69.4	75	63.2
Grafting ratio g [-][a]	3.3	4	9.3	9.7
Peptide-functionalized PEG-chains [%][a]	-	8	76.3	50.1
Polymer adsorption [ng/cm^2][b]	175	175	135	143
Protein adsorption [ng/cm^2][b]	< 5	< 5	< 5	< 5
Peptide surface density ρ_{ps} [pmol/cm^2]	-	5.1	20	15.8

[a]measured with NMR technique.

[b]measured with OWLS technique.

Prior to coating SLA discs, frozen batches of PLL-*g*-PEG and peptide-functionalized PLL-*g*-PEG were warmed to room temperature, dissolved in a salt buffer solution (HEPES 2) containing 10 mM HEPES (MicroSelect, Fluka Chemie GmbH, Buchs, Switzerland) and 150 mM NaCl at pH 7.4 (to reach a final concentration of 0.5 mg/ml), filter sterilized using a 0.22 µm filter (Milian, Basel, CH) and used to prepare the designated peptide surface densities. Solutions containing PLL-*g*-PEG/PEG-peptide were mixed with unfunctionalized PLL-*g*-PEG in order to yield desired surface peptide densities. Multi-peptide PLL-*g*-PEG surfaces were created by mixing solutions containing PLL-*g*-PEG/PEG-RGD and PLL-*g*-PEG/PEG-KRSR in varying peptide concentrations. All SLA discs used in this study were sterilized using an oxygen plasma cleaner (PDC-32G, Harrick Plasma, Ithaca, NY) for 5 minutes under low vacuum and then placed in 24-well plates. Solutions containing the desired polymer-peptide combinations were pipetted immediately onto the appropriate surfaces for 30 minutes followed by two washings in sterile HEPES 2 buffer solution.

Experimental Design

Control groups included **(1)** tissue culture polystyrene (TCPS), **(2)** plasma-cleaned titanium SLA, and **(3)** titanium SLA coated with unfunctionalized PLL-*g*-PEG. These groups are similar to the controls used in a previous study by Tosatti et al. [95], which examined the dose-dependent effects of RGD functionalized to PLL-*g*-PEG. Experimental groups were formed by coating disks with PLL-*g*-PEG solutions containing varying concentrations of RGD, KRSR, and K<u>S</u>SR. Figure 5-1 on the following page shows a schematic of the PLL-*g*-PEG surface and a chart of the RGD/KRSR combinations used in this study and the previous pilot study by Tosatti et al [95].

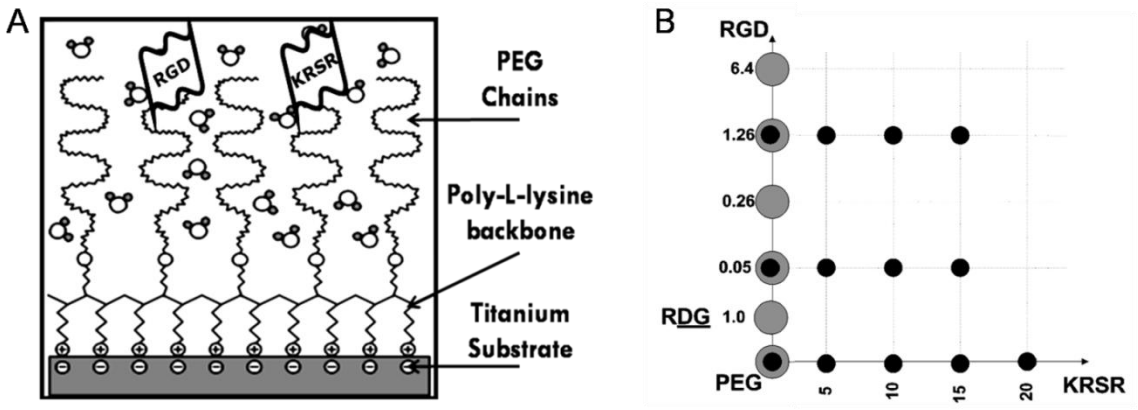

Figure 5-1: A) Schematic of peptide-functionalized poly-L-lysine grafted polyethylene glycol (PLL-*g*-PEG) following self-assembly on the titanium SLA surface. B) Array showing the experimental groups used in this study to evaluate the interaction of RGD and KRSR. The large gray dots represent the previous study by Tosatti et al [95]. Values are measured in pmol/cm^2.

KRSR surface peptide density was varied from 0, 5, 10, 15, to 20 pmol/cm^2, and RGD surface peptide density was varied from 0, 0.05, to 1.26 pmol/cm^2. K<u>S</u>SR surface peptide density was 10 pmol/cm^2 in combination with RGD varied at surface peptide densities of 0, 0.05, and 1.26 pmol/cm^2. The dose-dependent response to RGD was measured with the following experimental groups coated on titanium SLA: **(4)** PLL-*g*-PEG/PEG-RGD(0.05) and **(5)** PLL-*g*-PEG/PEG-RGD(1.26). The dose-dependent response to K<u>S</u>SR was measured with the following experimental groups coated on titanium SLA: **(6)** PLL-*g*-PEG/PEG-K<u>S</u>SR(10), **(7)** PLL-*g*-PEG/PEG-RGD(0.05)/PEG-K<u>S</u>SR(10), and **(8)** PLL-*g*-PEG/PEG-RGD(1.26)/PEG-K<u>S</u>SR(10). The dose-dependent response to KRSR was measured with the following experimental groups coated on titanium SLA: **(9)** PLL-*g*-PEG/PEG-KRSR(5), **(10)** PLL-*g*-PEG/PEG-KRSR(10), **(11)** PLL-*g*-PEG/PEG-KRSR(15), and **(12)** PLL-*g*-PEG/PEG-KRSR(20). Multifunctional peptide experimental groups included: **(13)** PLL-*g*-PEG/PEG-RGD(0.05)/PEG-KRSR(5), **(14)** PLL-*g*-PEG/PEG-RGD(0.05)/PEG-KRSR(10), **(15)** PLL-*g*-PEG/PEG-RGD(0.05)/PEG-KRSR(15), **(16)** PLL-*g*-PEG/PEG-RGD(1.26)/PEG-KRSR(5), **(17)** PLL-

g-PEG/PEG-RGD(1.26)/PEG-KRSR(10), and **(18)** PLL-*g*-PEG/PEG-RGD(1.26)/PEG-KRSR(15). KRSR at a surface peptide density of 20 pmol/cm^2 was near the saturating surface peptide density and therefore could not be combined with RGD.

Cell Culture and Biological Assays

Osteoblast-like MG63 cells were used in this study and are described extensively in chapter 2 and in the literature [69]. Following the coating and washing steps, MG63 cells were plated in 24-well plates at an initial density of 10,000 cells/cm^2. Cells were cultured in 500 µL Dulbecco's modified Eagle medium (DMEM) containing 10% fetal bovine serum (FBS) and 1% penicillin/streptomycin at 37˚C in an atmosphere of 5% CO_2 and 100% humidity. Media were changed at 24 hours and then every 48 hours. All groups were harvested 24 hours after confluence was reached for the cells on TCPS. Media were collected and the cell layers were washed twice with DMEM. Cells were released from the surfaces by two sequential 10 min incubations in 0.25% trypsin at 37˚C to ensure that all cells were removed from the SLA surfaces. The cells were collected to measure cell number, total protein, and alkaline phosphatase specific activity while the media were used to measure osteocalcin, TGF-β1, PGE_2 levels. Methods for these assays are described in chapter 2.

Statistical Analysis

Each data point was calculated from six independent cultures (n=6) and is presented as the mean ± SEM. The data were analyzed using ANOVA and significant differences between groups were determined using Bonferroni's modification of Student's t-test. $P<0.05$. All experiments were repeated to ensure validity of the results.

The data presented are from a representative experiment for each parameter. Observations were consistent among experiments unless otherwise stated, although the absolute baselines value differed between experiments.

5.3 Results

Cell number was regulated by both surface roughness and surface chemistry. Cell number was lower on SLA surfaces compared to TCPS, and was lower on PLL-*g*-PEG surfaces than both SLA and TCPS (Figure 5-2A). Functionalizing PLL-*g*-PEG with 1.26 pmol/cm^2 of RGD increased cell number, restoring it to near-SLA levels (Figure 5-2B). These results were expected and confirm earlier results by Tosatti et al. [95]. KSSR caused a further decrease in cell number compared to SLA and PEGylated surfaces. Cell number was partially restored on KSSR surfaces by the addition of RGD. The effects of KRSR were very weak. KRSR alone had no effect on cell number and only increased cell number at a relatively high peptide surface density of 15 pmol/cm^2 in combination with 1.26 pmol/cm^2 of RGD.

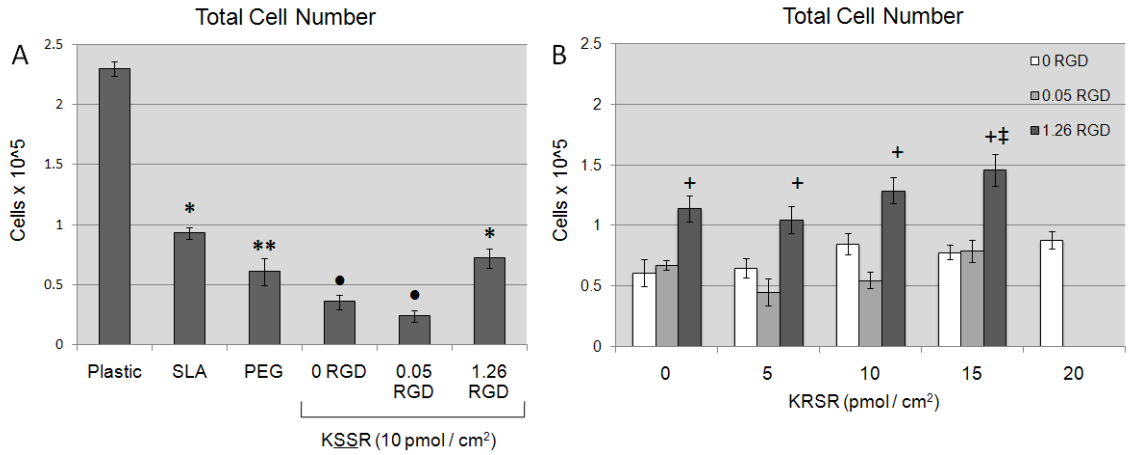

Figure 5-2: A) Comparison of cell number on TCPS, SLA, PLL-*g*-PEG controls, and KSSR surfaces. B) Comparison of cell number on KRSR and RGD surfaces at varying peptide densities. A: *p<0.05, Ti surfaces v. plastic; **p<0.05, PEG surfaces v. SLA • p<0.05, KSSR v. PEG. B: +p<0.05, RGD v. KRSR alone (0 RGD); ‡<0.05, KRSR v. RGD alone (0 KRSR).

Alkaline phosphatase activity was also regulated by surface roughness and surface chemistry. Alkaline phosphatase activity was increased on SLA surfaces coated with PLL-*g*-PEG (Figure 5-3A). KSSR did not affect alkaline phosphatase specific activity. The addition of 0.05 pmol/cm^2 or 1.26 pmol/cm^2 of RGD peptide decreased alkaline phosphatase activity (Figure 5-3B). Addition of KRSR also caused a decrease in alkaline phosphatase activity, though not as strongly as the decrease caused by RGD. The effect of combining RGD and KRSR seemed to be dominated by RGD, since there was weak supplemental inhibition by KRSR even at high peptide densities.

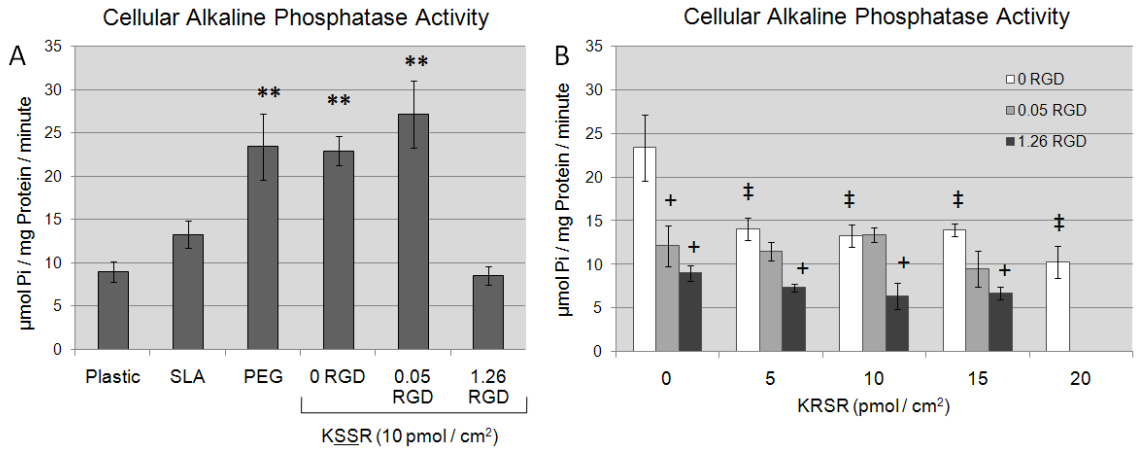

Figure 5-3: A) Comparison of alkaline phosphatase activity on TCPS, SLA, PLL-*g*-PEG controls, and KSSR surfaces. B) Comparison of alkaline phosphatase activity on KRSR and RGD surfaces at varying peptide densities. A: *p<0.05, Ti surfaces v. plastic; **p<0.05, PEG surfaces v. SLA; B: +p<0.05, RGD v. KRSR alone (0 RGD); ‡<0.05, KRSR v. RGD alone (0 KRSR).

Surface roughness and surface energy affected osteoblast differentiation as determined by osteocalcin levels. Osteocalcin levels increased on SLA surfaces and further increased on SLA surfaces coated with PLL-*g*-PEG (Figure 5-4A). The addition of RGD at a concentration of 1.26 pmol/cm^2 significantly decreased levels of osteocalcin. KSSR further increased osteocalcin levels, but this effect was masked with the addition of RGD. KRSR alone did not affect osteocalcin levels (Figure 5-4B). There was a slight

decrease in osteocalcin levels on PLL-*g*-PEG/PEG-RGD(1.26)/PEG-KRSR(15) surfaces, although no other peptide combinations showed any effect of KRSR.

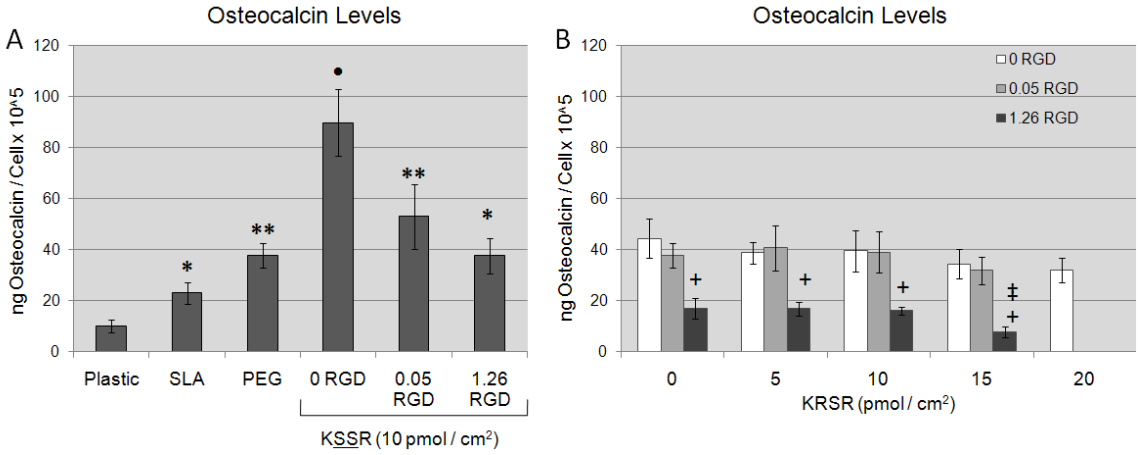

Figure 5-4: A) Comparison of osteocalcin levels on TCPS, SLA, PLL-*g*-PEG controls, and KSSR surfaces. B) Comparison of osteocalcin levels on KRSR and RGD surfaces at varying peptide densities. A: *p<0.05, Ti surfaces v. plastic; **p<0.05, PEG surfaces v. SLA • p<0.05, KSSR v. PEG. B: +p<0.05, RGD v. KRSR alone (0 RGD); ‡<0.05, KRSR v. RGD alone (0 KRSR).

Levels of autocrine and paracrine factors were also affected by changes in surface roughness and surface energy, and by the addition of bioactive peptides. Levels of latent and active TGF-β1 (Figures 5-5A and 5-5C) and PGE_2 (Figure 5-6A) were increased on SLA versus TCPS, and were further increased on PLL-*g*-PEG coated SLA surfaces. Addition of 1.26 pmol/cm^2 RGD to the PLL-*g*-PEG surfaces caused a significant decrease in levels of latent and total TGF-β1 (Figures 5-5A and 5-5C) and PGE_2 (Figure 5-6A), confirming earlier results [95]. Levels of latent and active TGF-β1 on K<u>S</u>SR coated surfaces were not statistically different from PEGylated controls; however, K<u>S</u>SR did increase levels of PGE_2 versus PEGylated and SLA surfaces.

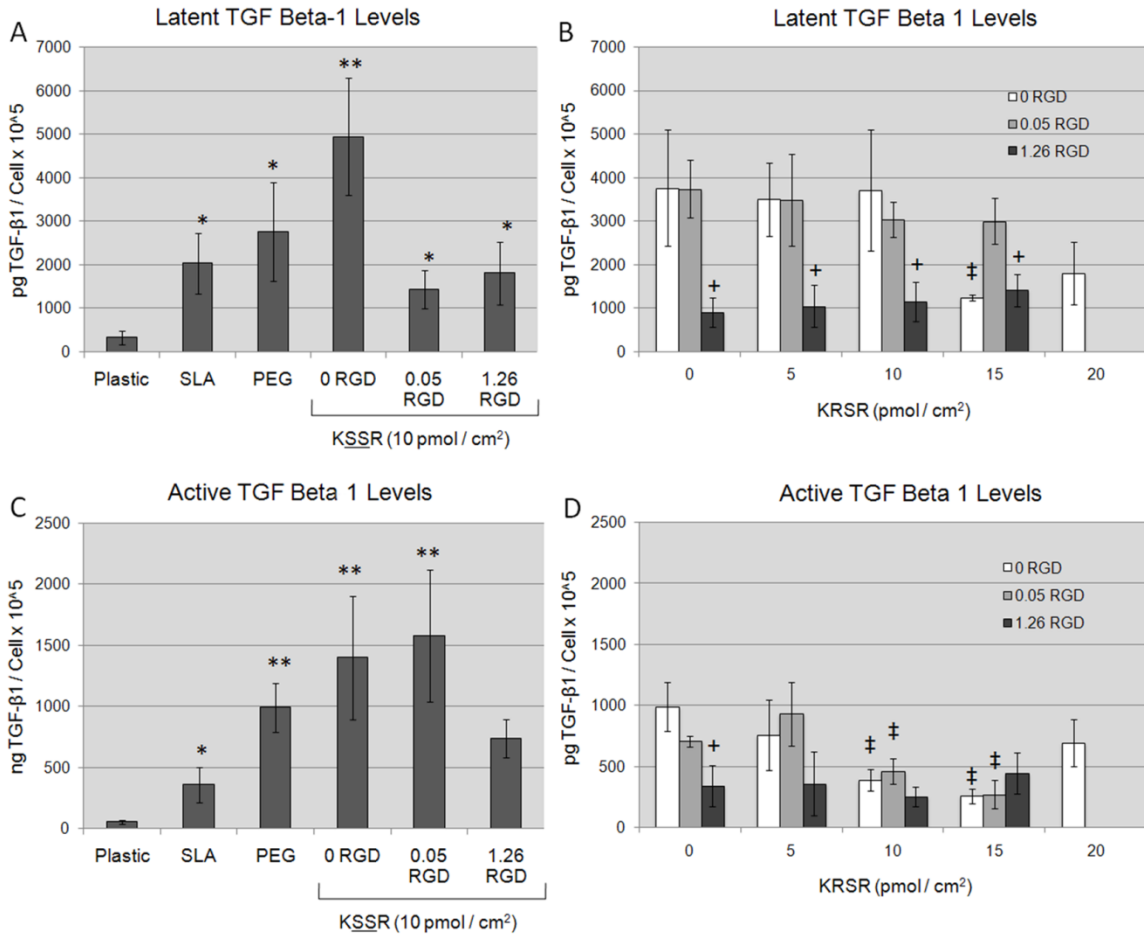

Figure 5-5: Comparison of latent (A) and active (B) TGF-β1 levels on TCPS, SLA, PLL-*g*-PEG controls, and KSSR surfaces. Comparison of latent (C) and active (D) TGF-β1 levels on KRSR and RGD surfaces at varying peptide densities. A: *p<0.05, Ti surfaces v. plastic; **p<0.05, PEG surfaces v. SLA • p<0.05, KSSR v. PEG. B: +p<0.05, RGD v. KRSR alone (0 RGD); ‡<0.05, KRSR v. RGD alone (0 KRSR).

Addition of 15 pmol/cm^2 of KRSR reduced levels of active and latent TGF-β1 (Figures 5-5Band 5-5D) and the addition of 10, 15, or 20 pmol/cm^2 of KRSR reduced levels of PGE_2 (Figure 5-6B). Interaction effects between RGD and KRSR were not observed. RGD appeared to be the dominant cause of reduction in TGF-β1 levels. Combining RGD and KRSR caused further inhibition of PGE_2 levels than using either ligand alone, but this combination did not lead to synergistic responses. Altogether, KRSR was observed to affect osteoblastic phenotype only at high surface peptide densities, and did not affect cell phenotype as strongly as RGD. Surprisingly, KSSR did

promote an osteoblastic phenotype, shown by decreased cell number and increased levels of osteocalcin and PGE_2.

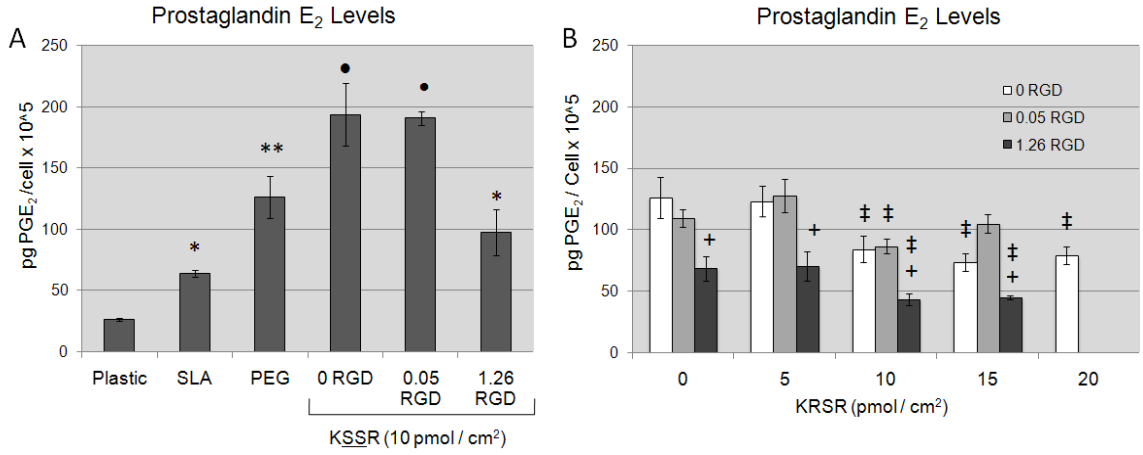

Figure 5-6: A) Comparison of PGE_2 levels on TCPS, SLA, PLL-*g*-PEG controls, and KSSR surfaces. B) Comparison of PGE_2 levels on KRSR and RGD surfaces at varying peptide densities. A: *p<0.05, Ti surfaces v. plastic; **p<0.05, PEG surfaces v. SLA • p<0.05, KSSR v. PEG. B: +p<0.05, RGD v. KRSR alone (0 RGD); ‡<0.05, KRSR v. RGD alone (0 KRSR).

5.4. Discussion

The results of this study support previous observations [95] showing that addition of attachment factors like RGD or KRSR to PEGylated surfaces promotes cell attachment and growth, but inhibits osteoblast differentiation. Addition of RGD to the PLL-*g*-PEG surface increased cell number, but reduced markers for differentiation and local factor production. The effects of KRSR on cell number were weak compared to RGD; the peptide had no effect on cell number or osteocalcin levels, but it did cause a decrease in TGF-β1 and PGE_2 levels at high surface peptide densities. In combination, KRSR and RGD at high surface peptide densities caused a decrease in alkaline phosphatase activity, and levels of osteocalcin, TGF-β1, and PGE_2. Surprisingly, KSSR, which does not promote osteoblast attachment to TCPS [192], caused an increase in osteoblastic differentiation. These results support the hypothesis that attachment and

proliferation are differentially regulated and further support the hypothesis that osteoblast differentiation is favored by reduced cell spreading.

The results from this study regarding the bioactivity of KRSR differ from other reports in the literature. Previous studies had suggested that KRSR increased both attachment and migration of rat calvarial osteoblasts [197]. Although KRSR increased outgrowth of osteoblasts from newborn rat calvarial bone chips after 8 days of incubation time, outgrowth on RGD-coated surfaces was much greater. Others have shown that human bone marrow stromal cells (hBMSCs) are sensitive to KRSR as well [198]. In the present study we did not examine cell attachment per se but the number of cells remaining on the surface at time of harvest. We found that KRSR did not increase cell number by itself, but did increase cell number in combination with RGD. This result confirms earlier observations that RGD supports greater proliferation than KRSR in newborn rat calvarial osteoblasts [197]. However, the previous report did indicate that KRSR increased cell number, while the current study does not. This difference may be due to the cell source or to differences in the state of maturation in the osteoblast lineage. The MG63 cell model we used is a relatively immature osteoblast cell line whereas the Schuler group used primary newborn rat calvarial osteoblasts obtained as outgrowths from bone chips.

The functional role of KRSR may depend in part on its presentation to responding cells, which can depend upon flanking amino acids, ligand presentation, and spatial patterning. RGD and KRSR were presented randomly at the surface and not at defined distances/positions of cell-binding and heparin-binding sites as found in native tissues. Previous studies suggest that proper spatial arrangement of heparin- and integrin-binding domains may enhance cell attachment and response, although these studies did not specifically consider KRSR [199, 200]. Flanking residues may also affect

the biological activity of KRSR. Both attachment and differentiation were increased when hBMSCs were cultured on surfaces functionalized with one of the binding domains in fibroblast growth factor-2 (FGF-2), residues 105-111, which has the sequence Y**KRSR**YT [198]. This sequence matches the XBBXBX pattern proposed by Cardin et al. to be a cell attachment peptide [191], but differs from the ligand used in the present study (GCRGYG**KRSR**G), which supported attachment but not differentiation of MG63 cells. The differences in the two outcomes could arise from using hBMSCs, which are a mixed population that includes osteoprogenitor cells, rather than osteoblast-like MG63 cells. This difference could also be due to using hydrophobic tyrosines to flank the KRSR binding region, compared to the hydrophilic glycines chosen in the present study.

In contrast to KRSR, the KSSR peptide used in the present study did increase osteoblast differentiation. This result could arise from specific biological activity of the KSSR, although no previous studies have suggested that KSSR has such activity. Alternatively, KSSR could promote differentiation by inhibiting cell attachment and spreading. PLL-*g*-PEG surfaces also limit cell attachment and spreading, which could explain why osteoblasts are more differentiated on PLL-*g*-PEG surfaces compared to SLA surfaces. Our results indicate that KRSR plays a weak inhibitory role on the differentiation of osteoblasts on PLL-*g*-PEG surfaces, though the KSSR results do support the possibility of strong biological activity for other ligands based on the XBBXBX design.

Osteoblast attachment is often one of the first properties of a peptide that researchers evaluate; however, this measure may not be a good indicator of whether a peptide will affect differentiation. As observed previously [192], KRSR increased attachment whereas KSSR did not. In contrast, KRSR did not increase osteoblast differentiation. As noted previously by Dee et al., KSSR was not shown to affect

osteoblast attachment, but our results indicate a potent effect on osteoblast differentiation. The additional information provided in the present study demonstrates that attachment and proliferation assessments alone are insufficient for characterizing the response of cells to peptides. Assays for differentiation should be a primary tool for characterizing the biological activity of peptides. Even still, studies examining attachment, proliferation, and differentiation *in vitro* cannot replace the full insight gained from *in vivo* studies since bone formation requires each of these actions at different timepoints. Future work will be needed to evaluate the osteointegrative potential of multifunctional PLL-*g*-PEG systems both *in vitro* and *in vivo*.

Successful multifunctional peptide surfaces should increase the osteoblast population at the implant surface, increase osteoblastic differentiation of attached cells, and discourage the development of inflammation and fibrosis; although the combinations of peptides we used did not achieve this goal with respect to *in vitro* demonstration of enhanced proliferation *and* osteogenic differentiation of attached cells. RGD has been used effectively to increase bone formation in some *in vivo* studies [5, 42, 179], but our results indicate its primary effect is on osteoblast proliferation, not differentiation. This role of RGD may certainly be important *in vivo* though, since increased attachment and proliferation of osteoprogenitors enhances bone formation. In fact, attachment of ligands promoting differentiation might actually be counterproductive to bone formation if they greatly mask the effects of attachment ligands such as RGD. Ligands promoting differentiation may be important at later stages of bone formation after a sufficient osteoblast population has arrived. While the present study suggests that K<u>S</u>SR does stimulate expression of an osteogenic phenotype, this effect was not increased when used in combination with RGD, nor did the combination of RGD and K<u>S</u>SR lead to a state of high proliferation *and* high differentiation. RGD and K<u>S</u>SR appeared to act in

opposite directions on osteoblast phenotype, although it is difficult to reach a definitive conclusion since high RGD levels masked the effect of KSSR. Moreover, the effects of KSSR may be non-specific by preventing cell attachment. Thus, the present study cannot definitively state whether the combination of attachment and differentiation ligands in a multifunctional surface would work synergistically or antagonistically to effect bone formation.

5.5. Conclusions

The present study examined the effects of PLL-*g*-PEG-based multifunctional RGD and KRSR peptide surfaces on the enhancement of markers for both osteoblast proliferation and differentiation. RGD was effective in increasing cell proliferation on the PLL-*g*-PEG surface, but RGD inhibited differentiation present on the PLL-*g*-PEG surface. KSSR promoted an osteogenic phenotype, shown by decreased cell number and increased levels of osteocalcin and PGE_2. Overall, KRSR had a very weak effect on osteoblast phenotype either alone or in combination with RGD. The combination of RGD and KSSR did not lead to a state of high osteoblast proliferation *and* high differentiation, although the non-specific nature of KSSR activity makes it difficult to reach broader conclusions regarding the efficacy of combining RGD with osteogenic peptides in multifunctional surfaces to promote initial osteoblast attachment and subsequent osteoblastic differentiation. Multifunctional peptide surfaces offer the ability to gain better control over the biological cues provided to cells at the surface; however, choosing which combinations of biological cues to provide is a daunting task, but one that will likely be necessary to achieve truly bioactive surfaces.

CHAPTER 6:

VDR Mediates the Osteogenic Effects of 1α,25(OH)$_2$D$_3$

6.1. Introduction

The vitamin D metabolite 1α,25(OH)$_2$D$_3$ is essential for mineral ion homeostasis and the normal development and structure of bone. 1α,25(OH)$_2$D$_3$ regulates bone turnover directly through its effects on osteoblasts, and indirectly through its regulation of blood calcium and phosphorus levels [101]. The biological actions of the 1α,25(OH)$_2$D$_3$ are mediated by VDR and by a membrane associated mechanism involving Pdia3, also known as ERp60, ERp57, and 1,25D$_3$-MARRS [51, 114]. The classical effects of 1α,25(OH)$_2$D$_3$ on osteoblasts are to promote an osteogenic phenotype, as evidenced by a decrease in proliferation and an increase in differentiation [100, 103]; however, the relative roles of the VDR and Pdia3 in 1α,25(OH)$_2$D$_3$ signaling in osteoblasts are only recently being defined. Moreover, increasing evidence suggests that integrin and membrane 1α,25(OH)$_2$D$_3$ signaling may act to modulate activity of VDR or other nuclear receptors in ways that could promote or inhibit differentiation depending on extracellular cues and the state of differentiation of the cell [108, 114, 201].

Understanding the differential contributions of the VDR and Pdia3 in 1α,25(OH)$_2$D$_3$ signaling could aid in the creation of pharmacological analogs of vitamin D for treatment of osteoporosis or for promoting improved osteointegration of orthopaedic implants [111]. Studies examining the response of osteoblasts to surfaces used on titanium dental implants show that when cells are grown on microstructured substrates, they exhibit increased levels of osteocalcin, PGE$_2$, TGF-β1, and OPG, as well as enhanced responsiveness to 1α,25(OH)$_2$D$_3$ in comparison to cells grown on smooth Ti or TCPS surfaces [69, 202]. This increase in expression of a differentiated phenotype due

to the surface microstructure appears to precede the enhanced response to $1\alpha,25(OH)_2D_3$, suggesting that activity of one or both receptors may be sensitive to integrin signaling, which could give rise to synergy between the effects of surface roughness and $1\alpha,25(OH)_2D_3$ on osteoblast differentiation.

It is currently unclear whether VDR and Pdia3 target transcription of different genes, or whether membrane $1\alpha,25(OH)_2D_3$ signaling modulates gene transcription via downstream phosphorylation of VDR. Studies have shown that Pdia3 is required for the $1\alpha,25(OH)_2D_3$-dependent increase in PKC activity and rapid release of intracellular Ca^{++} [113, 115]. Studies using osteoblasts and chondrocytes from VDR deficient mice show that these cells still exhibit $1\alpha,25(OH)_2D_3$-dependent rapid activation of PKC and release of intracellular Ca^{++} despite the lack a functional VDR [112]. Moreover, $1\alpha,25(OH)_2D_3$ treatment has been shown in chondrocytes to increase ERK1/2 and other MAP kinases known to broadly affect gene transcription [120]. While osteocalcin and osteopontin expression are known to be regulated by $1\alpha,25(OH)_2D_3$ via VDR binding to specific VDREs [101, 203], other genes upregulated by $1\alpha,25(OH)_2D_3$ lack such sites. For example, PGE_2 production is increased by $1\alpha,25(OH)_2D_3$-induced rapid production of diacylglycerol and arachidonic acid (AA) and the cyclooxygenase-mediated conversion of AA to PGE_2 [204]. These results demonstrate that the rapid, non-genomic events of $1\alpha,25(OH)_2D_3$ could occur independently of the VDR; however, there are still questions regarding how VDR and Pdia3 dependent $1\alpha,25(OH)_2D_3$ signaling pathways differentially affect osteoblast phenotype. Furthermore, the enhanced response of osteoblasts to $1\alpha,25(OH)_2D_3$ on roughened Ti surfaces may involve crosstalk between integrins and $1\alpha,25(OH)_2D_3$ signaling pathways, although it is not clear whether this response depends on VDR or Pdia3.

To address these questions, we took advantage of VDR(-/-) mice developed by Li et al [121]. These mice develop hypocalcemia, hypophosphatemia, hyperparathyroidism, rickets, osteomalacia, and alopecia. When VDR(-/-) mice are placed on a rescue diet containing high calcium, phosphate, and lactose, they exhibit normal mineral ion homeostasis and do not exhibit signs of rickets, thus demonstrating the critical systemic role of VDR in calcium and phosphate regulation [205, 206]. Still, studies using VDR deficient mice have supported the importance of the direct actions of $1\alpha,25(OH)_2D_3$ on osteoblast phenotype and bone morphology. Overexpression of VDR in mature osteoblasts leads to increases in bone formation, mineralization rate, and overall bone strength [207]. VDR(-/-) mice on a "rescue diet" have decreased trabecular bone volume, mineral apposition rate, alkaline phosphatase staining, and cbfaI/Runx2 expression compared to wild-type mice, indicating a role of $1\alpha,25(OH)_2D_3$ and VDR in promoting osteogenesis [206]. However, Sooy et al. suggest that VDR deficient osteoblasts have enhanced osteoblast activity *in vitro* due to a role of $1\alpha,25(OH)_2D_3$ in inhibiting osteogenesis [208]. Taken together, studies using VDR(-/-) mice suggest that while the most critical and best understood role of $1\alpha,25(OH)_2D_3$ is on mineral ion homeostasis, $1\alpha,25(OH)_2D_3$ also plays a complex role in controlling bone turnover via its direct effects on osteoblasts through VDR and Pdia3.

The present study uses VDR(+/+) and VDR(-/-) calvarial osteoblasts to examine whether VDR is required to mediate the osteogenic effects of $1\alpha,25(OH)_2D_3$, or whether VDR independent signaling, presumably through Pdia3, can lead to changes in osteoblastic phenotype. In addition, this study examines whether VDR is essential for synergistic signaling of $1\alpha,25(OH)_2D_3$ and integrins, or whether $1\alpha,25(OH)_2D_3$ can modify osteoblast response to increasing surface roughness in the absence of VDR.

6.2. Materials and Methods

Vitamin D Receptor Deficient Osteoblasts

The study used cavarial osteoblasts from knockout VDR(-/-) mice and "wild-type" VDR(+/+) littermates. Complete methods are described in Chapter 2.

Titanium Surfaces

Institut Straumann AG (Basel, Switzerland) supplied the PT, SLA, and TPS titanium disks used in this study. Surfaces were manufactured and characterized as described in chapter 2.

Cell Culture

Cells were cultured in DMEM plus 10% FBS and 1% penicillin/streptomycin. The culture media used in these studies contains 10% FBS. Because the FBS was not charcoal stirred it contained low levels of $1\alpha,25(OH)_2D_3$; thus, the culture media had 10^{-12} to 10^{-13} M $1\alpha,25(OH)_2D_3$. Initial experiments compared baseline production of osteocalcin in VDR(+/+) cells and VDR(-/-) osteoblasts. For these experiments second passage cells were grown to confluence on TCPS and osteocalcin in the media was assayed. To assess the effects of growth on microstructured titanium, VDR(+/+) or VDR(-/-) osteoblasts were plated at a density of 10,000 cells/cm^2 into 24-well plates containing 6 wells each of TCPS, PT, SLA, and TPS surfaces.

Physiological Responses of VDR(-/-) and VDR(+/+) Osteoblasts

At confluence, which was determined from cells on TCPS surfaces, each group was treated with 10^{-8} M $1\alpha,25(OH)_2D_3$ (Biomol, Plymouth Meeting, PA) or vehicle control

(ethanol) for 24 hours. At harvest, experimental media were collected and the cell layers were washed twice with DMEM. Osteoblasts were removed using two subsequent treatments for 10 minutes with 0.25% trypsin. Osteoblast phenotype was assessed by measuring cell number, total protein, alkaline phosphatase activity, and media levels of osteocalcin, TGF-β1, OPG, and PEG_2 according to protocols discussed in chapter 2.

Expression of VDR and Pdia3 in MG63 Cells

Expression of Pdia and VDR was measured in MG63 cells plated on TCPS, PT, SLA, and TPS surfaces. The purpose of this experiment was to determine if surface roughness directly affected expression of either Pdia3 or VDR. Cells were grown on four discs each of TCPS, PT, and SLA. At confluence, cells were treated with $1\alpha,25(OH)_2D_3$ for 24 hours and then harvested for mRNA using an RNeasy™ kit (Qiagen, Germantown, MD) according to the manufacturer's protocols. Quantitative RT-PCR was performed on an i-cycler™ (Bio-Rad Laboratories, Hercules, CA) using software i-cycler iQ™, version 3.0a. PCRs were carried out in a total volume of 25 µl in PCR master mix containing 12.5 µl SYBR® green, 200 ng each of sense and antisense primer, 25mM $MgCl_2$, and 3 µl of the reverse transcription product. The volume was adjusted with DEPC-treated water. The primers used were:

VDR	F	CAT CAG AAG GAG AAG GAA GG
	R	TGA GGC AAC AGC ATT ATC C
GapDH	F	GCT CTC CAG AAC ATC ATC C
	R	TGC TTC ACC ACC TTC TTG
PDIA3	F	GCC TAC CCT GGT GAT TAG AAC
	R	GAG CAG AGA ACA GTC CTT GG

The results from this preliminary study shown in the appendix in Figure A-3 demonstrate that surface roughness does not alter expression of VDR. Expression of Pdia3 was slightly decreased on SLA and TPS surfaces. Addition of 1α,25$(OH)_2D_3$ had no effect on expression of either VDR or Pdia3.

Gene Expression Changes in VDR(-/-) and VDR(+/+) Osteoblasts

Expression of the genes for GapDH (Control), Pdia3, integrin beta 1, integrin alpha 2, integrin alpha 5, caveolin-1, Runx2, and integrin beta 3 were measured in VDR(+/+) and VDR(-/-) osteoblasts. Cells were grown on six discs each of TCPS, PT, and SLA surfaces in a similar manner as described above. In addition, a separate set of experiments was grown on TCPS surfaces of 6-well plates and was treated at confluence for 24 hours with 1α,25$(OH)_2D_3$. Cells were harvested for mRNA using an RNeasy™ kit (Qiagen, Germantown, MD) according to the manufacturer's protocols. Following RNA isolation, RNA was quantified using a Nanodrop™ spectrophotometer (Thermo Scientific, Wilmington, DE). All samples were normalized to 1ug RNA/uL with diethylpyrocarbonate (DEPC)-treated water. Gene expression was assessed by qRT-PCR using a QuantiFast™ SYBR Green RT-PCR Kit (Qiagen) according to manufacturer's protocols. Briefly, 12.5 µL SYBR green master mix, 1 µL (1 µmol) of each primer, 0.25 µL RT mix, 1 µg mRNA, and DEPC-treated water were combined for a total volume of 25 µL. All reactions were carried out for 40 cycles on an i-cycler™ (Bio-Rad Laboratories, Hercules, CA) using software i-cycler iQ™, version 3.0a. The primers and annealing temperatures used in the experiments were:

CAV-1	R	ACA GTG AAG GTG GTG AAG C	54.2
	F	GAT TGA CTT TGA AGA TGT GAT TGC	

ITGA2	R	GGT CAA AGG CTT GTT TAG G	57.1
	F	ACT GTT CAA GGA GGA GAC	
ITGA5	R	AAG TTC CCT GGG TGT CTG	57.1
	F	ATC TGT GTG CCT GAC CTG	
ITGB1	R	TCC TCC TCA TTT CAT TCA TC	57.1
	F	ATT ACT CAG ATC CAA CCA C	
PDIA3	R	TTC ATA CTC AGG GGC AAG C	57.9
	F	CGA TGT GTT GGA ACT GAC G	
RUNX2	R	GAT AGG ATG CTG ACG AAG TAC C	56.0
	F	CCG CCA CCA CTC ACT ACC	
GAPDH	R	TCT CGC TCC TGG AAG ATG G	55.0
	F	TTC AAC GGC ACA GTC AAG G	
ITGB3	R	GCT CAC CGT GTC TCC AAT C	57.1
	F	AAT GCC ACC TGC CTC AAC	

Unfortunately, the data from qRT-PCR for VDR(+/+) and VDR(-/-) osteoblasts was not consistent between experiments for many of the genes tested. In addition, the yield of RNA harvested on SLA surfaces was low in all groups. Levels of GapDH (control) were also lower on SLA surfaces despite adjustment based on RNA measurements. Because of the low levels of RNA and inconsistency between experiments, it is difficult to draw definitive conclusion from the data. The data is shown in the appendix in Figures A-1, A-2, A-3, and A-4. The pooled data from all of the VDR(+/+) and VDR(-/-) experiments are shown in Tables A-1 and A-2.

Statistical Analysis

Data for each experiment were calculated from six independent cultures (n=6) per group and presented as the mean ± standard error of the mean (SEM). Data were analyzed via analysis of variance (AVONA) and statistical difference between groups determined using Bonferroni's modification of the Student's t-test. Values with $p<0.05$ were considered significant. Each experiment was performed twice to ensure the consistency of the results. The data presented are from one of two representative experiments for each end point assay.

6.3. Results

The levels of mRNA expression for the genes Pdia3 and VDR were measured in MG63 cells using quantitative PCR. The results show no statistical difference in either Pdia3 or VDR expression in response to changing surface roughness or treatment with $1\alpha25(OH)_2D_3$. There was a reduction in Pdia3 expression on some of the titanium surfaces versus TCPS (Figure 6-1). These results indicate that surface roughness and $1\alpha25(OH)_2D_3$ do not directly affect mRNA levels of either $1\alpha25(OH)_2D_3$ receptor in osteoblast-like MG63 cells.

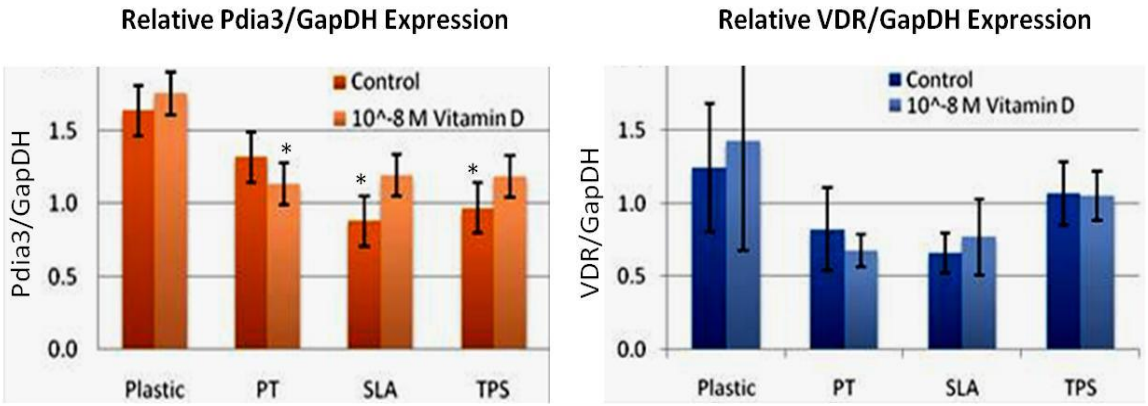

Figure 6-1: Pdia3 and VDR mRNA expression in osteoblast-like MG63 cells. * Titanium Surface vs. TCPS. Significant if $p < 0.05$.

At confluence on TCPS, VDR(-/-) osteoblasts produced 10-fold higher levels of osteocalcin than VDR(+/+) osteoblasts (Figure 6-4). Repeats of the experiment did not show significant differences in baseline levels osteocalcin or other factors (Figure 6-2), although alkaline phosphatase activity was significantly reduced in VDR(-/-) osteoblasts compared to VDR(+/+) osteoblasts. These differences may be due to experimental variance because of the nature of harvesting osteoblasts from separate batches of mice. VDR (-/-) osteoblasts did not respond to $1\alpha25(OH)_2D_3$, but neither did VDR(+/+) osteoblasts in this particular repeat. All other experiments showed a strong effect of $1\alpha25(OH)_2D_3$ on osteoblast phenotype.

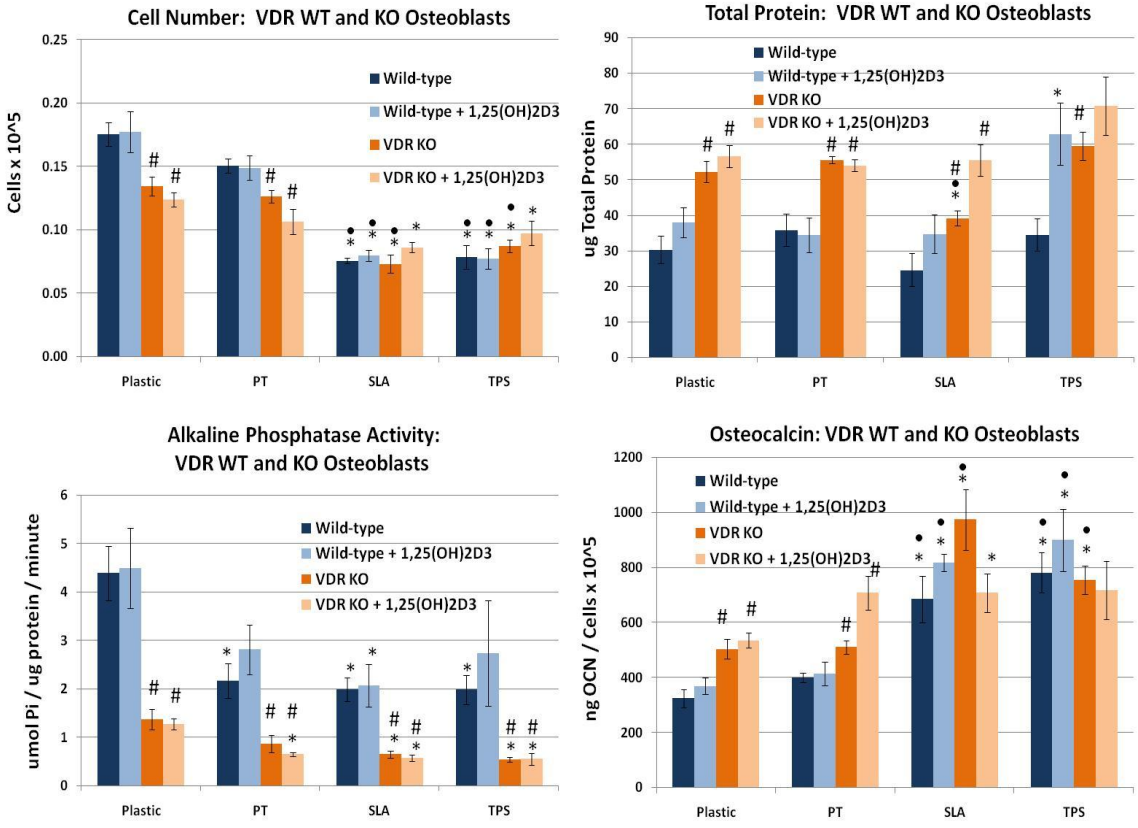

Figure 6-2: Baseline comparison of VDR (+/+) and 'Rescued' VDR (-/-) osteoblasts on TCPS, PT, SLA, and TPS surfaces. Statistics: * Surface vs. TCPS; • SLA/TPS vs. PT; # WT vs. KO. Significant if $p < 0.05$.

When the cells were grown on titanium substrates, VDR(-/-) and VDR(+/+) cells behaved in a similar manner. There was a decrease in cell number on all titanium substrates compared to TCPS with the greatest reduction in cultures grown on SLA and TPS (Figure 6-1). Both VDR(+/+) and VDR(-/-) osteoblasts displayed a similar reduction in cell number due to surface roughness, although cell number in VDR(-/-) osteoblasts was lower on all surfaces compared to VDR(+/+) osteoblasts.

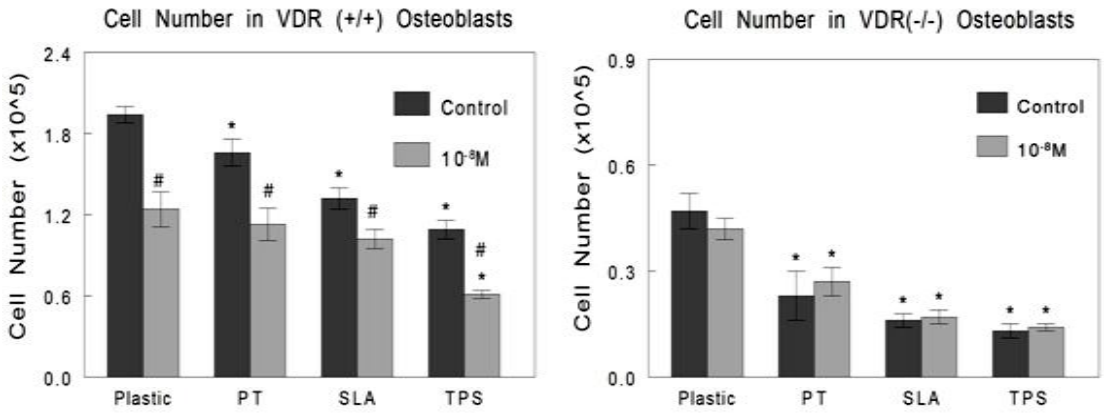

Figure 6-3: Comparison of cell number in VDR(+/+) and VDR(-/-) osteoblasts.

Measures for osteoblast differentiation show a loss in VDR(-/-) osteoblasts of responses typically observed following treatment with 1α,25$(OH)_2D_3$. VDR(+/+) and VDR(-/-) cells both exhibited increases in alkaline phosphatase specific activity on SLA and TPS substrates (Figure 6-2); however, VDR(+/+) osteoblasts treated with 1α,25$(OH)_2D_3$ exhibited an increase in alkaline phosphatase specific activity whereas no effects of 1α,25$(OH)_2D_3$ were evident in VDR(-/-) cells.

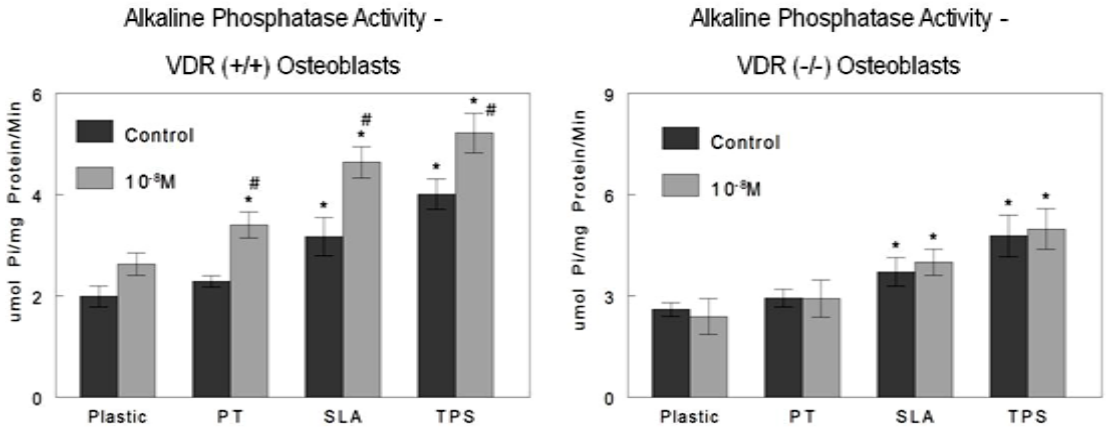

Figure 6-4: Comparison of alkaline phosphatase specific activity in VDR(+/+) and VDR(-/-) osteoblasts.

Osteocalcin levels were also increased in the media from VDR(+/+) and VDR(-/-) osteoblasts grown on SLA and TPS surfaces (Figure 6-3). Interestingly, osteocalcin levels were much higher on all surfaces in VDR(-/-) osteoblasts. 1α,25$(OH)_2D_3$ caused an increase in osteocalcin levels in VDR(+/+) osteoblasts that was synergistic with the effect of the microstructured surface on SLA and TPS. However, 1α,25$(OH)_2D_3$ did not cause any increase in osteocalcin levels in VDR(-/-) osteoblasts on any surfaces.

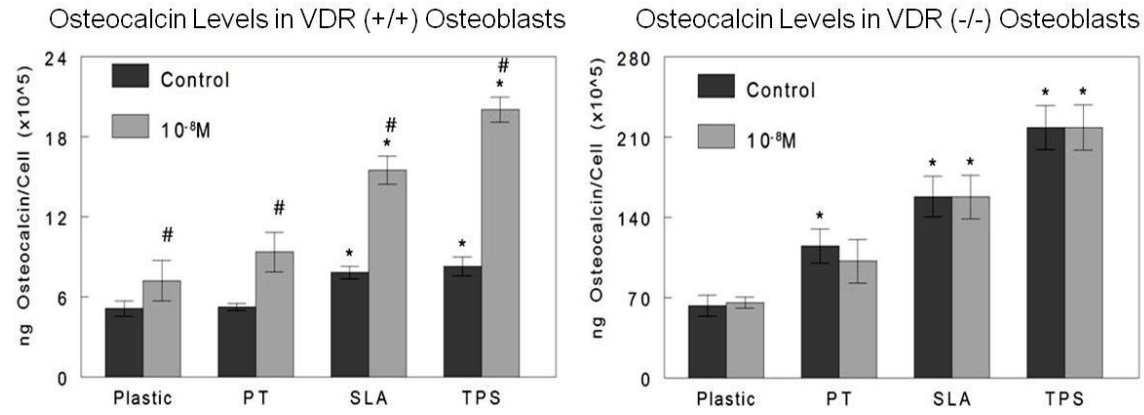

Figure 6-5: Comparison of osteocalcin levels in VDR(+/+) and VDR(-/-) osteoblasts.

Local factor production was also increased by surface roughness and 1α,25$(OH)_2D_3$ treatment in VDR(+/+) osteoblasts. Levels of PGE_2 increased in response

to increasing surface roughness in both VDR(+/+) and VDR(-/-) osteoblasts (Figure 6-4). Addition of 1α,25$(OH)_2D_3$ caused an increase in levels of PGE_2 in VDR(+/+) osteoblasts, but 1α,25$(OH)_2D_3$ did not affect PGE_2 levels in VDR(-/-) regardless of the surface.

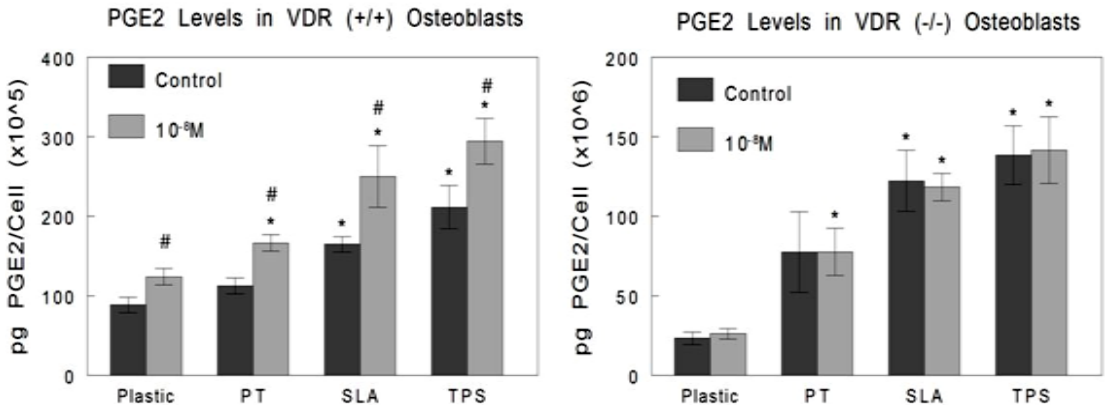

Figure 6-6: Comparison of PGE_2 levels in VDR(+/+) and VDR(-/-) osteoblasts.

Production of latent and active TGF-β1 was modulated in a similar manner as PGE_2. Both VDR(+/+) and VDR(-/-) osteoblasts had greater amounts of latent and active growth factor in their conditioned media when grown on titanium substrates compared to TCPS (Figure 6-5) with the greatest levels on TPS. Interestingly, TGF-β1 levels were higher on all surfaces in VDR(-/-) osteoblasts compared to VDR(+/+) osteoblasts. In VDR(+/+) osteoblasts 1α,25$(OH)_2D_3$ increased levels of active and latent TGF-β1 on nearly all substrates. In contrast, in VDR(-/-) osteoblasts 1α,25$(OH)_2D_3$ did not increase levels of a active or latent TGF-β1 on any substrates.

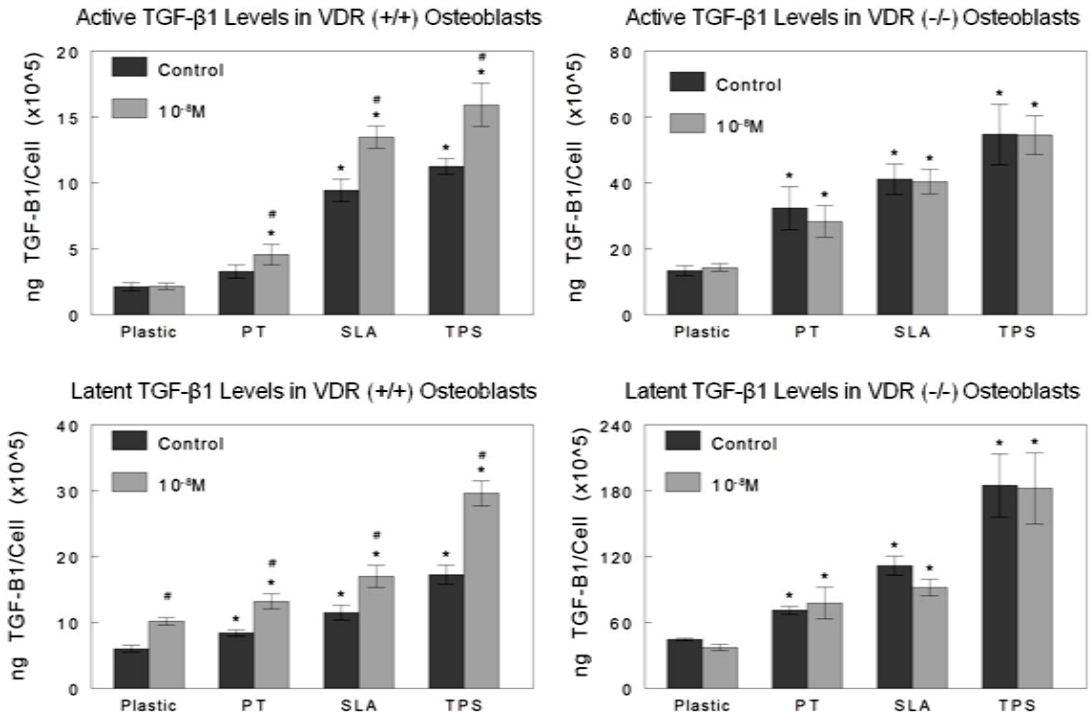

Figure 6-7: Comparison of active (Top) and latent (bottom) TGF-β1 levels in VDR(+/+) and VDR(-/-) osteoblasts.

6.4. Discussion

These results clearly demonstrate that VDR is required for the effects of 1α,25$(OH)_2D_3$ on osteoblast phenotype. In osteoblasts lacking a functional VDR, 1α,25$(OH)_2D_3$ did not alter cell proliferation, osteogenic differentiation, or levels of osteogenic paracrine factors. Previous studies have shown that VDR does not mediate the rapid effects of 1α,25$(OH)_2D_3$ on PKC activity and intracellular calcium release [177]. Despite the fact that these membrane pathways remain intact, 1α,25$(OH)_2D_3$ is not able to alter osteoblast phenotype in the absence of VDR. This result corroborates *in vivo* results from other groups that have suggested a similar role for VDR in promoting an osteogenic phenotype. *Gardiner et al.* showed that overexpression of VDR leads to increases in bone formation and mineralization rate [207], while *Panda et al.* showed that VDR(-/-) mice on a "rescue diet" have impaired bone formation and mineralization

[206]. These results support the conclusion that the directs effects of 1α,25$(OH)_2D_3$ on osteoblast phenotype are mediated by VDR and lead to increased osteogenic phenotype both *in vitro* and *in vivo*.

While this study shows that 1α,25$(OH)_2D_3$ does not directly alter osteoblast phenotype via VDR independent pathways, it does not rule out a role for Pdia3 in 1α,25$(OH)_2D_3$ signaling in osteoblasts. Pdia3 is highly expressed in osteoblasts and is found in the cell membrane, caveolae, and matrix vesicles [113, 117]. It is still hypothesized that Pdia3-mediated 1α,25$(OH)_2D_3$ signaling could modulate VDR transcriptional activity through action of PKC, MAPK, casein kinase II, or $Ca2^{++}$/calmodulin-dependent kinase IV (CaMKIV)kinases [105, 123, 124], although direct evidence of such action has not been established. Such a role for rapid 1α,25$(OH)_2D_3$ signaling would require an intact VDR and so was not observed in the present study.

Rapid 1α,25$(OH)_2D_3$ signaling may also be important in the matrix mineralization, but these actions were not tested in the present study. Previous studies by *Boyan et al* using chondrocytes showed that 1α,25$(OH)_2D_3$ acts through Pdia3 to release lysophospholipids that destabilize matrix vesicles [122]. It is theorized that these vesicles could then release stored calcium, phosphate, matrix metalloproteinases, and a myriad of proteins that may be involved in matrix mineralization. This theory is supported by evidence that caveolin-1 and Pdia3 are present both in caveolae and matrix vesicles in chondrocytes and osteoblasts [122]. A recent study by *Sawada et al.* demonstrated that overexpression of caveolin-1 leads to a large increase in osteoblast matrix mineralization [134]. This possibility would mean that both VDR and Pdia3 are important in the formation and turnover of bone in response to 1α,25$(OH)_2D_3$.

The results in this study demonstrate that absence of VDR does not alter the effects of increasing surface roughness on osteoblast phenotype, although VDR is

required for any enhanced osteoblastic differentiation due to the combination of 1α,25$(OH)_2D_3$ and increasing surface roughness. Differences in the response to surfaces alone in VDR(+/+) and VDR(-/-) osteoblasts might have been expected since basal levels (10^{-13} M) of 1α,25$(OH)_2D_3$ exist in non-treated media and since previous work by *Sooy et al.* that showed VDR(-/-) osteoblasts had enhanced osteoblastic activity versus VDR(+/+) osteoblasts [208]. 1α,25$(OH)_2D_3$ is also known to act through VDR to repress Runx2 expression, although it promotes other osteoblast genes including osteocalcin and osteopontin [107, 123]. Still, the results herein demonstrate that the effects of surface roughness alone are consistent in VDR(+/+) and VDR(-/-) osteoblasts, which means that baseline levels of signaling in the VDR-1α,25$(OH)_2D_3$ system do not alter osteoblast phenotype.

The results suggest that the synergistic response of osteoblasts to surface roughness and 1α,25$(OH)_2D_3$ is controlled by genomic VDR signaling, rather than through events downstream of rapid Pdia3-mediated signaling. Synergy between integrin and 1α,25$(OH)_2D_3$ signaling may occur via upregulation of integrin pathways by traditional VDR-mediated 1α,25$(OH)_2D_3$ signaling. This theory is supported by earlier work by *Raz et al* showing that 1α,25$(OH)_2D_3$ increased expression of the β_1 integrin [40], an integrin subunit shown to be critical in osteoblast differentiation on surfaces [32, 188]. Although it was hypothesized that increasing surface roughness would increase expression of VDR, qRT-PCR data showed that mRNA levels of VDR were not affected by surface roughness (Appendix, Figure A-3). Pdia3 was decreased on SLA and TPS surfaces, perhaps suggesting an inhibitory role of Pdia3 on osteoblastic differentiation. However, whatever 1α,25$(OH)_2D_3$-mediated effect Pdia3 has on osteoblastic differentiation appears to require an intact VDR. The findings in this study suggest that synergy between surface roughness and 1α,25$(OH)_2D_3$ requires VDR for crosstalk between integrins and 1α,25$(OH)_2D_3$ signaling pathways, although there could still be a

role of membrane 1α,25$(OH)_2D_3$ signaling in modulating VDR signaling. Further work will be necessary to determine exactly which genes and signaling pathways are involved in these interactions.

6.5. Conclusions

This study demonstrates that VDR is essential to the inhibitory effects of 1α,25$(OH)_2D_3$ on osteoblast proliferation, and to the stimulatory effects of 1α,25$(OH)_2D_3$ on osteoblast differentiation and production of osteogenic paracrine factors. Furthermore, this study demonstrates that VDR is required for the effects of 1α,25$(OH)_2D_3$ in modulating the response of osteoblasts to substrate microtopography, possibly via upregulation of osteoblast-specific proteins and integrin expression. These results do not rule out a role for Pdia3 in modulating VDR activity, nor do they rule out a role of Pdia3 in bone matrix deposition and mineralization. Studies using Pdia3 knockdown or knockout models may be necessary to fully elucidate the role of membrane 1α,25$(OH)_2D_3$ signaling in bone. The effects of 1α,25$(OH)_2D_3$ on bone are complex and intertwined with other signaling pathways; however, fully understanding the relative roles of membrane and nuclear 1α,25$(OH)_2D_3$ signaling in osteoblasts could yield new insights for the treatment of bone diseases such as osteoporosis.

CHAPTER 7:

Altered Response of Caveolin-1 Deficient Osteoblasts to $1\alpha,25(OH)_2D_3$ and Surface Microtopography

7.1. Introduction

Caveolae are a specialized form of cholesterol-enriched lipid rafts that are involved in endocytosis, lipid and cholesterol regulation, and a wide variety of cellular signaling pathways. As discussed extensively in chapter 1, caveolae are 60-80 nm 'cave-like' organelles in the cell membrane that are stabilized by caveolin-1 [129, 130]. In bone cells, caveolae are involved in the modulation of extracellular matrix and integrin interactions, mechanical stress transduction, bone morphogenic protein (BMP) signaling, and $1\alpha,25(OH)_2D_3$ signaling [129, 131-133]. Moreover, caveolae may also serve as a nexus for crosstalk between many of these signaling pathways, giving rise to potential synergies between ECM and growth factor signaling.

Despite the presence of so many different signaling molecules located in caveolae, Cav-1(-/-) mice exhibit a mild phenotype without any gross abnormalities, suggesting other lipid rafts or endosomes compensate for the lack of caveolae and the loss of caveolae-dependent signaling pathways [135]. Surprisingly, loss of caveolin-1 in Cav-1(-/-) mice actually causes an increase in bone mass. The growth plates of Cav-1(-/-) mice are widened and have abnormally high numbers of hypertrophic cells [117]. The femurs of Cav-1(-/-) mice show a significant increase in bone mass, cortical bone thickness, elastic modulus, stiffness, and overall yield strength compared to wild-type bones [137]. Osteoblasts in Cav-1(-/-) mice also display increased mineral apposition rate and bone formation rate compared to osteoblasts in Cav-1(+/+) mice.

The molecular mechanism by which loss of caveolae increases the rate of bone formation is unclear; however, studies suggest that caveolae might function to suppress signals for osteoblastic differentiation, thus slowing the rate of bone formation. Knockdown of cav-1 has been shown to lead to enhanced MAP kinase activity in NIH 3T3 cells [209], and has been shown to lead to increased levels of runx2 and osterix bone marrow stromal cells [137]. In addition, caveolae have been shown sequester β-catenin, which suppresses canonical Wnt/β-catenin signaling important in the osteoblastic differentiation of osteoprogenitors cells [139]. However, the role of caveolin-1 in osteoblast function may not be as simple as just repressing differentiation. Because of the involvement of caveolae such a wide variety of signaling pathways, it is likely that caveolae act to enhance, suppress, or modulate different osteogenic signals depending on extracellular cues or the state of differentiation of the cell. For instance, caveolin-1 has been shown to either enhance or inhibit BMP receptor function depending on which isoform of cav-1 binds to BMP receptors I or II. Cav-1β appears to inhibit BMP signaling, whereas Cav-1α appears to promote it [133]. Caveolae may also act in concert with Pdia3-mediated membrane 1α,25$(OH)_2D_3$ pathways to modulate VDR activity through phosphorylation by PKC or other kinases [105, 124], although this possibility has not been directly proven. While it appears that caveolin-1 delays early differentiation, it appears that it might actually promote mineralization [136] by mediating matrix vesicle biogenesis. This theory is supported by evidence that caveolin-1 is present both in caveolae and matrix vesicles in chondrocytes and osteoblasts [134]. Furthermore, overexpression of caveolin-1 leads to a large increase in osteoblast matrix mineralization. Overall, these findings point to a complex and dynamic role of caveolae in osteoblast function depending on the state of differentiation of the cell.

Rough surface microtopography and 1α,25$(OH)_2D_3$ treatment cause a synergistic increase in markers for osteoblastic differentiation, including alkaline phosphatase

activity, and levels of osteocalcin, OPG, and PGE_2 [69]. Caveolae may be involved in cell response to each of these stimuli individually, and may also be responsible for crosstalk that leads to synergistic effects on osteoblast differentiation. Osteoblast response to surfaces is mediated by integrin binding to adsorbed proteins. Separate studies have shown that integrins $\alpha_2\beta_1$ and $\alpha_5\beta_1$ can traffic through caveolae. Loss of cav-1 decreases the stability and number of focal adhesions [144], alters Ras/Erk, PI3K/Akt and Rac/Pak signaling downstream of integrins [138], and disrupts cell polarization and migration [143]. Moreover, integrin binding has been shown to regulate caveolae internalization, which may enhance spatial and temporal control of signaling by quickly up- or downregulating caveolae-dependent signaling pathways [138, 145]. However, it is not clear if loss of these functions of caveolae actually would alter how cells response to changes in surface topography and chemistry.

Caveolae also play a critical role in membrane $1\alpha,25(OH)_2D_3$ signaling. Recent studies have shown that both VDR and Pdia3 are present in caveolae [117, 141]. More importantly, chondrocytes deficient in caveolin-1 and caveolae lack a rapid increase in PKC activity and intracellular calcium concentration normally associated with treatment of $1\alpha,25(OH)_2D_3$ [117]. Rapid membrane $1\alpha,25(OH)_2D_3$ signaling leads to activation of MAP kinases such as ERK 1/2 [120], although the exact effects on gene transcription remain to be elucidated. Interaction between integrin and $1\alpha,25(OH)_2D_3$ signaling pathways may occur at multiple points in the signaling cascade. [136, 142]. Signaling of $1\alpha,25(OH)_2D_3$ could be affected through attachment mediated control over caveolae internalization or through crosstalk between secondary signaling molecules. Alternatively, $1\alpha,25(OH)_2D_3$ signaling could alter integrin signaling directly, through downstream crosstalk, or through changes in integrin or ECM component gene expression. The purpose of the present study is not to determine the exact nature of

such crosstalk between integrin and 1α,25$(OH)_2D_3$ signaling, rather, the purpose is to determine whether caveolae are necessary for such crosstalk to occur.

The present study uses Cav-1(+/+) and Cav-1(-/-) calvarial osteoblasts to examine whether caveolae are required to mediate the osteogenic effects of 1α,25$(OH)_2D_3$ via rapid response mechanisms involving Pdia3 and/or VDR. The present study also examines whether loss of caveolae alters osteoblast response to surface energy and topography, and whether loss of caveolae disrupts synergistic signaling between 1α,25$(OH)_2D_3$ and integrin signaling pathways.

7.2. Materials and Methods

Caveolin-1 Deficient Osteoblasts

Cavarial osteoblasts from knockout Cav-1(-/-) mice and "wild-type" Cav-1(+/+) littermates. Complete methods are described in Chapter 2.

Titanium Surfaces

Institut Straumann AG (Basel, Switzerland) supplied the PT, SLA, and TPS titanium disks used in this study. Surfaces were manufactured and characterized as described in chapter 2.

Cell Culture

Cells were cultured in DMEM plus 10% FBS and 1% penicillin/streptomycin. The culture media used in these studies contains 10% FBS. Because the FBS was not charcoal stirred it contained low levels of 1α,25$(OH)_2D_3$; thus, the culture media had 10^-

^{12} to 10^{-13} M 1α,25$(OH)_2D_3$. Initial experiments compared baseline production of osteocalcin in Cav-1(+/+) cells and Cav-1(-/-) osteoblasts. For these experiments second passage cells were grown to confluence on TCPS and osteocalcin in the media was assayed. To assess the effects of growth on microstructured titanium, Cav-1(+/+) or Cav-1(-/-) osteoblasts were plated at a density of 10,000 cells/cm^2 into 24-well plates containing 6 wells each of TCPS, PT, SLA, and TPS surfaces.

Physiological Responses of Cav-1(+/+) and Cav-1(-/-) Osteoblasts

At confluence, which was determined from cells on TCPS surfaces, each group was treated with 10^{-8} M 1α,25$(OH)_2D_3$ (Biomol, Plymouth Meeting, PA) or vehicle control (ethanol) for 24 hours. At harvest, experimental media were collected and the cell layers were washed twice with DMEM. Osteoblasts were removed using two subsequent treatments for 10 minutes with 0.25% trypsin. Osteoblast phenotype was assessed by measuring cell number, total protein, alkaline phosphatase activity, and media levels of osteocalcin, TGF-β1, OPG, and PEG_2 according to protocols discussed in chapter 2.

Gene Expression Changes in Cav-1(+/+) and Cav-1(-/-) Osteoblasts

Expression of the genes for GapDH (Control), VDR, integrin beta 1, integrin alpha 2, integrin alpha 5, caveolin-1, Runx2, and integrin beta 3 were measured in Cav-1(+/+) and Cav-1(-/-) osteoblasts. Cells were grown on six discs each of TCPS, PT, and SLA surfaces in a similar manner as described above. In addition, a separate set of experiments was grown on TCPS surfaces of 6-well plates and was treated at confluence for 24 hours with 1α,25$(OH)_2D_3$. Cells were harvested for mRNA using an RNeasy™ kit (Qiagen, Germantown, MD) according to the manufacturer's protocols. Following RNA isolation, RNA was quantified using a Nanodrop™ spectrophotometer

(Thermo Scientific, Wilmington, DE). All samples were normalized to 1ug RNA/uL with diethylpyrocarbonate (DEPC)-treated water. Gene expression was assessed by qRT-PCR using a QuantiFast™ SYBR Green RT-PCR Kit (Qiagen) according to manufacturer's protocols. Briefly, 12.5 µL SYBR green master mix, 1 µL (1 µmol) of each primer, 0.25 µL RT mix, 1 µg mRNA, and DEPC-treated water were combined for a total volume of 25 µL. All reactions were carried out for 40 cycles on an i-cycler™ (Bio-Rad Laboratories, Hercules, CA) using software i-cycler iQ™, version 3.0a. The primers and annealing temperatures used in the experiments were the same as described on page 110, although VDR primers were used instead of cav-1 primers. The VDR primers are:

VDR	R	AGG GAT GAT GGG TAG GTT GTG	59.4
	F	AGG CAG GCA GAA GAG ATG AG	

Unfortunately, the data from qRT-PCR for Cav-1(+/+) and Cav-1(-/-) osteoblasts exhibited similar problems as the qRT-PCR study using VDR(+/+) and VDR(-/-) osteoblasts from the previous chapter. Results were not consistent between experiments and RNA yields were low on SLA surfaces. Levels of GapDH (control) were also lower on SLA surfaces despite adjustment based on RNA measurements. Because of the low levels of RNA and inconsistency between experiments, it is difficult to draw definitive conclusion from the data. The data is shown in the appendix in Figures A-5, A-6, A-7, and A-8. The pooled data from all of the Cav-1(+/+) and Cav-1(-/-) experiments are shown in Tables A-3 and A-4.

Statistical Analysis

Data for each experiment were calculated from six independent cultures (n=6) per group and presented as the mean ± standard error of the mean (SEM). Data were

analyzed via analysis of variance (AVONA) and statistical difference between groups determined using Bonferroni's modification of the Student's t-test. Values with $p<0.05$ were considered significant. Each experiment was performed twice to ensure the consistency of the results. The data presented are from one of two representative experiments for each end point assay.

7.3. Results

The results indicate that caveolae have a role in proliferation, differentiation, and local factor production of osteoblasts, although the results are somewhat perplexing since not all markers for osteoblast phenotype were affected. The osteogenic effects of surface roughness do not appear to require functional caveolae, as decreases in proliferation and increases in osteogenic differentiation and local factor production are present on SLA and TPS surfaces in both Cav-1(+/+) and Cav-1(-/-) osteoblasts. However, $1\alpha,25(OH)_2D_3$ does appear to require caveolae for some of its effects.

Cell number in Cav-1(-/-) osteoblasts was lower on all surfaces compared to Cav-1(+/+) osteoblasts (Figure 7-2); however repeats varied in baseline cell number values depending on the harvest batch (Figure 7-1). A repeat on TCPS, PT, and SLA surfaces using Cav-1(+/+) and Cav-1(-/-) osteoblasts was performed using batches of cells grown in parallel and harvested at the same time. No differences in cell number, alkaline phosphatase activity, or osteocalcin levels were observed between Cav-1(+/+) and Cav-1(-/-) osteoblasts. This result suggests that differences in baseline levels of osteocalcin or other factors measured are due to experimental variance inherent with using cells harvested from separate batches of mice.

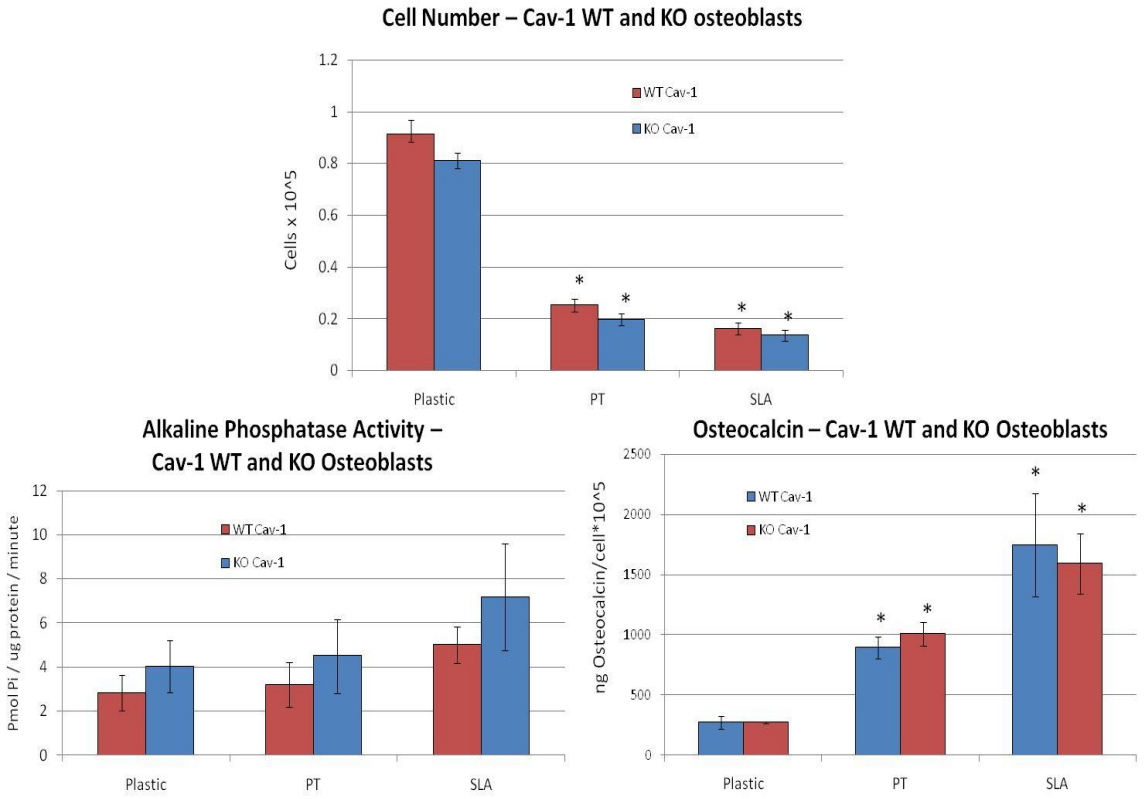

Figure 7-1: Baseline comparison of Cav-1 (+/+) and Cav-1 (-/-) osteoblasts on TCPS, PT, and SLA surfaces. Statistics: * Surface vs. TCPS. Significant if $p < 0.05$.

In the full experiment using TCPS, PT, SLA, and TPS surfaces, loss of caveolin-1 appeared to affect proliferation of osteoblasts. Increasing surface roughness caused a decrease in cell number in both Cav-1(+/+) and Cav-1(-/-) osteoblasts (Figure 7-2). $1\alpha,25(OH)_2D_3$ caused a further decrease in cell number in Cav-1(+/+) osteoblasts. The $1\alpha,25(OH)_2D_3$-dependent decrease was minimal in Cav-1(-/-) osteoblasts, suggesting that effects of $1\alpha,25(OH)_2D_3$ on cell number were impaired.

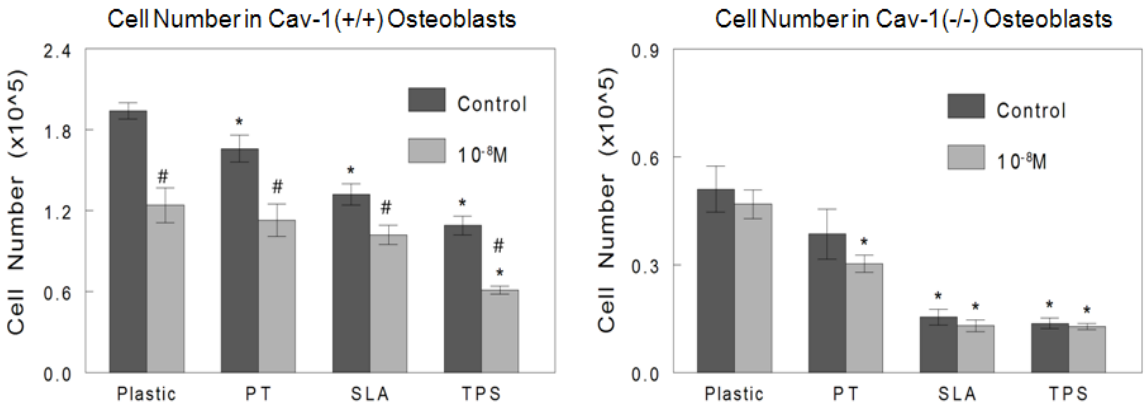

Figure 7-2: Comparison of cell number in Cav-1(+/+) and Cav-1(-/-) osteoblasts. * Ti surface vs. Plastic (TCPS); # 1,25 treatment vs. vehicle control.

Alkaline phosphatase specific activity was also altered by the absence of caveolae. Increasing surface roughness caused an increase in alkaline phosphatase specific activity in both Cav-1(+/+) and Cav-1(-/-) osteoblasts (Figure 7-2). 1α,25$(OH)_2D_3$ caused a further increase in alkaline phosphatase activity in Cav-1(+/+) osteoblasts; however, treatment with 1α,25$(OH)_2D_3$ on Cav-1(-/-) osteoblasts caused a decrease in alkaline phosphatase activity on all surfaces. Cav-1(-/-) osteoblasts treated with 1α,25$(OH)_2D_3$ also did not display an effect of surface roughness. These results suggest a role for caveolae in 1α,25$(OH)_2D_3$ signaling, although it is unclear why alkaline phosphatase activity was reduced below control levels after 1α,25$(OH)_2D_3$ treatment.

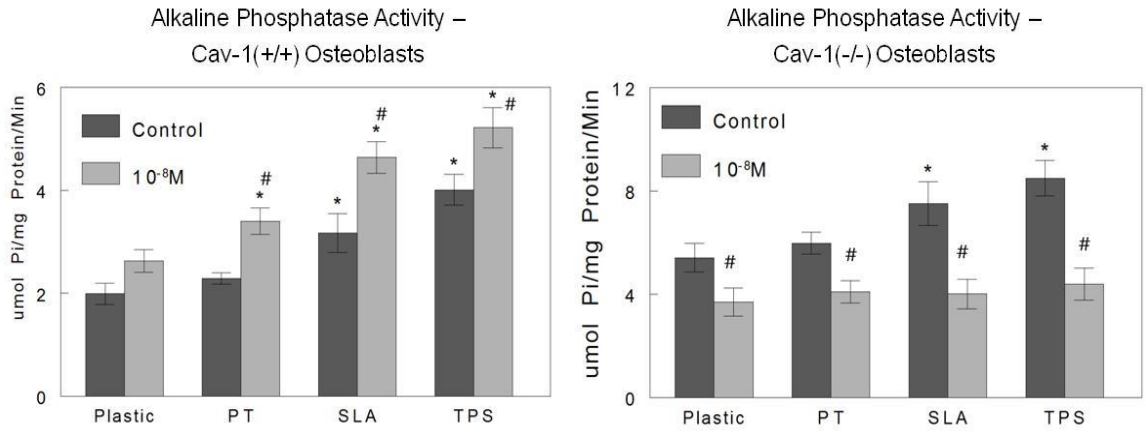

Figure 7-3: Comparison of alkaline phosphatase specific activity in Cav-1(+/+) and Cav-1(-/-) osteoblasts. * Ti surface vs. Plastic (TCPS); # 1,25 treatment vs. vehicle control.

One obvious observation in Cav-1(-/-) osteoblasts is the nearly 100-fold increase in levels of osteocalcin in all groups compared to Cav-1(+/+) controls (Figure 7-3). These baseline differences were not observed in Cav-1(+/+) and Cav-1(-/-) osteoblasts grown, harvested, and tested at the same time (Appendix, A-2). Previous studies have indicated increases in differentiation in Cav-1(-/-) osteoblast compared to Cav-1(+/+) controls [137], although it is not clear if that is the case in this study. Osteocalcin levels increased in both Cav-1(+/+) and Cav-1(-/-) osteoblasts due to increasing surface roughness. 1α,25$(OH)_2D_3$ caused an increase in osteocalcin levels on all surfaces in Cav-1(+/+) and Cav-1(-/-) osteoblasts.

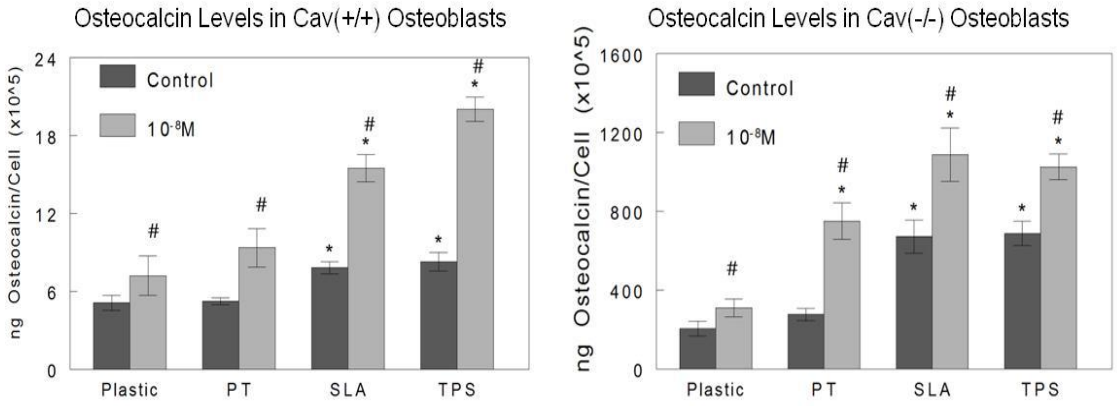

Figure 7-4: Comparison of osteocalcin levels in Cav-1(+/+) and Cav-1(-/-) osteoblasts. * Ti surface vs. Plastic (TCPS); # 1,25 treatment vs. vehicle control.

Local factor production was also affected in osteoblasts lacking caveolin-1. PGE_2 levels were nearly 100-fold higher in Cav-1(-/-) osteoblasts than Cav-1(+/+) osteoblasts (Figure 7-4). PGE_2 levels increased in both Cav-1(+/+) and Cav-1(-/-) osteoblasts due to increasing surface roughness. 1α,25$(OH)_2D_3$ caused an increase in osteocalcin levels on all surfaces in both Cav-1(+/+) and Cav-1(-/-) osteoblasts.

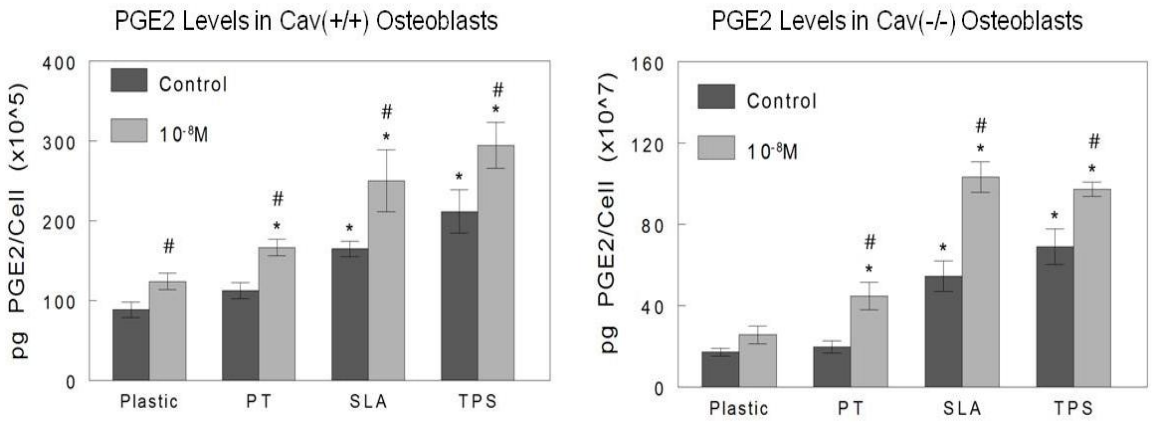

Figure 7-5: Comparison of PGE_2 levels in Cav-1(+/+) and Cav-1(-/-) osteoblasts. * Ti surface vs. Plastic (TCPS); # 1,25 treatment vs. vehicle control.

TGF-β1 levels were also nearly 100-fold higher in Cav-1(-/-) osteoblasts than Cav-1(+/+) osteoblasts. TGF-β1 levels increased in both Cav-1(+/+) and Cav-1(-/-) osteoblasts due to increasing surface roughness (Figure 7-5). $1\alpha,25(OH)_2D_3$ caused a further increase in latent TGF-β1 levels on all surfaces and active TGF-β1 levels on SLA and TPS surfaces. $1\alpha,25(OH)_2D_3$ did not have in effect on active or latent TGF-β1 levels in Cav-1(-/-) osteoblasts.

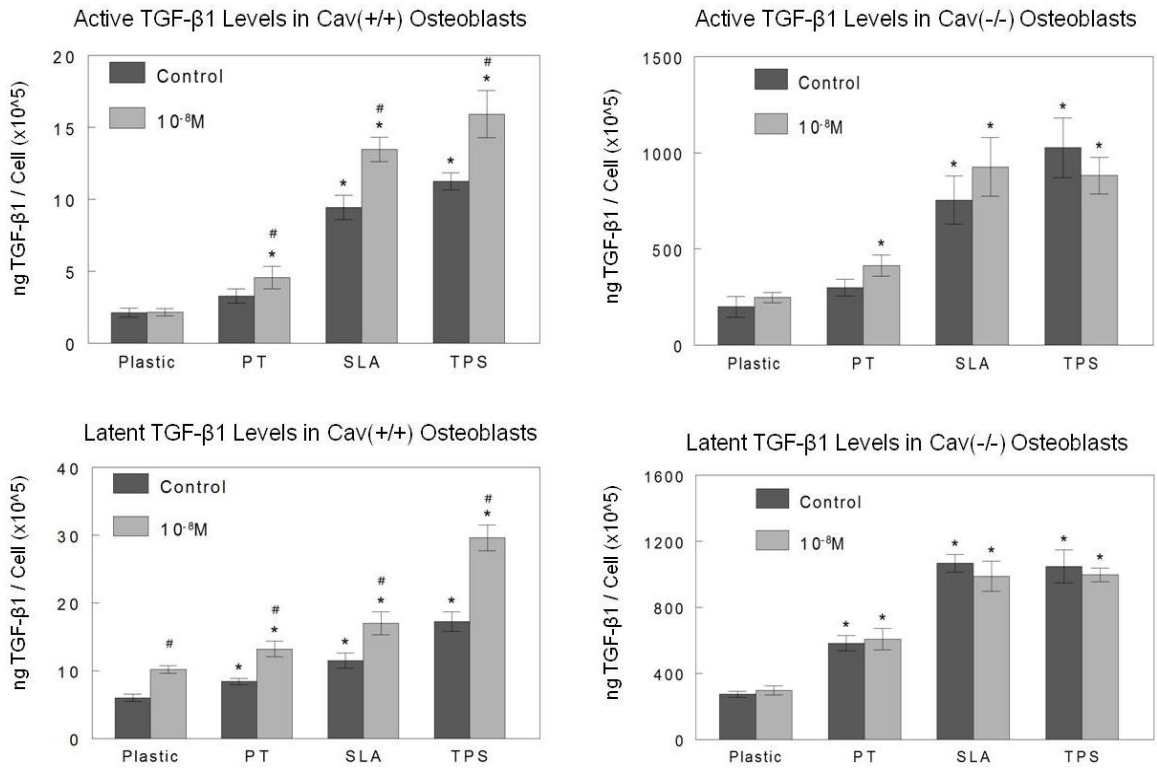

Figure 7-6: Comparison of active (top) and latent (bottom) TGF-β1 levels in Cav-1(+/+) and Cav-1(-/-) osteoblasts.

7.4. Discussion

The results demonstrate that loss of caveolae do affect osteoblast phenotype and responsiveness to 1α,25$(OH)_2D_3$; however, osteoblast response to surface roughness did not appear to be impaired. Interestingly, levels of osteocalcin, active and latent TGF-β1, and PGE_2 were nearly 100-fold higher in the absence of caveolae. Part of this effect may be due to lower cell number observed in Cav-1(-/-), although even non-normalized levels of these factors were still 30-fold higher in caveolae deficient cells. Part of this effect may also be due to experimental variance. All cells is the experiment were primary osteoblasts harvested from separate batches of Cav-1(+/+) and Cav-1(-/-) mice. Repeats did not show differences in levels of osteocalcin (Appendix, Figure A-2). TGF-β1, and PGE_2 levels were not measured again. Still, the fact that levels of

osteocalcin, active and latent TGF-β1, and PGE_2 were so highly expressed in Cav-1(-/-) osteoblasts from both primary experiments suggests that this result cannot be ignored. Previous studies suggest that one of the main roles of caveolae in osteoblasts is to repress signals for differentiation [136, 137]. These findings include higher levels in Cav-1(-/-) osteoblasts of runx2 and osterix, both of which are potent osteoblast transcription factors. Previous work has also shown that MAP kinase activity appears to be hyperactive in cav-1 deficient cells [209]. MAP kinase activity is known upregulate runx2 and other transcription factors to promote osteoblast differentiation. Alternatively, canonical Wnt/β-catenin signaling or BMP-signaling could also be increased in Cav-1(-/-) osteoblasts due to the inability of caveolin-1 to sequester β-catenin or BMP receptors, respectively. Finally, TGF-β1 levels could be increased given reports that caveolae are involved in internalization and degradation of TGF-β receptors [210]. Each of these possible scenarios could partially explain why Cav-1(-/-) osteoblasts undergo more rapid differentiation than their wild-type counterparts.

Despite multiple reports that caveolae are involved in cell polarity, migration, integrin signaling, and the assembly of focal adhesions [138, 143, 144], this study did not demonstrate any alteration in the response of Cav-1(-/-) osteoblasts to increasing surface roughness. Previous studies have investigated the role of caveolae under more dynamic conditions, whereas the present study measured markers for osteoblast proliferation and differentiation at a set time point 24 hours post-confluence. Although It is still possible that cav-1(-/-) osteoblasts might have impaired or delayed response to surface roughness at short time points, the present results clearly show that loss of caveolae does not affect osteoblast response to surface roughness at the time points investigated.

Osteoblast response to 1α,25$(OH)_2D_3$ appears to be partially under the control of caveolae. The results show that without caveolae, 1α,25$(OH)_2D_3$ was not able to decrease cell number. In addition, lack of caveolae disrupted 1α,25$(OH)_2D_3$-mediated increases in alkaline phosphatase activity and levels of active and latent TGF-β1. However, 1α,25$(OH)_2D_3$-dependent increases in osteocalcin and PGE_2 levels were not affected by the lack of caveolae. These findings suggest the possibility that these phenotypic responses are regulated by caveolae-dependent and independent mechanisms. For instance, it is well known that traditional 1α,25$(OH)_2D_3$ binding to VDR is able to upregulate osteocalcin transcription through VDR-RXR binding to VDREs in the promoter region of the osteocalcin gene [107]. Loss of a 1α,25$(OH)_2D_3$-mediated decrease in cell number in Cav-1(-/-) osteoblasts is also not surprising given reports that cav-1(-/-) cells shown changes in proliferation [136, 138]. It has been suggested that rapid membrane signaling can activate multiple kinases that either directly affect G1-S transition or act through crosstalk with the VDR to upregulate VDR target genes [51].

The finding that 1α,25$(OH)_2D_3$-mediated upregulation of PGE_2 is not regulated via caveolae is surprising given that previous reports showed that rapid membrane 1α,25$(OH)_2D_3$ signaling can increase PGE_2 production via increases in arachidonic acid [204]. The finding that 1α,25$(OH)_2D_3$-mediated increases in active TGF-β1 require caveolae supports earlier work that shows that rapid 1α,25$(OH)_2D_3$ produces stromelysin-1 (MMP-3), which releases and activates latent TGF-β1 in the ECM [211]. However, the 1α,25$(OH)_2D_3$ signaling mechanisms regulating latent TGF-β1 levels via caveolae are unclear. In addition, effects of 1α,25$(OH)_2D_3$ on reducing alkaline phosphatase activity in Cav-1(-/-) osteoblasts are difficult to explain given the fact that 1α,25$(OH)_2D_3$ treatment appeared to inhibit any surface effects. Overall, the findings that caveolae regulate, some, but not all of the effects of 1α,25$(OH)_2D_3$ points to

increased complexity in 1α,25$(OH)_2D_3$ signaling, perhaps due to extensive crosstalk between membrane and nuclear 1α,25$(OH)_2D_3$ signaling pathways.

7.5. Conclusion

The data suggest that caveolin-1 deficient osteoblasts exhibited differences in state of differentiation and responsiveness to 1α,25$(OH)_2D_3$ compared to littermate controls. Levels of osteocalcin, active and latent TGF-β1, and PGE_2 were nearly 100-fold higher in the absence of caveolae, although it is not clear whether this is due to enhanced differentiation or is an artifact of the experiment. When osteoblasts lacking caveolae were treated with 1α,25$(OH)_2D_3$, they did not exhibit decreases in cell number and increases in alkaline phosphatase activity and active and latent TGF-β1 characteristic of 'wild-type' osteoblasts treated similarly. Lack of caveolae did not affect osteoblast response to surface energy or roughness, nor did lack of caveolae affect 1α,25$(OH)_2D_3$-induced increases in osteocalcin or PGE_2 levels. Overall, the results support other reports that suggest that lack of caveolae enhances osteoblastic differentiation. Moreover, the results suggest that 1α,25$(OH)_2D_3$ signaling relies on both membrane and nuclear vitamin D pathways to properly regulate target genes.

CHAPTER 8: Discussion

The results highlighted in the previous chapters of this thesis demonstrate that integrins, VDR, and caveolae play important roles in mediating osteoblast response to implant surface properties and $1\alpha,25(OH)_2D_3$. While these studies have answered questions regarding the roles of the β_1 integrin or VDR in mediating these responses, the studies have also opened up many more questions regarding the complexity of the mechanisms regulating interaction between integrins, caveolae, and vitamin D mediated signaling. The following sections will discuss the findings with regard to cell-surface interactions, the design of multifunctional peptide-based surfaces, and vitamin D signaling. The thesis will conclude with a discussion of potential future directions in light of these findings and other reports in the scientific literature.

8.1. Cell Response to Surfaces

Osteoblast response to increasing surface roughness was shown in Chapter 3 to be regulated by the β_1 integrin subunit. While much of the research in the literature has focused on the roles of the $\alpha_2\beta_1$ and $\alpha_5\beta_1$ integrins in osteoblast biology, many other integrins likely play supportive roles in differentiation. Osteoblasts express multiple integrin pairs that vary at different times as osteoblasts mature from osteoprogenitor cells to mature, mineralizing osteoblasts. These osteoblasts include integrins $\alpha_1\beta_1$, $\alpha_2\beta_1$ $\alpha_3\beta_1$, $\alpha_4\beta_1$, $\alpha_5\beta_1$, $\alpha_6\beta_1$, $\alpha_8\beta_1$, $\alpha_V\beta_3$, $\alpha_V\beta_5$, [34], and possibly others that have not been measured. It has been shown that surface roughness and time in culture increases β_1 and α_2 expression and decreases α_5 expression, which demonstrates that integrin expression varies not only by surface properties, but also by the state of differentiation of the cells. Such differences in integrin expression, particularly $\alpha_2\beta_1$ and $\alpha_5\beta_1$, along with changes in osteocalcin and other markers for differentiation, suggest that changes in

integrin expression could associated with increased osteoblast differentiation [40]. However, for many integrins it is not known whether increased expression is the cause of or the result of increased osteoblastic differentiation.

Variance in integrin expression and the existence of disparate integrin functions is expected given the requirements of osteoblasts in producing bone. Early osteoprogenitor cells must reach the implant surface where they attach to a provisional matrix containing both fibronectin and collagen I. Reports in the literature suggest that the $\alpha_5\beta_1$ integrin is important in the early attachment, proliferation, and differentiation of osteoprogenitor cells [146, 162, 163]. Silencing of the α_5-integrin did not have any effect on the response of immature osteoblast-like MG63 cells to surface roughness; however, confirmation of these results is necessary given the possibly of insufficient silencing of the α_5-integrin at the cell surface. While studies suggest that the $\alpha_5\beta_1$ integrin is critical to osteoprogenitor cell differentiation [146, 162, 163], its role may change as these cells mature into osteoblasts. The $\alpha_5\beta_1$ integrin likely plays a central role in providing cell survival and proliferative cues necessary to generate sufficient osteoblast population from osteoprogenitor cells. However, as osteoblasts begin to mature, they tend to produce less fibronectin and more collagen I and bone-specific proteins like osteocalcin. Thus, a switch from $\alpha_5\beta_1$ to $\alpha_2\beta_1$ signaling might be important in switching from signals promoting proliferation/survival to those promoting osteoblastic differentiation and mineralization. The α_5-silencing study presented in this thesis only investigated the role of the $\alpha_5\beta_1$ integrin in immature osteoblasts. Even if issues with α_5 silencing efficiency are ignored and we conclude that $\alpha_5\beta_1$ does not mediate the effects of surface roughness in MG63 cells, it is not clear whether this finding would hold true in normal human osteoblasts or other osteoblast cell models.

In an effort to limit variables, experimenters must often look at the role of single integrins or peptides. This simplification is necessary, but ignores the complexity of biological systems. Multiple integrins other than $\alpha_2\beta_1$ and $\alpha_5\beta_1$ are involved in osteoblast interaction with the ECM including $\alpha_1\beta_1$, $\alpha_3\beta_1$, $\alpha_V\beta_3$, and others. It is well known that the binding of multiple different ligands to different components of the ECM can lead to synergies in signals for proliferation or differentiation. Thus, while $\alpha_2\beta_1$ has been shown to be critical to differentiation in mature osteoblasts, other integrins could also play important supporting roles. This possibility suggests that knockdown of some of these others integrins might also impair osteoblast response to surface microtopography.

Integrin binding has been shown to affect growth factor signaling through caveolae or other mechanisms. In this manner, the osteogenic functions of some integrin signaling pathways can be amplified in a way by enhancing the actions of various growth factors or steroid hormones. It is likely that integrin expression and binding affects growth factor signaling, and vice versa, growth factors can alter integrin expression or activity. For example, treatment with $1\alpha,25(OH)_2D_3$ leads to increased expression of the β_1 integrin [40]. In addition, cells often require both the proper attachment signals and growth factor signals to maximize signaling. For instance, internalization of caveolae, and thus caveolae based signaling, can be mediated by association of pY14Cav-1 with the β_1 integrin [138]. Thus, better understanding of cell-surface interactions requires indentifying not only the integrins involved in osteoblastic differentiation, but also other associated signaling molecules that interact with integrins to enhance or repress osteoblastic differentiation.

8.2. Multifunctional Peptide Coated Implant Surfaces

The use of proteins, peptides, or other molecules to modify surfaces to elicit specific biological responses is a rapidly developing field of research. One of the keys to designing successful peptide-based surfaces is being able to understand the biology well enough to design ligands that can enhance osteoblast differentiation. The results using RGD and KRSR surfaces were disappointing in this regard because of lack of biological activity of KRSR. RGD on the other hand had biological activity, but promoted osteoblast proliferation, not differentiation. Unfortunately, it is difficult to predict whether a ligand will promote differentiation, especially since many ligands are selected based on initial attachment studies rather than actual measures for differentiation. Selection of ligands for even initial tests can be difficult. While the RGD sequence is found in many different proteins, KRSR is based off a BBXB design where the amino acid sequence varies by protein, making biologically active BBXB groups difficult to identify without resorting to complex screening assays.

Interestingly, K<u>S</u>SR was able to promote an osteoblastic phenotype, although the exact mechanism for this effect is unknown. Earlier reports show that K<u>S</u>SR was not able to increase cell attachment [192], which creates doubt regarding any biological specificity of the sequence. An alternative hypothesis is that the K<u>S</u>SR ligand inhibits cell attachment and reduces cell spreading. The PLL-*g*-PEG coating has a similar effect on cells although it is even more pronounced by addition of K<u>S</u>SR. The mechanisms behind how these surfaces act to enhance osteoblast differentiation are largely unknown. Much of the discussion of osteoblast differentiation in this thesis has focused on the role of integrin binding and attachment, so it seems almost counterintuitive that surfaces limiting attachment would enhance differentiation. One possible theory is that the types of integrins binding adsorbed proteins on such surfaces strongly promote

osteoblast differentiation, but not proliferation. This point reiterates earlier suggestions that signals for proliferation and differentiation may compete against one another. Still, very little is known regarding which integrins are expressed differentially on PLL-*g*-PEG or modSLA surfaces, or how a reduction in cell spreading leads to increased differentiation.

KSSR was effective in promoting osteoblast differentiation, but the combination of RGD and KSSR did not lead to a state of enhanced osteoblast proliferation and differentiation. Instead, RGD at high peptide densities appeared to mask the effects of KSSR. Clearly, ligands used in multifunctional peptide surfaces should work synergistically, not antagonistically. Other multifunctional peptide surfaces, such as those composed of RGD/GFOGER, RGD/FHRRIKA, or RGD/PHSRN have demonstrated enhanced binding [42, 186-188], which suggests that selectivity of ligands is critical to achieving enhanced cell attachment, proliferation, or differentiation. Thus, the development of truly advanced multifunctional peptide surfaces requires better understanding of ligand bioactivity, ligand combinations, spacing, and surface attachment chemistries in order to eliminate much of trial and error that is currently the basis for ligand design and evaluation.

8.3. Vitamin D and Caveolae

The combination of surface microtopography and 1α,25$(OH)_2D_3$ treatment leads to synergistic effects on osteoblast differentiation, although it is still unclear how 1α,25$(OH)_2D_3$ and integrin signaling pathways interact to give rise to this synergy. The results in Chapter 6 suggest that VDR is required for the effects of 1α,25$(OH)_2D_3$ on all measured markers for osteoblastic differentiation; however, this finding is somewhat surprising given the role of VDR-independent pathways in increasing Ca^{++} and PKC

[212]. The very fact that these responses exist suggests that some downstream effects of rapid 1α,25$(OH)_2D_3$ signaling exist and are yet to be identified. One of the most plausible explanations for this finding is that both Pdia3 and VDR are required for the rapid responses to 1α,25$(OH)_2D_3$. Both VDR and Pdia3 have been found in the caveolae [117], although no evidence has yet shown that these proteins interact. Interestingly, VDR transcriptional activity can be mediated by multiple phosphorylation sites that can be targeted by PKC-β, CaMKIV, casein kinase II, MAPK, and PKA [105], although it is not clear which, if any of these signaling molecules might be affected by rapid 1α,25$(OH)_2D_3$ signaling. The existence of such modulation of nuclear receptor activity by rapid membrane pathways is not uncommon in either growth factor or steroid hormone signaling [213], so it would not be surprising if membrane signaling did in fact modulate VDR transcriptional activity and activation of target genes. This possibility will have to be explored in future studies.

Surprisingly, lack of caveolae did not affect cell response to the surface properties tested in this study despite reports that lack of caveolae affects focal adhesion assembly, cell polarity, migration, proliferation, and differentiation [136]. None of these functions were totally inhibited by lack of caveolae in these referenced studies, but the spatial and temporal control over these events was impaired. Previous tests in the literature examined short time points, whereas the experiments in this thesis measured cell response at confluence, possibly making these differences in dynamics irrelevant. Still, given previous reports of increased differentiation in cav-1(-/-) osteoblasts and the increased levels of osteocalcin, TGFβ1, and PGE_2 observed in this study, it is surprising that no differences were seen in the relative responses of cav-1(-/-) and cav-1(+/+) osteoblasts to changing surface roughness.

It is well known that lipid rafts or other mechanisms can compensate for the critical roles of caveolae, therefore making it difficult to determine exactly what functions are mediated by caveolae and what functions are mediated by signaling molecules or lipid rafts that are simply associated with caveolae. Still, the interplay between caveolae and integrins is certainly an area of intense interest. The fact that integrin binding can directly affect caveolae internalization and signaling suggests the possibility that there is anchorage dependent modulation of many growth factor signaling pathways [136, 145]. Moreover, growth factor signaling can in turn affect integrin binding and focal adhesion stability through the interactions with phosphorylated caveolin-1. Further work will be needed to explore whether these actions of caveolae have direct roles in crosstalk between integrin and $1\alpha,25(OH)_2D_3$ signaling pathways.

8.4. Future Studies

Although rough implant topographies have been used in orthopaedic and dental implants for several decades now, there is still a tremendous amount of work that needs to be performed to understand how these surface features actually affect integrin signaling and osteoblast phenotype. The design of advanced implant surfaces or combination therapies based on such increased understanding of osteoblast biology will also require advances in surface engineering and improvements our ability to select appropriate signaling motifs. Understanding how osteoblasts interact with implant surfaces requires a deeper understanding of cell-surface interactions and a deeper understanding of the mechanisms promoting osteointegration. Integrins certainly play a significant role in the ability of osteoblasts to respond to surface roughness; however, studies investigating the roles of integrins in bone turnover and peri-implant healing *in vivo* are still lacking in large numbers. Some studies have focused on the $\alpha_2\beta_1$ and $\alpha_5\beta_1$ integrins in osteoblast interactions with surfaces, but few studies have deeply

investigated the role of the integrins in affecting *in vivo* bone formation. Moreover, there is a need for more comprehensive studies examining temporal expression of multiple integrins throughout both bone turnover *in vivo* and osteoblast response to titanium surface properties *in vitro*. Such studies would provide better information about when different integrins are expressed, thus providing insight on how integrin expression progresses as osteoblasts differentiate. This information would be useful to bioengineers in terms of indentifying targets for the design of peptide coated surfaces.

Experiments on protein or peptide based surfaces appear to be limited by the biological activity of the ligands attached to the surfaces. As demonstrated with the KRSR peptide, even ligands proven to increase osteoblast-specific adhesion do not necessarily lead to promotion of an osteoblastic phenotype. In theory, a ligand like KRSR that increases osteoblast-specific adhesion but actually promotes osteoblastic differentiation would be an important discovery. While it is very difficult to identify and prove the osteogenic capability of new ligands, such discoveries could lead to novel surfaces that promote osteointegration *in vivo*. Furthermore, studies exploring the combination of ligands on titanium implant surfaces may show increased osteogenic potential than single ligands.

Better understanding of the relative roles of the membrane and nuclear $1\alpha,25(OH)_2D_3$ pathways could lead to novel targets for drug design. While the results herein this thesis demonstrate that VDR is required for the effects of $1\alpha,25(OH)_2D_3$ on all measured markers for osteoblast proliferation and differentiation, the results do not rule out a role for membrane $1\alpha,25(OH)_2D_3$ signaling in modulating VDR transcriptional activity and affecting VDR target gene transcription. Future studies should specifically investigate the role of rapid $1\alpha,25(OH)_2D_3$ signaling in activating PKC-β, PKA, casein kinase II, MAPK, or $Ca2^{++}$/calmodulin-dependent kinase IV (CaMKIV) dependent

signaling mechanisms that have been previously shown to phosphorylate the VDR [105, 124]. These studies should further attempt to establish a direct link between rapid 1α,25$(OH)_2D_3$ signaling, phosphorylation of the VDR, and altered transcriptional activity of target genes. Furthermore, the role of caveolae should be explored to determine if and how these signaling pathways are modulating by integrin signaling. Such a discovery regarding interactions between membrane 1α,25$(OH)_2D_3$ and traditional VDR pathways would finally answer questions regarding the downstream effects of rapid 1α,25$(OH)_2D_3$ signaling.

REFERENCES

1. Ratner B, Hoffman, A., Schoen, F., Lemons, J. Biomaterials Science. San Diego, CA: Academic Press, 1996.
2. Spector M. Prostheses: Materials, design, and strategies for fixation. Orthopaedic Knowledge Update 3 1990:115-199.
3. Long PH. Medical devices in orthopedic applications. Toxicol Pathol 2008;36(1):85-91.
4. Sakiyama-Elbert SE, Hubbell JA. Functional biomaterials: Design of novel biomaterials. Annual Review of Materials Research 2001;31:183-201.
5. Schuler M, Trentin D, Textor M, Tosatti SG. Biomedical interfaces: titanium surface technology for implants and cell carriers. Nanomed 2006 Dec;1(4):449-463.
6. Bostrom M, Bosket, A., Kaufman, JK., Einhorn, TA. Form and Function of Bone. In: Buckwalter J, Einhorn, TA., Simon, SR., editor. Orthopaedic Basic Science. 2nd ed. Rosemont, IL: American Academy of Orthopaedic Surgeons, 2000.
7. Long M, Rack HJ. Titanium alloys in total joint replacement--a materials science perspective. Biomaterials 1998 Sep;19(18):1621-1639.
8. Boron WF, Boulpaep, E.L. Medical Physiology. 1st ed: Saunders, 2003.
9. Rho JY, Kuhn-Spearing L, Zioupos P. Mechanical properties and the hierarchical structure of bone. Med Eng Phys 1998 Mar;20(2):92-102.
10. Kumar V, Cotran, R., Robbins, S. Basic Pathology. Philadelphia, PA: Saunders, 2003.
11. Blair HC, Robinson LJ, Zaidi M. Osteoclast signalling pathways. Biochem Biophys Res Commun 2005 Mar 18;328(3):728-738.
12. Green GA. Understanding NSAIDs: from aspirin to COX-2. Clin Cornerstone 2001;3(5):50-60.
13. Hunter DJ, McDougall JJ, Keefe FJ. The symptoms of osteoarthritis and the genesis of pain. Rheum Dis Clin North Am 2008 Aug;34(3):623-643.
14. Hunziker EB. Articular cartilage repair: basic science and clinical progress. A review of the current status and prospects. Osteoarthritis Cartilage 2002 Jun;10(6):432-463.
15. Iorio R, Robb WJ, Healy WL, Berry DJ, Hozack WJ, Kyle RF, et al. Orthopaedic surgeon workforce and volume assessment for total hip and knee replacement in the United States: preparing for an epidemic. J Bone Joint Surg Am 2008 Jul;90(7):1598-1605.
16. Kurtz S, Ong K, Lau E, Mowat F, Halpern M. Projections of primary and revision hip and knee arthroplasty in the United States from 2005 to 2030. J Bone Joint Surg Am 2007 Apr;89(4):780-785.
17. Nizard R, Pourreyron D, Raould A, Hannouche D, Sedel L. Alumina-on-alumina hip arthroplasty in patients younger than 30 years old. Clin Orthop Relat Res 2008 Feb;466(2):317-323.
18. Lee K, Goodman SB. Current state and future of joint replacements in the hip and knee. Expert Rev Med Devices 2008 May;5(3):383-393.
19. A patient's guide to artificial joint replacement of the hip. Medical Multimedia Group, 2002.
20. Geetha M, Singh AK, Asokamani R, Gogia AK. Ti based biomaterials, the ultimate choice for orthopaedic implants - A review. Progress in Materials Science 2009;54:397-425.
21. Hallab N, Merritt K, Jacobs JJ. Metal sensitivity in patients with orthopaedic implants. J Bone Joint Surg Am 2001 Mar;83-A(3):428-436.

22. Netter FH HG, Kozinn SC, Wilson PD Jr, Pellicci PM. The Ciba Collection of Medical Illustrations, Vol 8, Musculoskeletal System, Pt. II. In: Freyberg RH HR, Dingle RV., editor. Summit, NJ: Ciba-Geigy Corporation, 1989. p. 235-246.
23. Drees P, Eckardt A, Gay RE, Gay S, Huber LC. Mechanisms of disease: Molecular insights into aseptic loosening of orthopedic implants. Nat Clin Pract Rheumatol 2007 Mar;3(3):165-171.
24. Castner DG, Ratner B. Biomedical surface science: Foundations to frontiers. Surface Science 2002;500:28-60.
25. Israelachvili J. Intermolecular and surface forces. 2nd ed. London: Academic Press, 1991.
26. Garcia AJ, Boettiger D. Integrin-fibronectin interactions at the cell-material interface: initial integrin binding and signaling. Biomaterials 1999 Dec;20(23-24):2427-2433.
27. Davies JE, Hosseini MM. Histodynamics of endosseous wound healing. In: Davies JE, editor. Bone Engineering. Toronto, Canada: em squared inc., 2000. p. 1-14.
28. Anderson JM. The Cellular Cascades of Wound Healing. In: Davies JE, editor. Bone Engineering. Toronto, Canada: em squared inc., 2000. p. 81-93.
29. Chaudhary LR, Hofmeister AM, Hruska KA. Differential growth factor control of bone formation through osteoprogenitor differentiation. Bone 2004 Mar;34(3):402-411.
30. Cochran DL, Nummikoski PV, Higginbottom FL, Hermann JS, Makins SR, Buser D. Evaluation of an endosseous titanium implant with a sandblasted and acid-etched surface in the canine mandible: radiographic results. Clin Oral Implants Res 1996 Sep;7(3):240-252.
31. Boyan BD, Hummert TW, Dean DD, Schwartz Z. Role of material surfaces in regulating bone and cartilage cell response. Biomaterials 1996 Jan;17(2):137-146.
32. Garcia AJ. Get a grip: integrins in cell-biomaterial interactions. Biomaterials 2005 Dec;26(36):7525-7529.
33. Moser M, Legate KR, Zent R, Fassler R. The tail of integrins, talin, and kindlins. Science 2009 May 15;324(5929):895-899.
34. Petrie TA, Garcia AJ. Extracellular matrix-derived ligands for selective integrin binding to control cell function. In: Puleo DA, Bizios R, editors. Biological Interactions on Materials Surfaces. New York, New York: Springer, 2009. p. 133-156.
35. Anselme K. Osteoblast adhesion on biomaterials. Biomaterials 2000 Apr;21(7):667-681.
36. Siebers MC, ter Brugge PJ, Walboomers XF, Jansen JA. Integrins as linker proteins between osteoblasts and bone replacing materials. A critical review. Biomaterials 2005 Jan;26(2):137-146.
37. Sinha RK, Tuan RS. Regulation of human osteoblast integrin expression by orthopedic implant materials. Bone 1996 May;18(5):451-457.
38. Clover J, Dodds RA, Gowen M. Integrin subunit expression by human osteoblasts and osteoclasts in situ and in culture. J Cell Sci 1992 Sep;103 (Pt 1):267-271.
39. Wilson CJ, Clegg RE, Leavesley DI, Pearcy MJ. Mediation of biomaterial-cell interactions by adsorbed proteins: a review. Tissue Eng 2005 Jan-Feb;11(1-2):1-18.
40. Raz P, Lohmann CH, Turner J, Wang L, Poythress N, Blanchard C, et al. 1alpha,25(OH)2D3 regulation of integrin expression is substrate dependent. J Biomed Mater Res A 2004 Nov 1;71(2):217-225.
41. Olivares-Navarrete R, Raz P, Zhao G, Chen J, Wieland M, Cochran DL, et al. Integrin alpha2beta1 plays a critical role in osteoblast response to micron-scale surface structure and surface energy of titanium substrates. Proc Natl Acad Sci U S A 2008 Oct 14;105(41):15767-15772.

42. Garcia AJ, Reyes CD. Bio-adhesive surfaces to promote osteoblast differentiation and bone formation. J Dent Res 2005 May;84(5):407-413.
43. Danen EH, Aota S, van Kraats AA, Yamada KM, Ruiter DJ, van Muijen GN. Requirement for the synergy site for cell adhesion to fibronectin depends on the activation state of integrin alpha 5 beta 1. J Biol Chem 1995 Sep 15;270(37):21612-21618.
44. Giancotti FG, Ruoslahti E. Integrin signaling. Science 1999 Aug 13;285(5430):1028-1032.
45. Harburger DS, Calderwood DA. Integrin signalling at a glance. J Cell Sci 2009 Jan 15;122(Pt 2):159-163.
46. Ridley AJ, Schwartz MA, Burridge K, Firtel RA, Ginsberg MH, Borisy G, et al. Cell migration: integrating signals from front to back. Science 2003 Dec 5;302(5651):1704-1709.
47. Kaabeche K, Guenou H, Bouvard D, Didelot N, Listrat A, Marie PJ. Cbl-mediated ubiquitination of alpha5 integrin subunit mediates fibronectin-dependent osteoblast detachment and apoptosis induced by FGFR2 activation. J Cell Sci 2005 Mar 15;118(Pt 6):1223-1232.
48. Dufour C, Holy X, Marie PJ. Skeletal unloading induces osteoblast apoptosis and targets alpha5beta1-PI3K-Bcl-2 signaling in rat bone. Exp Cell Res 2007 Jan 15;313(2):394-403.
49. Cowles EA, Brailey LL, Gronowicz GA. Integrin-mediated signaling regulates AP-1 transcription factors and proliferation in osteoblasts. J Biomed Mater Res 2000 Dec 15;52(4):725-737.
50. Xiao G, Jiang D, Thomas P, Benson MD, Guan K, Karsenty G, et al. MAPK pathways activate and phosphorylate the osteoblast-specific transcription factor, Cbfa1. J Biol Chem 2000 Feb 11;275(6):4453-4459.
51. Fleet JC. Rapid, membrane-initiated actions of 1,25 dihydroxyvitamin D: what are they and what do they mean? J Nutr 2004 Dec;134(12):3215-3218.
52. Schwartz MA, Ginsberg MH. Networks and crosstalk: integrin signalling spreads. Nat Cell Biol 2002 Apr;4(4):E65-68.
53. Assoian RK, Schwartz MA. Coordinate signaling by integrins and receptor tyrosine kinases in the regulation of G1 phase cell-cycle progression. Curr Opin Genet Dev 2001 Feb;11(1):48-53.
54. Karsenty G. Transcriptional control of skeletogenesis. Annu Rev Genomics Hum Genet 2008;9:183-196.
55. Franceschi RT, Ge C, Xiao G, Roca H, Jiang D. Transcriptional regulation of osteoblasts. Ann N Y Acad Sci 2007 Nov;1116:196-207.
56. Byers BA, Pavlath GK, Murphy TJ, Karsenty G, Garcia AJ. Cell-type-dependent up-regulation of in vitro mineralization after overexpression of the osteoblast-specific transcription factor Runx2/Cbfal. J Bone Miner Res 2002 Nov;17(11):1931-1944.
57. Gersbach CA, Byers BA, Pavlath GK, Garcia AJ. Runx2/Cbfa1 stimulates transdifferentiation of primary skeletal myoblasts into a mineralizing osteoblastic phenotype. Exp Cell Res 2004 Nov 1;300(2):406-417.
58. Jones DC, Wein MN, Oukka M, Hofstaetter JG, Glimcher MJ, Glimcher LH. Regulation of adult bone mass by the zinc finger adapter protein Schnurri-3. Science 2006 May 26;312(5777):1223-1227.
59. Nishio Y, Dong Y, Paris M, O'Keefe RJ, Schwarz EM, Drissi H. Runx2-mediated regulation of the zinc finger Osterix/Sp7 gene. Gene 2006 May 10;372:62-70.
60. Jilka RL, Weinstein RS, Parfitt AM, Manolagas SC. Quantifying osteoblast and osteocyte apoptosis: challenges and rewards. J Bone Miner Res 2007 Oct;22(10):1492-1501.

61. Westendorf JJ, Kahler RA, Schroeder TM. Wnt signaling in osteoblasts and bone diseases. Gene 2004 Oct 27;341:19-39.
62. Wall I, Donos N, Carlqvist K, Jones F, Brett P. Modified titanium surfaces promote accelerated osteogenic differentiation of mesenchymal stromal cells in vitro. Bone 2009 Jul;45(1):17-26.
63. Wan M, Cao X. BMP signaling in skeletal development. Biochem Biophys Res Commun 2005 Mar 18;328(3):651-657.
64. Huang W, Yang S, Shao J, Li YP. Signaling and transcriptional regulation in osteoblast commitment and differentiation. Front Biosci 2007;12:3068-3092.
65. Tamura Y, Takeuchi Y, Suzawa M, Fukumoto S, Kato M, Miyazono K, et al. Focal adhesion kinase activity is required for bone morphogenetic protein--Smad1 signaling and osteoblastic differentiation in murine MC3T3-E1 cells. J Bone Miner Res 2001 Oct;16(10):1772-1779.
66. Shah AK, Lazatin J, Sinha RK, Lennox T, Hickok NJ, Tuan RS. Mechanism of BMP-2 stimulated adhesion of osteoblastic cells to titanium alloy. Biol Cell 1999 Mar;91(2):131-142.
67. Takebe J, Champagne CM, Offenbacher S, Ishibashi K, Cooper LF. Titanium surface topography alters cell shape and modulates bone morphogenetic protein 2 expression in the J774A.1 macrophage cell line. J Biomed Mater Res A 2003 Feb 1;64(2):207-216.
68. Le Guehennec L, Soueidan A, Layrolle P, Amouriq Y. Surface treatments of titanium dental implants for rapid osseointegration. Dent Mater 2007 Jul;23(7):844-854.
69. Boyan BD, Lohmann CH, Dean DD, Sylvia VL, Cochran DL, Schwartz Z. Mechanisms involved in osteoblast response to implant surface morphology. Annual Review of Materials Research 2001;31:357-371.
70. Kieswetter K, Schwartz Z, Dean DD, Boyan BD. The role of implant surface characteristics in the healing of bone. Crit Rev Oral Biol Med 1996;7(4):329-345.
71. Martin JY, Schwartz Z, Hummert TW, Schraub DM, Simpson J, Lankford J, Jr., et al. Effect of titanium surface roughness on proliferation, differentiation, and protein synthesis of human osteoblast-like cells (MG63). J Biomed Mater Res 1995 Mar;29(3):389-401.
72. Zhao G, Zinger O, Schwartz Z, Wieland M, Landolt D, Boyan BD. Osteoblast-like cells are sensitive to submicron-scale surface structure. Clin Oral Implants Res 2006 Jun;17(3):258-264.
73. Mendonca G, Mendonca DB, Aragao FJ, Cooper LF. Advancing dental implant surface technology--from micron- to nanotopography. Biomaterials 2008 Oct;29(28):3822-3835.
74. Zhao G, Raines AL, Wieland M, Schwartz Z, Boyan BD. Requirement for both micron- and submicron scale structure for synergistic responses of osteoblasts to substrate surface energy and topography. Biomaterials 2007 Jun;28(18):2821-2829.
75. Eriksson C, Nygren H, Ohlson K. Implantation of hydrophilic and hydrophobic titanium discs in rat tibia: cellular reactions on the surfaces during the first 3 weeks in bone. Biomaterials 2004 Aug;25(19):4759-4766.
76. Zhao G, Schwartz Z, Wieland M, Rupp F, Geis-Gerstorfer J, Cochran DL, et al. High surface energy enhances cell response to titanium substrate microstructure. J Biomed Mater Res A 2005 Jul 1;74(1):49-58.
77. Keselowsky BG, Collard DM, Garcia AJ. Integrin binding specificity regulates biomaterial surface chemistry effects on cell differentiation. Proc Natl Acad Sci U S A 2005 Apr 26;102(17):5953-5957.

78. Keselowsky BG, Collard DM, Garcia AJ. Surface chemistry modulates fibronectin conformation and directs integrin binding and specificity to control cell adhesion. J Biomed Mater Res A 2003 Aug 1;66(2):247-259.
79. Buser D, Broggini N, Wieland M, Schenk RK, Denzer AJ, Cochran DL, et al. Enhanced bone apposition to a chemically modified SLA titanium surface. J Dent Res 2004 Jul;83(7):529-533.
80. Sun L, Berndt CC, Gross KA, Kucuk A. Material fundamentals and clinical performance of plasma-sprayed hydroxyapatite coatings: a review. J Biomed Mater Res 2001;58(5):570-592.
81. Lee JJ, Rouhfar L, Beirne OR. Survival of hydroxyapatite-coated implants: a meta-analytic review. J Oral Maxillofac Surg 2000 Dec;58(12):1372-1379; discussion 1379-1380.
82. de Assis AF, Beloti MM, Crippa GE, de Oliveira PT, Morra M, Rosa AL. Development of the osteoblastic phenotype in human alveolar bone-derived cells grown on a collagen type I-coated titanium surface. Clin Oral Implants Res 2009 Mar;20(3):240-246.
83. Morra M, Cassinelli C, Cascardo G, Bollati D. Collagen I-Coated Titanium Surfaces for Bone Implantation. In: Puleo DA, Bizios R, editors. Biological Interactions on Materials Surfaces. New York, New York: Springer, 2009.
84. van den Dolder J, Bancroft GN, Sikavitsas VI, Spauwen PH, Mikos AG, Jansen JA. Effect of fibronectin- and collagen I-coated titanium fiber mesh on proliferation and differentiation of osteogenic cells. Tissue Eng 2003 Jun;9(3):505-515.
85. Rammelt S, Schulze E, Bernhardt R, Hanisch U, Scharnweber D, Worch H, et al. Coating of titanium implants with type-I collagen. J Orthop Res 2004 Sep;22(5):1025-1034.
86. Elmengaard B, Bechtold JE, Soballe K. In vivo effects of RGD-coated titanium implants inserted in two bone-gap models. J Biomed Mater Res A 2005 Nov 1;75(2):249-255.
87. Germanier Y, Tosatti S, Broggini N, Textor M, Buser D. Enhanced bone apposition around biofunctionalized sandblasted and acid-etched titanium implant surfaces. A histomorphometric study in miniature pigs. Clin Oral Implants Res 2006 Jun;17(3):251-257.
88. Schuler M, Owen GR, Hamilton DW, de Wild M, Textor M, Brunette DM, et al. Biomimetic modification of titanium dental implant model surfaces using the RGDSP-peptide sequence: a cell morphology study. Biomaterials 2006 Jul;27(21):4003-4015.
89. Barber TA, Ho JE, De Ranieri A, Virdi AS, Sumner DR, Healy KE. Peri-implant bone formation and implant integration strength of peptide-modified p(AAM-co-EG/AAC) interpenetrating polymer network-coated titanium implants. J Biomed Mater Res A 2007 Feb;80(2):306-320.
90. Petrie TA, Raynor JE, Reyes CD, Burns KL, Collard DM, Garcia AJ. The effect of integrin-specific bioactive coatings on tissue healing and implant osseointegration. Biomaterials 2008 Jul;29(19):2849-2857.
91. Petrie TA, Capadona JR, Reyes CD, Garcia AJ. Integrin specificity and enhanced cellular activities associated with surfaces presenting a recombinant fibronectin fragment compared to RGD supports. Biomaterials 2006 Nov;27(31):5459-5470.
92. Gallant ND, Michael KE, Garcia AJ. Cell adhesion strengthening: contributions of adhesive area, integrin binding, and focal adhesion assembly. Mol Biol Cell 2005 Sep;16(9):4329-4340.

93. Tosatti S. Functionalized Titanium Surfaces for Biomedial Applications: Physico-chemical Characterization and Biological In Vitro Evaluation Zurich, Switzerland: Swiss Federal Institute of Technology (ETH Zurich); 2003.
94. Tosatti S, De Paul SM, Askendal A, VandeVondele S, Hubbell JA, Tengvall P, et al. Peptide functionalized poly(L-lysine)-g-poly(ethylene glycol) on titanium: resistance to protein adsorption in full heparinized human blood plasma. Biomaterials 2003 Dec;24(27):4949-4958.
95. Tosatti S, Schwartz Z, Campbell C, Cochran DL, VandeVondele S, Hubbell JA, et al. RGD-containing peptide GCRGYGRGDSPG reduces enhancement of osteoblast differentiation by poly(L-lysine)-graft-poly(ethylene glycol)-coated titanium surfaces. J Biomed Mater Res A 2004 Mar 1;68(3):458-472.
96. Holick MF. Vitamin D deficiency. N Engl J Med 2007 Jul 19;357(3):266-281.
97. Chapuy MC, Arlot ME, Duboeuf F, Brun J, Crouzet B, Arnaud S, et al. Vitamin D3 and calcium to prevent hip fractures in the elderly women. N Engl J Med 1992 Dec 3;327(23):1637-1642.
98. Jackson RD, LaCroix AZ, Gass M, Wallace RB, Robbins J, Lewis CE, et al. Calcium plus vitamin D supplementation and the risk of fractures. N Engl J Med 2006 Feb 16;354(7):669-683.
99. Kelly J, Lin A, Wang CJ, Park S, Nishimura I. Vitamin D and Bone Physiology: Demonstration of Vitamin D Deficiency in an Implant Osseointegration Rat Model. J Prosthodont 2009 Mar 26.
100. Holick MF. Evolution and function of vitamin D. Recent Results Cancer Res 2003;164:3-28.
101. Christakos S, Dhawan P, Liu Y, Peng X, Porta A. New insights into the mechanisms of vitamin D action. J Cell Biochem 2003 Mar 1;88(4):695-705.
102. Wang L, Zhao G, Olivares-Navarrete R, Bell BF, Wieland M, Cochran DL, et al. Integrin beta1 silencing in osteoblasts alters substrate-dependent responses to 1,25-dihydroxy vitamin D3. Biomaterials 2006 Jul;27(20):3716-3725.
103. DeLuca HF, Zierold C. Mechanisms and functions of vitamin D. Nutr Rev 1998 Feb;56(2 Pt 2):S4-10; discussion S 54-75.
104. Norman AW. Minireview: vitamin D receptor: new assignments for an already busy receptor. Endocrinology 2006 Dec;147(12):5542-5548.
105. Jurutka PW, Bartik L, Whitfield GK, Mathern DR, Barthel TK, Gurevich M, et al. Vitamin D receptor: key roles in bone mineral pathophysiology, molecular mechanism of action, and novel nutritional ligands. J Bone Miner Res 2007 Dec;22 Suppl 2:V2-10.
106. Wang TT, Tavera-Mendoza LE, Laperriere D, Libby E, MacLeod NB, Nagai Y, et al. Large-scale in silico and microarray-based identification of direct 1,25-dihydroxyvitamin D3 target genes. Mol Endocrinol 2005 Nov;19(11):2685-2695.
107. Pike JW, Meyer MB, Watanuki M, Kim S, Zella LA, Fretz JA, et al. Perspectives on mechanisms of gene regulation by 1,25-dihydroxyvitamin D3 and its receptor. J Steroid Biochem Mol Biol 2007 Mar;103(3-5):389-395.
108. Haussler MR, Haussler CA, Bartik L, Whitfield GK, Hsieh JC, Slater S, et al. Vitamin D receptor: molecular signaling and actions of nutritional ligands in disease prevention. Nutr Rev 2008 Oct;66(10 Suppl 2):S98-112.
109. Farach-Carson MC, Sergeev I, Norman AW. Nongenomic actions of 1,25-dihydroxyvitamin D3 in rat osteosarcoma cells: structure-function studies using ligand analogs. Endocrinology 1991 Oct;129(4):1876-1884.
110. Boyan BD, Dean DD, Sylvia VL, Schwartz Z. Steroid hormone action in musculoskeletal cells involves membrane receptor and nuclear receptor mechanisms. Connect Tissue Res 2003;44 Suppl 1:130-135.

111. Farach-Carson MC, Nemere I. Membrane receptors for vitamin D steroid hormones: potential new drug targets. Curr Drug Targets 2003 Jan;4(1):67-76.
112. Wali RK, Kong J, Sitrin MD, Bissonnette M, Li YC. Vitamin D receptor is not required for the rapid actions of 1,25-dihydroxyvitamin D3 to increase intracellular calcium and activate protein kinase C in mouse osteoblasts. J Cell Biochem 2003 Mar 1;88(4):794-801.
113. Khanal RC, Nemere I. The ERp57/GRp58/1,25D3-MARRS receptor: multiple functional roles in diverse cell systems. Curr Med Chem 2007;14(10):1087-1093.
114. Khanal R, Nemere I. Membrane receptors for vitamin D metabolites. Crit Rev Eukaryot Gene Expr 2007;17(1):31-47.
115. Nemere I, Schwartz Z, Pedrozo H, Sylvia VL, Dean DD, Boyan BD. Identification of a membrane receptor for 1,25-dihydroxyvitamin D3 which mediates rapid activation of protein kinase C. J Bone Miner Res 1998 Sep;13(9):1353-1359.
116. Nemere I, Farach-Carson MC, Rohe B, Sterling TM, Norman AW, Boyan BD, et al. Ribozyme knockdown functionally links a 1,25(OH)2D3 membrane binding protein (1,25D3-MARRS) and phosphate uptake in intestinal cells. Proc Natl Acad Sci U S A 2004 May 11;101(19):7392-7397.
117. Boyan BD, Wong KL, Wang L, Yao H, Guldberg RE, Drab M, et al. Regulation of growth plate chondrocytes by 1,25-dihydroxyvitamin D3 requires caveolae and caveolin-1. J Bone Miner Res 2006 Oct;21(10):1637-1647.
118. Schwartz Z, Graham EJ, Wang L, Lossdorfer S, Gay I, Johnson-Pais TL, et al. Phospholipase A2 activating protein (PLAA) is required for 1alpha,25(OH)2D3 signaling in growth plate chondrocytes. J Cell Physiol 2005 Apr;203(1):54-70.
119. Sylvia VL, Schwartz Z, Curry DB, Chang Z, Dean DD, Boyan BD. 1,25(OH)2D3 regulates protein kinase C activity through two phospholipid-dependent pathways involving phospholipase A2 and phospholipase C in growth zone chondrocytes. J Bone Miner Res 1998 Apr;13(4):559-569.
120. Schwartz Z, Ehland H, Sylvia VL, Larsson D, Hardin RR, Bingham V, et al. 1alpha,25-dihydroxyvitamin D(3) and 24R,25-dihydroxyvitamin D(3) modulate growth plate chondrocyte physiology via protein kinase C-dependent phosphorylation of extracellular signal-regulated kinase 1/2 mitogen-activated protein kinase. Endocrinology 2002 Jul;143(7):2775-2786.
121. Li YC, Pirro AE, Amling M, Delling G, Baron R, Bronson R, et al. Targeted ablation of the vitamin D receptor: an animal model of vitamin D-dependent rickets type II with alopecia. Proc Natl Acad Sci U S A 1997 Sep 2;94(18):9831-9835.
122. Boyan BD, Wong KL, Fang M, Schwartz Z. 1alpha,25(OH)2D3 is an autocrine regulator of extracellular matrix turnover and growth factor release via ERp60 activated matrix vesicle metalloproteinases. J Steroid Biochem Mol Biol 2007 Mar;103(3-5):467-472.
123. Jurutka PW, Whitfield GK, Hsieh JC, Thompson PD, Haussler CA, Haussler MR. Molecular nature of the vitamin D receptor and its role in regulation of gene expression. Rev Endocr Metab Disord 2001 Apr;2(2):203-216.
124. Hsieh JC, Jurutka PW, Galligan MA, Terpening CM, Haussler CA, Samuels DS, et al. Human vitamin D receptor is selectively phosphorylated by protein kinase C on serine 51, a residue crucial to its trans-activation function. Proc Natl Acad Sci U S A 1991 Oct 15;88(20):9315-9319.
125. Qi X, Pramanik R, Wang J, Schultz RM, Maitra RK, Han J, et al. The p38 and JNK pathways cooperate to trans-activate vitamin D receptor via c-Jun/AP-1 and sensitize human breast cancer cells to vitamin D(3)-induced growth inhibition. J Biol Chem 2002 Jul 19;277(29):25884-25892.

126. Ellison TI, Dowd DR, MacDonald PN. Calmodulin-dependent kinase IV stimulates vitamin D receptor-mediated transcription. Mol Endocrinol 2005 Sep;19(9):2309-2319.
127. Simboli-Campbell M, Gagnon A, Franks DJ, Welsh J. 1,25-Dihydroxyvitamin D3 translocates protein kinase C beta to nucleus and enhances plasma membrane association of protein kinase C alpha in renal epithelial cells. J Biol Chem 1994 Feb 4;269(5):3257-3264.
128. Farach-Carson MC, Bergh JJ, Xu Y. Integrating rapid responses to 1,25-dihydroxyvitamin D3 with transcriptional changes in osteoblasts: Ca2+ regulated pathways to the nucleus. Steroids 2004 Aug;69(8-9):543-547.
129. Parton RG, Simons K. The multiple faces of caveolae. Nat Rev Mol Cell Biol 2007 Mar;8(3):185-194.
130. Parton RG. Caveolae--from ultrastructure to molecular mechanisms. Nat Rev Mol Cell Biol 2003 Feb;4(2):162-167.
131. Thomas CM, Smart EJ. Caveolae structure and function. J Cell Mol Med 2008 Jun;12(3):796-809.
132. Pike LJ. Growth factor receptors, lipid rafts and caveolae: an evolving story. Biochim Biophys Acta 2005 Dec 30;1746(3):260-273.
133. Nohe A, Keating E, Underhill TM, Knaus P, Petersen NO. Dynamics and interaction of caveolin-1 isoforms with BMP-receptors. J Cell Sci 2005 Feb 1;118(Pt 3):643-650.
134. Sawada N, Taketani Y, Amizuka N, Ichikawa M, Ogawa C, Nomoto K, et al. Caveolin-1 in extracellular matrix vesicles secreted from osteoblasts. Bone 2007 Jul;41(1):52-58.
135. Le Lay S, Kurzchalia TV. Getting rid of caveolins: phenotypes of caveolin-deficient animals. Biochim Biophys Acta 2005 Dec 30;1746(3):322-333.
136. Serra M, Scotlandi K. Caveolins in the development and diseases of musculoskeletal system. Cancer Lett 2009 Apr 2.
137. Rubin J, Schwartz Z, Boyan BD, Fan X, Case N, Sen B, et al. Caveolin-1 knockout mice have increased bone size and stiffness. J Bone Miner Res 2007 Sep;22(9):1408-1418.
138. Salanueva IJ, Cerezo A, Guadamillas MC, del Pozo MA. Integrin regulation of caveolin function. J Cell Mol Med 2007 Sep-Oct;11(5):969-980.
139. Galbiati F, Volonte D, Brown AM, Weinstein DE, Ben-Ze'ev A, Pestell RG, et al. Caveolin-1 expression inhibits Wnt/beta-catenin/Lef-1 signaling by recruiting beta-catenin to caveolae membrane domains. J Biol Chem 2000 Jul 28;275(30):23368-23377.
140. Boyd ND, Chan BM, Petersen NO. Beta1 integrins are distributed in adhesion structures with fibronectin and caveolin and in coated pits. Biochem Cell Biol 2003 Oct;81(5):335-348.
141. Huhtakangas JA, Olivera CJ, Bishop JE, Zanello LP, Norman AW. The vitamin D receptor is present in caveolae-enriched plasma membranes and binds 1 alpha,25(OH)2-vitamin D3 in vivo and in vitro. Mol Endocrinol 2004 Nov;18(11):2660-2671.
142. Wei Y, Yang X, Liu Q, Wilkins JA, Chapman HA. A role for caveolin and the urokinase receptor in integrin-mediated adhesion and signaling. J Cell Biol 1999 Mar 22;144(6):1285-1294.
143. Grande-Garcia A, Echarri A, de Rooij J, Alderson NB, Waterman-Storer CM, Valdivielso JM, et al. Caveolin-1 regulates cell polarization and directional migration through Src kinase and Rho GTPases. J Cell Biol 2007 May 21;177(4):683-694.

144. Goetz JG, Joshi B, Lajoie P, Strugnell SS, Scudamore T, Kojic LD, et al. Concerted regulation of focal adhesion dynamics by galectin-3 and tyrosine-phosphorylated caveolin-1. J Cell Biol 2008 Mar 24;180(6):1261-1275.
145. del Pozo MA, Balasubramanian N, Alderson NB, Kiosses WB, Grande-Garcia A, Anderson RG, et al. Phospho-caveolin-1 mediates integrin-regulated membrane domain internalization. Nat Cell Biol 2005 Sep;7(9):901-908.
146. Hamidouchea Z, Fromiguea O, Ringeb J, Hauplb T, Vaudinc P, Sroujid S, et al. Priming integrin alpha5 promotes human mesenchymal stromal cell osteoblast differentiation and osteogenesis. ECTS 36th European Symposium on Calcified Tissues; 2009 May 23-27; Vienna, Austria; 2009.
147. Zhao G. Interaction of Surface Energy and Microarchitecture in Determining Cell and Tissue Response to Biomaterials. Atlanta, GA: Georgia Institute of Technology; 2007.
148. Steinemann SG, Claes, L., inventor; Institut Straumann AG, assignee. Metallic implant anchorable to bone tissue for replacing a broken diseased bone. United States Patent No. 5456723 August 17, 1992.
149. Zinger O, Zhao G, Schwartz Z, Simpson J, Wieland M, Landolt D, et al. Differential regulation of osteoblasts by substrate microstructural features. Biomaterials 2005 May;26(14):1837-1847.
150. Boyan BD, Schwartz Z, Lohmann CH, Sylvia VL, Cochran DL, Dean DD, et al. Pretreatment of bone with osteoclasts affects phenotypic expression of osteoblast-like cells. J Orthop Res 2003 Jul;21(4):638-647.
151. Schuler M. Multifunctional Titanium Dental Implant Surface Based on Biochemically Modified Molecular Assembly Systems. Zurich, Switzerland: Swiss Federal Institute of Technology (ETH Zurich); 2006.
152. Ducy P, Desbois C, Boyce B, Pinero G, Story B, Dunstan C, et al. Increased bone formation in osteocalcin-deficient mice. Nature 1996 Aug 1;382(6590):448-452.
153. Atkin I, Dean DD, Muniz OE, Agundez A, Castiglione G, Cohen G, et al. Enhancement of osteoinduction by vitamin D metabolites in rachitic host rats. J Bone Miner Res 1992 Aug;7(8):863-875.
154. Bucay N, Sarosi I, Dunstan CR, Morony S, Tarpley J, Capparelli C, et al. osteoprotegerin-deficient mice develop early onset osteoporosis and arterial calcification. Genes Dev 1998 May 1;12(9):1260-1268.
155. Lim YJ, Oshida Y, Andres CJ, Barco MT. Surface characterizations of variously treated titanium materials. Int J Oral Maxillofac Implants 2001 May-Jun;16(3):333-342.
156. Francois P, Vaudaux P, Taborelli M, Tonetti M, Lew DP, Descouts P. Influence of surface treatments developed for oral implants on the physical and biological properties of titanium. (II) Adsorption isotherms and biological activity of immobilized fibronectin. Clin Oral Implants Res 1997 Jun;8(3):217-225.
157. Schwartz Z, Lohmann CH, Oefinger J, Bonewald LF, Dean DD, Boyan BD. Implant surface characteristics modulate differentiation behavior of cells in the osteoblastic lineage. Adv Dent Res 1999 Jun;13:38-48.
158. Lohmann CH, Tandy EM, Sylvia VL, Hell-Vocke AK, Cochran DL, Dean DD, et al. Response of normal female human osteoblasts (NHOst) to 17beta-estradiol is modulated by implant surface morphology. J Biomed Mater Res 2002 Nov;62(2):204-213.
159. Boyan BD, Batzer R, Kieswetter K, Liu Y, Cochran DL, Szmuckler-Moncler S, et al. Titanium surface roughness alters responsiveness of MG63 osteoblast-like cells to 1 alpha,25-(OH)2D3. J Biomed Mater Res 1998 Jan;39(1):77-85.

160. Xiao G, Wang D, Benson MD, Karsenty G, Franceschi RT. Role of the alpha2-integrin in osteoblast-specific gene expression and activation of the Osf2 transcription factor. J Biol Chem 1998 Dec 4;273(49):32988-32994.
161. Takeuchi Y, Suzawa M, Kikuchi T, Nishida E, Fujita T, Matsumoto T. Differentiation and transforming growth factor-beta receptor down-regulation by collagen-alpha2beta1 integrin interaction is mediated by focal adhesion kinase and its downstream signals in murine osteoblastic cells. J Biol Chem 1997 Nov 14;272(46):29309-29316.
162. Dedhar S. Signal transduction via the beta 1 integrins is a required intermediate in interleukin-1 beta induction of alkaline phosphatase activity in human osteosarcoma cells. Exp Cell Res 1989 Jul;183(1):207-214.
163. Dedhar S, Argraves WS, Suzuki S, Ruoslahti E, Pierschbacher MD. Human osteosarcoma cells resistant to detachment by an Arg-Gly-Asp-containing peptide overproduce the fibronectin receptor. J Cell Biol 1987 Sep;105(3):1175-1182.
164. Gronowicz G, McCarthy MB. Response of human osteoblasts to implant materials: integrin-mediated adhesion. J Orthop Res 1996 Nov;14(6):878-887.
165. Nakayamada S, Okada Y, Saito K, Tamura M, Tanaka Y. Beta1 integrin/focal adhesion kinase-mediated signaling induces intercellular adhesion molecule 1 and receptor activator of nuclear factor kappaB ligand on osteoblasts and osteoclast maturation. J Biol Chem 2003 Nov 14;278(46):45368-45374.
166. Saito T, Albelda SM, Brighton CT. Identification of integrin receptors on cultured human bone cells. J Orthop Res 1994 May;12(3):384-394.
167. Rychly J, Pommerenke H, Durr F, Schreiber E, Nebe B. Analysis of spatial distributions of cellular molecules during mechanical stressing of cell surface receptors using confocal microscopy. Cell Biol Int 1998;22(1):7-12.
168. Henning W, Bohn W, Nebe B, Knopp A, Rychly J, Strauss M. Local increase of beta 1-integrin expression in cocultures of immortalized hepatocytes and sinusoidal endothelial cells. Eur J Cell Biol 1994 Oct;65(1):189-199.
169. McManus MT, Sharp PA. Gene silencing in mammals by small interfering RNAs. Nat Rev Genet 2002 Oct;3(10):737-747.
170. Paul CP, Good PD, Winer I, Engelke DR. Effective expression of small interfering RNA in human cells. Nat Biotechnol 2002 May;20(5):505-508.
171. Stein GS, Lian JB, Stein JL, Van Wijnen AJ, Montecino M. Transcriptional control of osteoblast growth and differentiation. Physiol Rev 1996 Apr;76(2):593-629.
172. Hughes DE, Salter DM, Dedhar S, Simpson R. Integrin expression in human bone. J Bone Miner Res 1993 May;8(5):527-533.
173. Boyan BD, Lohmann CH, Sisk M, Liu Y, Sylvia VL, Cochran DL, et al. Both cyclooxygenase-1 and cyclooxygenase-2 mediate osteoblast response to titanium surface roughness. J Biomed Mater Res 2001 Jun 5;55(3):350-359.
174. Lossdorfer S, Schwartz Z, Wang L, Lohmann CH, Turner JD, Wieland M, et al. Microrough implant surface topographies increase osteogenesis by reducing osteoclast formation and activity. J Biomed Mater Res A 2004 Sep 1;70(3):361-369.
175. Schwartz Z, Lohmann CH, Sisk M, Cochran DL, Sylvia VL, Simpson J, et al. Local factor production by MG63 osteoblast-like cells in response to surface roughness and 1,25-(OH)2D3 is mediated via protein kinase C- and protein kinase A-dependent pathways. Biomaterials 2001 Apr;22(7):731-741.
176. Cancela L, Nemere I, Norman AW. 1 alpha,25(OH)2 vitamin D3: a steroid hormone capable of producing pleiotropic receptor-mediated biological responses by both genomic and nongenomic mechanisms. J Steroid Biochem 1988;30(1-6):33-39.

177. Boyan BD, Wang L, Wong KL, Jo H, Schwartz Z. Plasma membrane requirements for 1alpha,25(OH)2D3 dependent PKC signaling in chondrocytes and osteoblasts. Steroids 2006 Apr;71(4):286-290.
178. Keselowsky BG, Wang L, Schwartz Z, Garcia AJ, Boyan BD. Integrin alpha(5) controls osteoblastic proliferation and differentiation responses to titanium substrates presenting different roughness characteristics in a roughness independent manner. J Biomed Mater Res A 2007 Mar 1;80(3):700-710.
179. Morra M. Biochemical modification of titanium surfaces: peptides and ECM proteins. Eur Cell Mater 2006;12:1-15.
180. Meyer A, Auernheimer J, Modlinger A, Kessler H. Targeting RGD recognizing integrins: drug development, biomaterial research, tumor imaging and targeting. Curr Pharm Des 2006;12(22):2723-2747.
181. Ruoslahti E, Pierschbacher MD. New perspectives in cell adhesion: RGD and integrins. Science 1987 Oct 23;238(4826):491-497.
182. Ruoslahti E. RGD and other recognition sequences for integrins. Annu Rev Cell Dev Biol 1996;12:697-715.
183. Pierschbacher MD, Ruoslahti E. Cell Attachment Activity of Fibronectin Can Be Duplicated by Small Synthetic Fragments of the Molecule. Nature 1984;309(5963):30-33.
184. Cutler SM, Garcia AJ. Engineering cell adhesive surfaces that direct integrin alpha5beta1 binding using a recombinant fragment of fibronectin. Biomaterials 2003 May;24(10):1759-1770.
185. Zreiqat H, Akin FA, Howlett CR, Markovic B, Haynes D, Lateef S, et al. Differentiation of human bone-derived cells grown on GRGDSP-peptide bound titanium surfaces. J Biomed Mater Res A 2003 Jan 1;64(1):105-113.
186. Dettin M, Conconi MT, Gambaretto R, Pasquato A, Folin M, Di Bello C, et al. Novel osteoblast-adhesive peptides for dental/orthopedic biomaterials. J Biomed Mater Res 2002 Jun 5;60(3):466-471.
187. Healy KE, Rezania A, Stile RA. Designing biomaterials to direct biological responses. Ann N Y Acad Sci 1999 Jun 18;875:24-35.
188. Reyes CD, Garcia AJ. Alpha2beta1 integrin-specific collagen-mimetic surfaces supporting osteoblastic differentiation. J Biomed Mater Res A 2004 Jun 15;69(4):591-600.
189. Cavalcanti-Adam EA, Volberg T, Micoulet A, Kessler H, Geiger B, Spatz JP. Cell spreading and focal adhesion dynamics are regulated by spacing of integrin ligands. Biophys J 2007 Apr 15;92(8):2964-2974.
190. Cavalcanti-Adam EA, Micoulet A, Blummel J, Auernheimer J, Kessler H, Spatz JP. Lateral spacing of integrin ligands influences cell spreading and focal adhesion assembly. Eur J Cell Biol 2006 Apr;85(3-4):219-224.
191. Cardin AD, Weintraub HJR. Molecular Modeling of Protein-Glycosaminoglycan Interactions. Arteriosclerosis 1989 Jan-Feb;9(1):21-32.
192. Dee KC, Andersen TT, Bizios R. Design and function of novel osteoblast-adhesive peptides for chemical modification of biomaterials. Journal of Biomedical Materials Research 1998 Jun 5;40(3):371-377.
193. Boyan BD, Schwartz Z, Hambleton JC. Response of bone and cartilage cells to biomaterials in vivo and in vitro. J Oral Implantol 1993;19(2):116-122; discussion 136-117.
194. Mrksich M, Whitesides GM. Using self-assembled monolayers to understand the interactions of man-made surfaces with proteins and cells. Annual Review of Biophysics and Biomolecular Structure 1996;25:55-78.

195. Huang NP, Michel R, Voros J, Textor M, Hofer R, Rossi A, et al. Poly(L-lysine)-g-poly(ethylene glycol) layers on metal oxide surfaces: Surface-analytical characterization and resistance to serum and fibrinogen adsorption. Langmuir 2001 Jan 23;17(2):489-498.
196. Pasche S, De Paul SM, Voros J, Spencer ND, Textor M. Poly(L-lysine)-graft-poly(ethylene glycol) assembled monolayers on niobium oxide surfaces: A quantitative study of the influence of polymer interfacial architecture on resistance to protein adsorption by ToF-SIMS and in situ OWLS. Langmuir 2003 Oct 28;19(22):9216-9225.
197. Schuler M, Hamilton DW, Kunzler TP, Sprecher CM, de Wild M, Brunette DM, et al. Comparison of the response of cultured osteoblasts and osteoblasts outgrown from rat calvarial bone chips to nonfouling KRSR and FHRRIKA-peptide modified rough titanium surfaces. J Biomed Mater Res B Appl Biomater 2009 Jul 6.
198. Lee JY, Choo JE, Choi YS, Lee KY, Min DS, Pi SH, et al. Characterization of the surface immobilized synthetic heparin binding domain derived from human fibroblast growth factor-2 and its effect on osteoblast differentiation. J Biomed Mater Res A 2007 Jun 19.
199. Dalton BA, McFarland CD, Underwood PA, Steele JG. Role of the heparin binding domain of fibronectin in attachment and spreading of human bone-derived cells. J Cell Sci 1995 May;108 (Pt 5):2083-2092.
200. Sharma A, Askari JA, Humphries MJ, Jones EY, Stuart DI. Crystal structure of a heparin- and integrin-binding segment of human fibronectin. EMBO J 1999 Mar 15;18(6):1468-1479.
201. Kochupillai N. The physiology of vitamin D : current concepts. Indian J Med Res 2008 Mar;127(3):256-262.
202. Schwartz Z, Nasazky E, Boyan BD. Surface microtopography regulates osteointegration: the role of implant surface microtopography in osteointegration. Alpha Omegan 2005 Jul;98(2):9-19.
203. Haussler MR, Jurutka PW, Hsieh JC, Thompson PD, Selznick SH, Haussler CA, et al. New understanding of the molecular mechanism of receptor-mediated genomic actions of the vitamin D hormone. Bone 1995 Aug;17(2 Suppl):33S-38S.
204. Boyan BD, Sylvia VL, Dean DD, Pedrozo H, Del Toro F, Nemere I, et al. 1,25-(OH)2D3 modulates growth plate chondrocytes via membrane receptor-mediated protein kinase C by a mechanism that involves changes in phospholipid metabolism and the action of arachidonic acid and PGE2. Steroids 1999 Jan-Feb;64(1-2):129-136.
205. Li YC, Amling M, Pirro AE, Priemel M, Meuse J, Baron R, et al. Normalization of mineral ion homeostasis by dietary means prevents hyperparathyroidism, rickets, and osteomalacia, but not alopecia in vitamin D receptor-ablated mice. Endocrinology 1998 Oct;139(10):4391-4396.
206. Panda DK, Miao D, Bolivar I, Li J, Huo R, Hendy GN, et al. Inactivation of the 25-hydroxyvitamin D 1alpha-hydroxylase and vitamin D receptor demonstrates independent and interdependent effects of calcium and vitamin D on skeletal and mineral homeostasis. J Biol Chem 2004 Apr 16;279(16):16754-16766.
207. Gardiner EM, Baldock PA, Thomas GP, Sims NA, Henderson NK, Hollis B, et al. Increased formation and decreased resorption of bone in mice with elevated vitamin D receptor in mature cells of the osteoblastic lineage. FASEB J 2000 Oct;14(13):1908-1916.
208. Sooy K, Sabbagh Y, Demay MB. Osteoblasts lacking the vitamin D receptor display enhanced osteogenic potential in vitro. J Cell Biochem 2005 Jan 1;94(1):81-87.
209. Galbiati F, Volonte D, Engelman JA, Watanabe G, Burk R, Pestell RG, et al. Targeted downregulation of caveolin-1 is sufficient to drive cell transformation and

hyperactivate the p42/44 MAP kinase cascade. EMBO J 1998 Nov 16;17(22):6633-6648.
210. Chen YG. Endocytic regulation of TGF-beta signaling. Cell Res 2009 Jan;19(1):58-70.
211. Boyan BD, Schwartz Z. Rapid vitamin D-dependent PKC signaling shares features with estrogen-dependent PKC signaling in cartilage and bone. Steroids 2004 Aug;69(8-9):591-597.
212. Boyan BD, Jennings EG, Wang L, Schwartz Z. Mechanisms regulating differential activation of membrane-mediated signaling by 1alpha,25(OH)2D3 and 24R,25(OH)2D3. J Steroid Biochem Mol Biol 2004 May;89-90(1-5):309-315.
213. Norman AW, Mizwicki MT, Norman DP. Steroid-hormone rapid actions, membrane receptors and a conformational ensemble model. Nat Rev Drug Discov 2004 Jan;3(1):27-41.

APPENDIX

Selected Gene Expression in VDR (+/+) and VDR(-/-) Osteoblasts on Surfaces

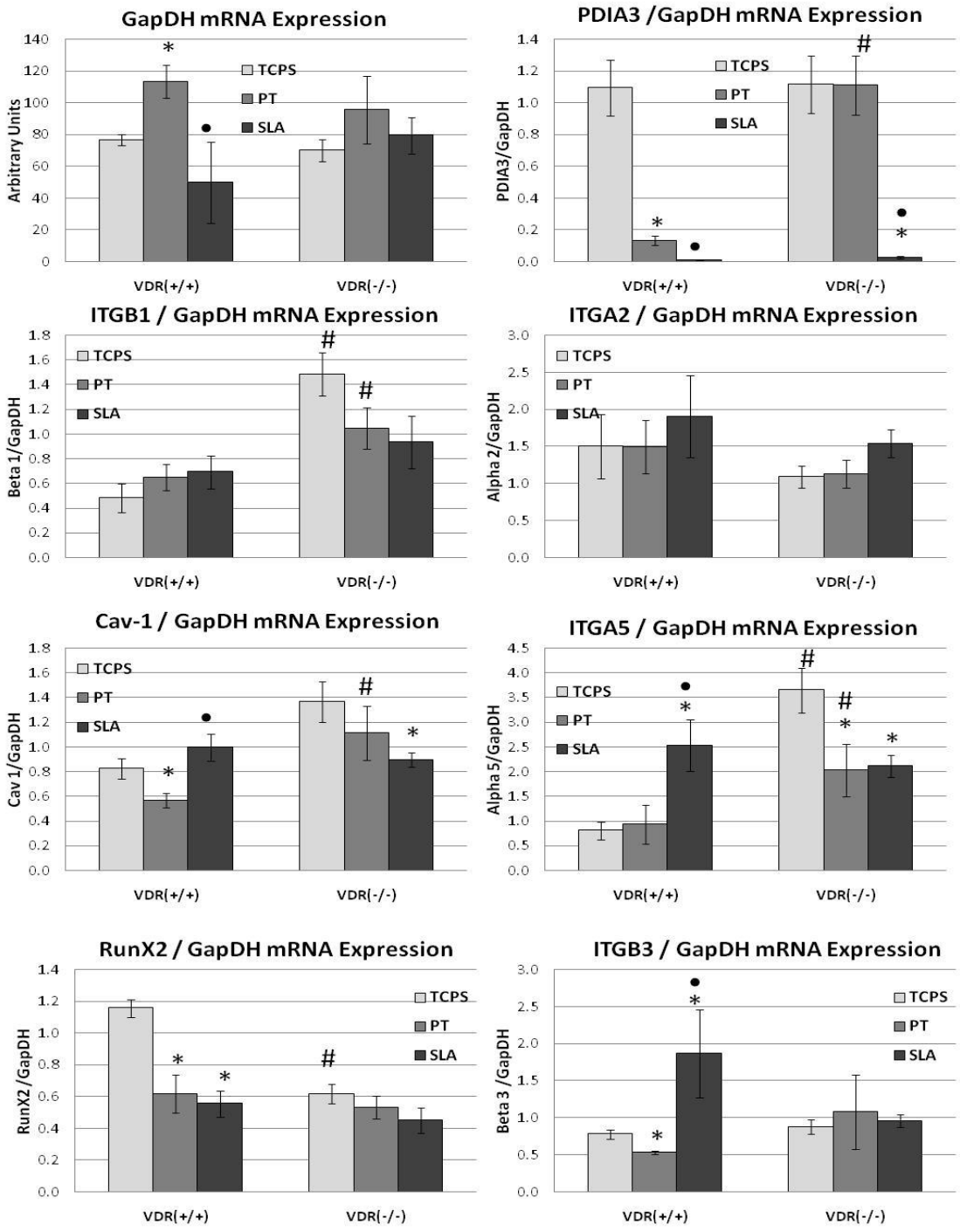

Figure A-1: Effect of changing surface roughness on expression of GapDH (Control), Pdia3, integrin beta 1, integrin alpha 2, integrin alpha 5, caveolin-1, Runx2, and integrin beta 3 in osteoblasts harvested from VDR(+/+) and VDR(-/-) mice. Statistics: * Surface vs. TCPS; • SLA vs. PT; # WT vs. KO. Significant if $p < 0.05$. Experiment #1.

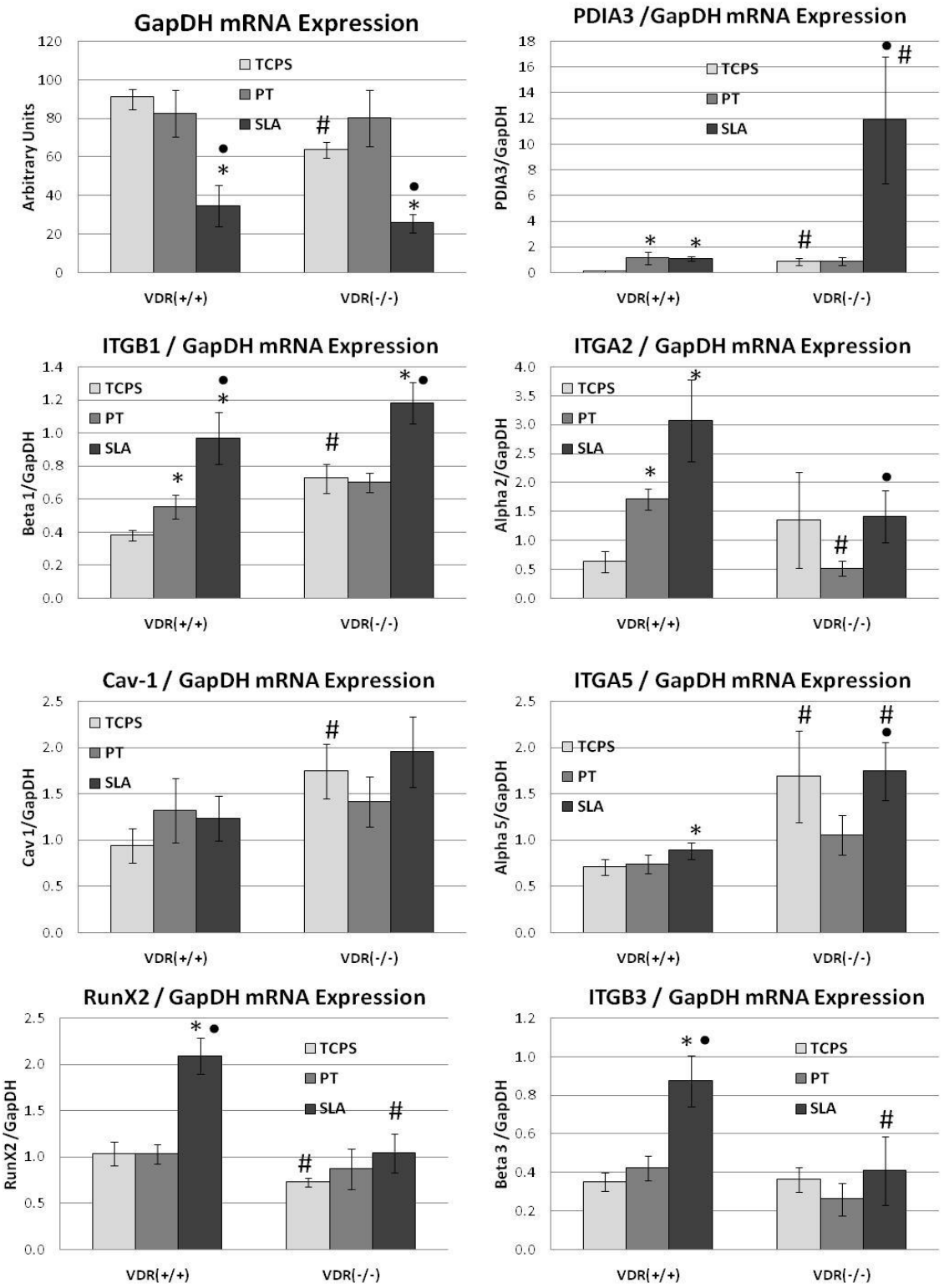

Figure A-2: Effect of changing surface roughness on expression of GapDH (Control), Pdia3, integrin beta 1, integrin alpha 2, integrin alpha 5, caveolin-1, Runx2, and integrin beta 3 in osteoblasts harvested from VDR(+/+) and VDR(-/-) mice. Statistics: * Surface vs. TCPS; • SLA vs. PT; # WT vs. KO. Significant if $p < 0.05$. Experiment #2.

Selected Gene Expression in VDR (+/+) and VDR(-/-) Osteoblasts ± 1α25(OH)$_2$D$_3$

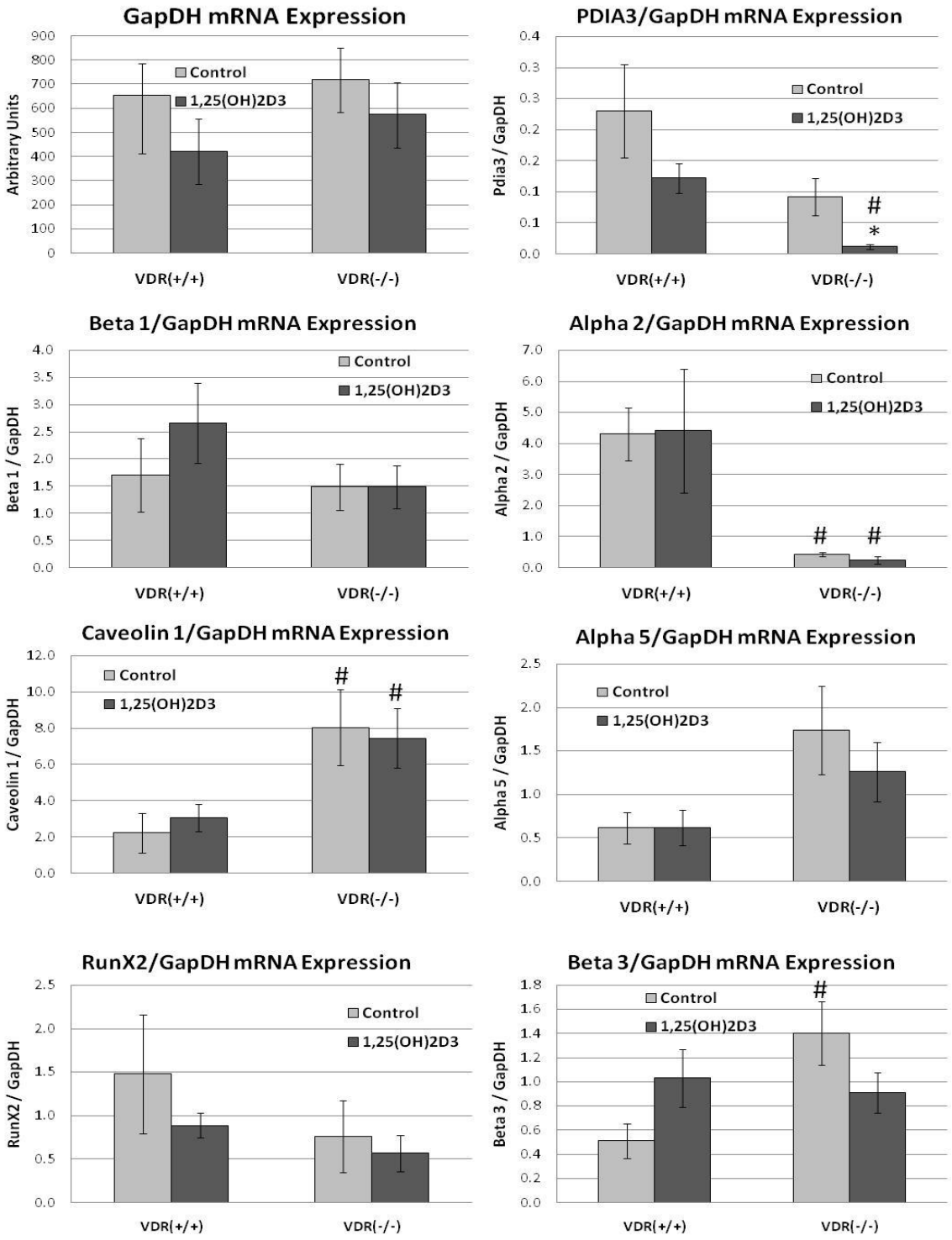

Figure A-3: Effect of 1α25(OH)$_2$D$_3$ on expression of GapDH (Control), Pdia3, integrin beta 1, integrin alpha 2, integrin alpha 5, caveolin-1, Runx2, and integrin beta 3 in osteoblasts harvested from VDR(+/+) and VDR(-/-) mice. Statistics: * Control vs. 1α25(OH)$_2$D$_3$; # WT vs. KO. Significant if $p < 0.05$. Experiment #1.

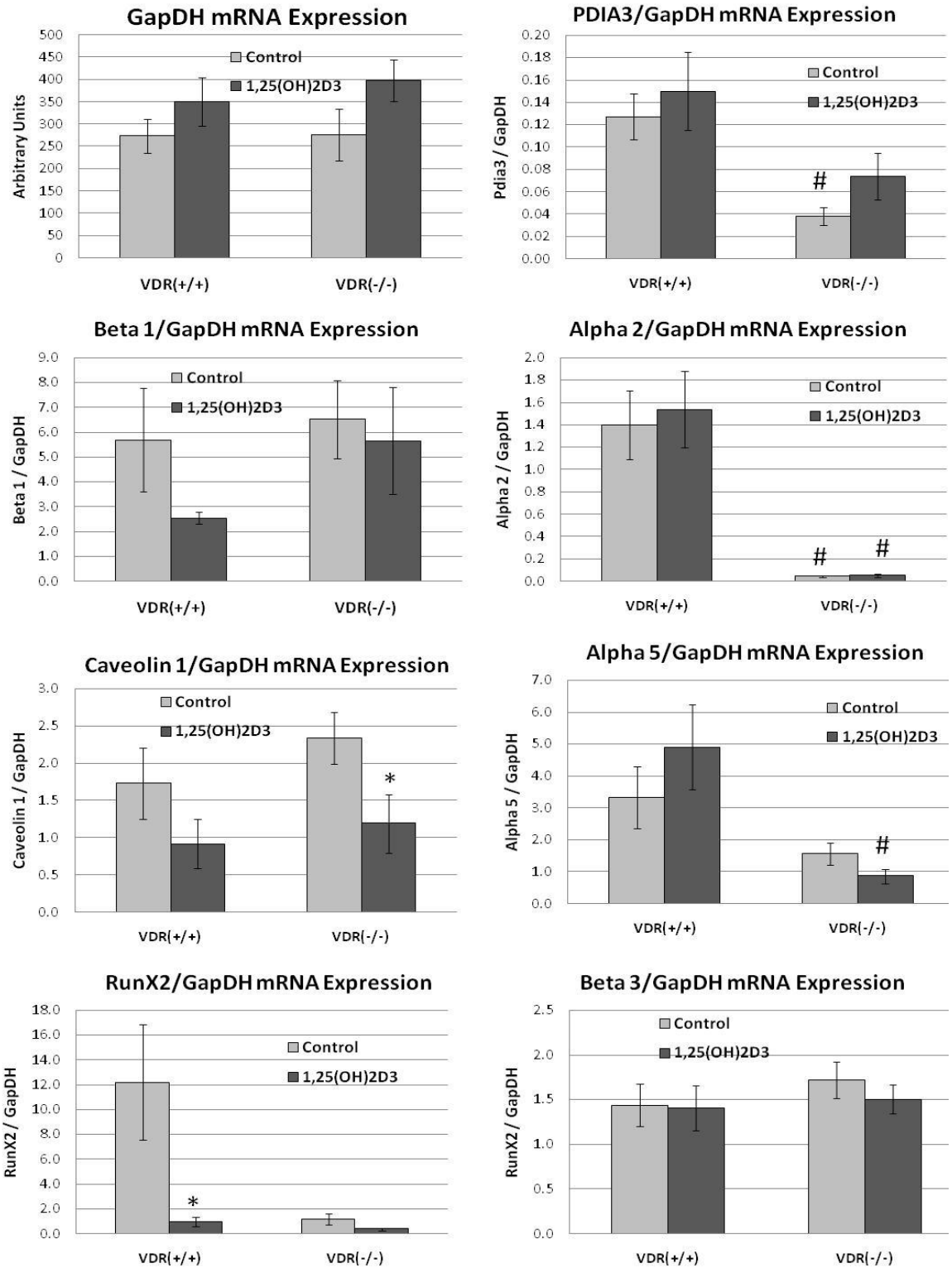

Figure A-4: Effect of $1\alpha25(OH)_2D_3$ on expression of GapDH (Control), Pdia3, integrin beta 1, integrin alpha 2, integrin alpha 5, caveolin-1, Runx2, and integrin beta 3 in osteoblasts harvested from VDR(+/+) and VDR(-/-) mice. Statistics: * Control vs. $1\alpha25(OH)_2D_3$; # WT vs. KO. Significant if $p < 0.05$. Experiment #2.

Selected Gene Expression in Cav-1 (+/+) and Cav-1(-/-) Osteoblasts on Surfaces

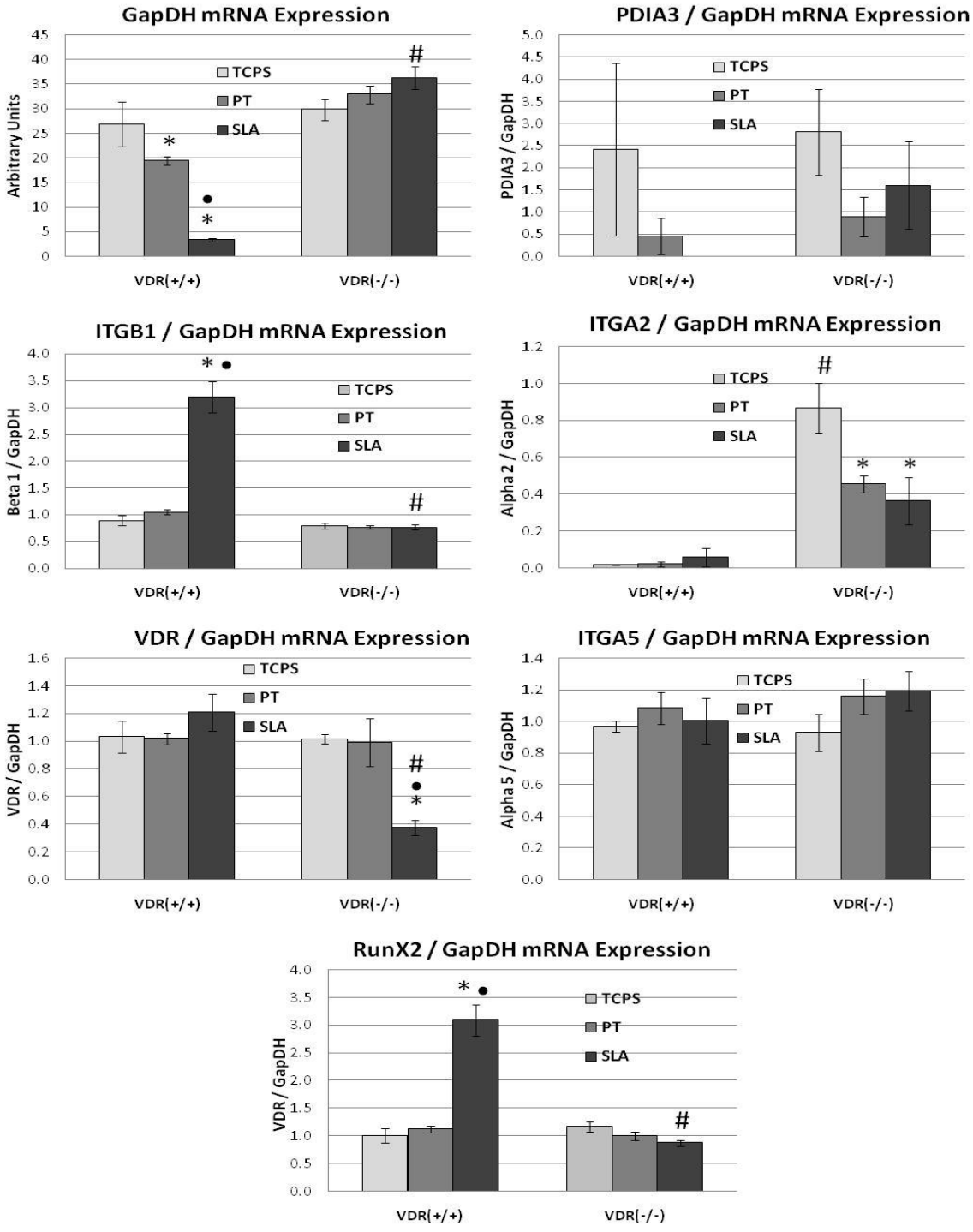

Figure A-5: Effect of changing surface roughness on expression of GapDH (Control), Pdia3, integrin beta 1, integrin alpha 2, integrin alpha 5, VDR, and Runx2 in osteoblasts harvested from Cav-1(+/+) and Cav-1(-/-) mice. Statistics: * Surface vs. TCPS; • SLA vs. PT; # WT vs. KO. Significant if $p < 0.05$. Experiment #1.

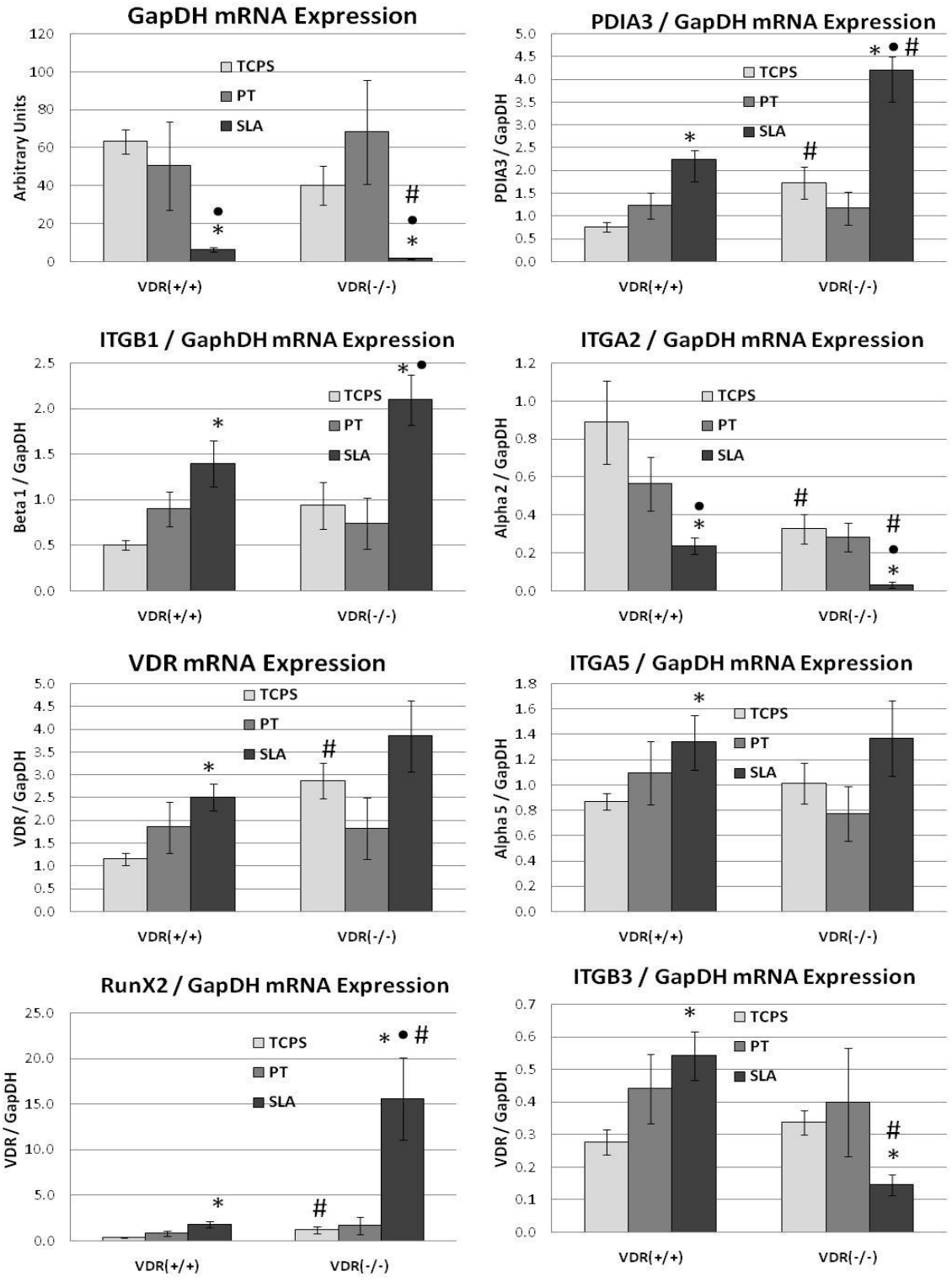

Figure A-6: Effect of changing surface roughness on expression of GapDH (Control), Pdia3, integrin beta 1, integrin alpha 2, integrin alpha 5, VDR, Runx2, and integrin beta 3 in osteoblasts harvested from Cav-1(+/+) and Cav-1(-/-) mice. Statistics: * Surface vs. TCPS; • SLA vs. PT; # WT vs. KO. Significant if $p < 0.05$. Experiment #2.

Selected Gene Expression in Cav-1 (+/+) and Cav-1(-/-) Osteoblasts ± 1α25(OH)$_2$D$_3$

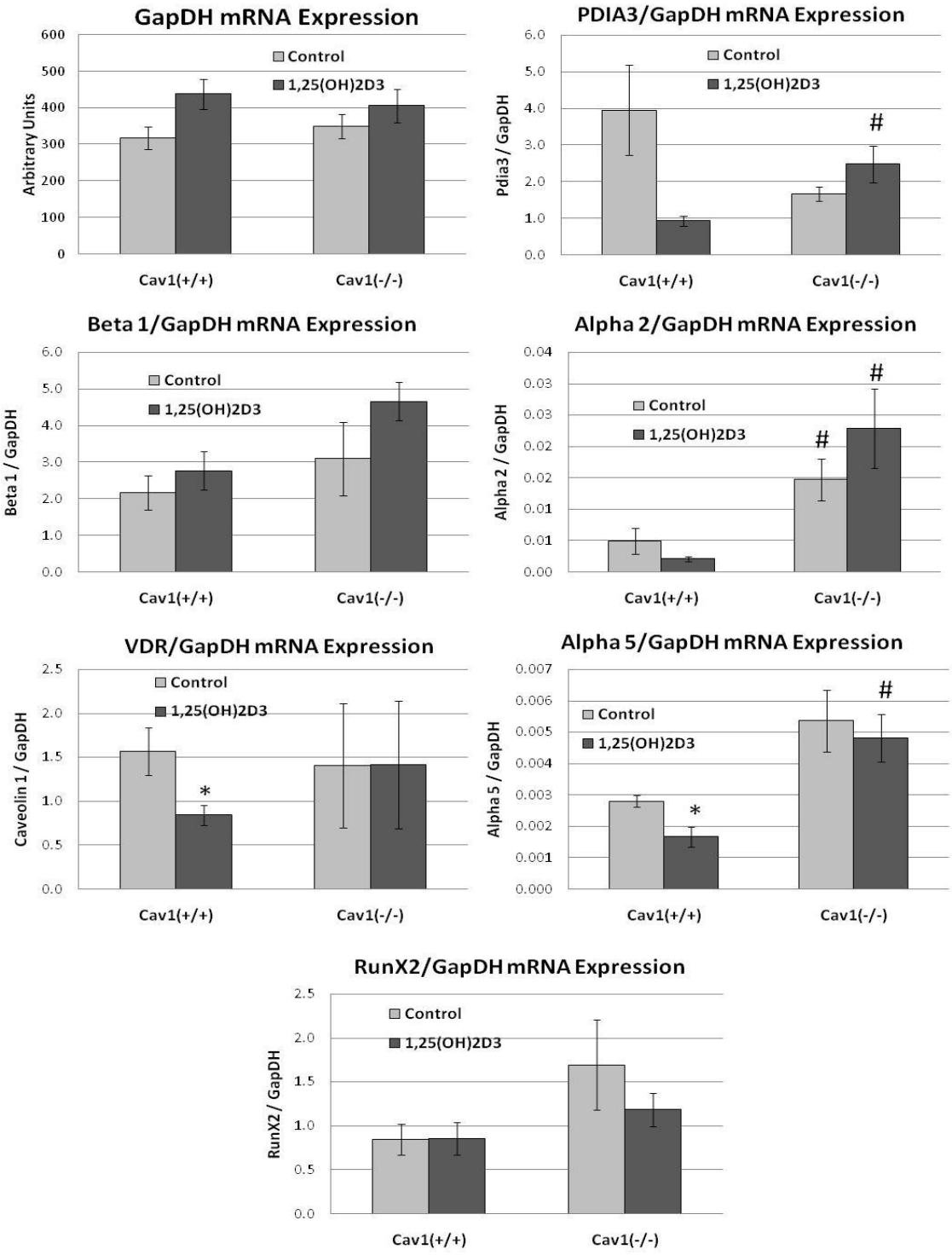

Figure A-7: Effect of 1α25(OH)$_2$D$_3$ on expression of GapDH (Control), Pdia3, integrin beta 1, integrin alpha 2, integrin alpha 5, VDR, and Runx2 in osteoblasts harvested from Cav-1(+/+) and Cav-1(-/-) mice. Statistics: * Control vs. 1α25(OH)$_2$D$_3$; # WT vs. KO. Significant if $p < 0.05$. Experiment #1.

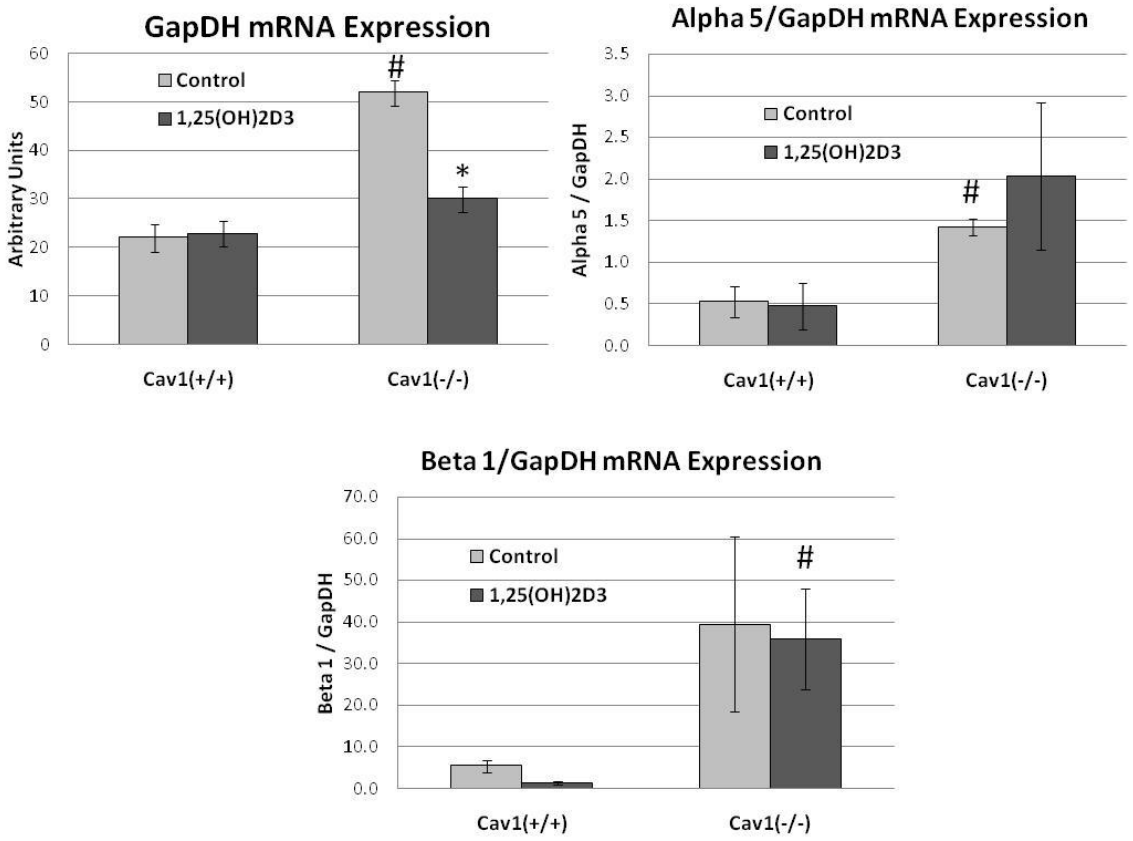

Figure A-8: Effect of $1\alpha25(OH)_2D_3$ on expression of GapDH (Control), integrin beta 1, and integrin alpha 5 in osteoblasts from Cav-1(+/+) and Cav-1(-/-) mice. Statistics: * Control vs. $1\alpha25(OH)_2D_3$; # WT vs. KO. Significant if $p < 0.05$. Experiment #2.

Pooled Gene Expression in VDR (+/+) and VDR (-/-) Osteoblasts

Table A-1: Pooled VDR(+/+) and VDR(-/-) data investigating the effect of surface roughness on expression of GapDH (Control), Pdia3, integrin beta 1, integrin alpha 2, integrin alpha 5, caveolin-1, Runx2, and integrin beta 3. Data is shown as mean ± 95% confidence interval. The bottom table displays ratios of gene expression on SLA versus PT surfaces in VDR(+/+) and VDR(-/-) osteoblasts. All data is pooled from two different experiments each with an n=6 per group.

Cell Type	Surface	GapDH	PDIA3	CAV1	ITGB1	ITGA2	ITGA5	RUNX2	ITGB3
WT	TCPS	84.1± 8.3	0.6± 0.3	0.9± 0.2	0.4± 0.1	1.1± 0.5	0.8± 0.2	1.1± 0.1	0.6± 0.2
WT	PT	98.1± 17.6	0.6± 0.5	0.1± 0.4	0.6± 0.1	1.6± 0.4	0.9± 0.4	0.8± 0.2	0.5± 0.1
WT	SLA	42.3± 26.4	0.6± 0.4	1.1± 0.3	0.9± 0.2	2.5± 0.9	1.7± 0.7	1.3± 0.5	1.4± 0.7
VDR KO	TCPS	67.0± 7.8	1.0± 0.3	1.6± 0.3	1.1± 0.3	0.9± 0.3	2.7± 0.9	0.7± 0.1	0.6± 0.2
VDR KO	PT	88.0± 24.5	1.0± 0.3	1.3± 0.3	0.9± 0.2	0.8± 0.3	1.5± 0.6	0.7± 0.2	0.7± 0.5
VDR KO	SLA	52.8± 19.7	6.5± 6.2	1.4± 0.5	1.1± 0.2	1.7± 0.3	1.9± 0.4	0.7± 0.3	0.7± 0.2

Cell Type	Surface	GapDH	PDIA3	CAV1	ITGB1	ITGA2	ITGA5	RUNX2	ITGB3
WT	SLA/PT	0.4	0.9	1.2	1.4	1.6	2.0	1.5	3.0
VDRKO	SLA/PT	0.6	6.4	1.1	1.2	2.0	1.3	1.0	1.1

Table A-2: Pooled VDR(+/+) and VDR(-/-) data only on TCPS surfaces to establish differences in baseline expression of the genes listed below. Data is shown as mean ± 95% confidence interval. Statistically significant values are shown in bold. Significance has been verified using ANOVAs blocked for the experimental batch. All data is pooled from the TCPS controls from four different experiments each with an n=6 per group.

Cell Type	Treatment	GapDH	PDIA3	CAV1	ITGB1	ITGA2	ITGA5	RUNX2	ITGB3
WT	Control	273.5 ± 146.1	0.3 ± 0.1	1.4 ± 0.6	1.5± 0.8	**1.7 ± 0.5**	1.4± 0.7	**2.0 ± 0.8**	0.8 ± 0.2
VDRKO	Control	282.1 ± 127.6	0.5 ± 0.3	3.4 ± 1.5	2.6± 1.2	**0.5 ± 0.2**	2.2± 0.6	**0.8 ± 0.3**	1.1 ± 0.3

Pooled Gene Expression in Cav-1 (+/+) and Cav-1 (-/-) Osteoblasts

Table A-3: Pooled Cav-1(+/+) and Cav-1(-/-) data only on TCPS surfaces to establish differences in baseline expression of the genes listed below. Data is shown as mean ± 95% confidence interval. Statistically significant values are shown in bold. Significance has been verified using ANOVAs blocked for the experimental batch. All data is pooled from two different experiments each with an n=6 per group.

Cell Type	Surface	GapDH	PDIA3	VDR	ITGB1	ITGA2	ITGA5	RUNX2	ITGB3
WT	TCPS	45.1± 13.0	1.5± 1.7	1.1± 0.2	0.7± 0.2	0.4± 0.3	1.0± 0.3	0.7± 0.2	0.3± 0.1
WT	PT	35.0± 23.7	0.9± 0.5	1.4± 0.6	1.0± 0.2	0.2± 0.2	1.0± 0.2	1.0± 0.3	0.4± 0.2
WT	SLA	4.9± 1.4	1.7± 1.0	1.9± 0.5	**2.3± 0.6**	0.2± 0.1	1.2± 0.3	**2.5± 0.6**	0.5± 0.2
Cav-1 KO	TCPS	35.1± 10.4	2.3± 1.0	2.0± 0.7	0.9± 0.3	0.6± 0.2	0.9± 0.2	1.2± 0.3	0.3± 0.1
Cav-1 KO	PT	50.7± 27.7	1.1± 0.5	1.4± 0.7	0.8± 0.3	0.4± 0.1	1.0± 0.3	1.4± 0.9	0.4± 0.3
Cav-1 KO	SLA	19.0± 10.5	3.0± 1.4	2.3± 1.4	1.4± 0.5	0.2± 0.2	1.3± 0.3	**9.3± 7.5**	0.2± 0.1

Cell Type	Surface	GapDH	PDIA3	VDR	ITGB1	ITGA2	ITGA5	RUNX2	ITGB3
WT	SLA/PT	0.1	2.0	1.3	2.4	0.7	1.2	2.5	1.2
Cav-1 KO	SLA/PT	0.4	2.9	1.6	1.9	0.6	1.3	6.8	0.4

Table A-4: Pooled Cav-1(+/+) and Cav-1(-/-) data only on TCPS surfaces to establish differences in baseline expression of the genes listed below. Data is shown as mean ± 95% confidence interval. Statistically significant values are shown in bold. Significance has been verified using ANOVAs blocked for the experimental batch. All data is pooled from the TCPS controls from four different experiments each with an n=6 per group.

Cell Type	Treatment	GapDH	PDIA3	VDR	ITGB1	ITGA2	ITGA5	RUNX2	ITGB3
WT	Control	107.6± 52.0	2.4± 1.5	1.3 ± 0.2	1.2 ± 0.5	0.3 ± 0.2	0.6± 0.2	**0.8 ± 0.2**	0.3 ± 0.1
Cav-1 KO	Control	117.8± 57.0	2.1± 0.7	1.8 ± 0.6	1.6 ± 0.8	0.4 ± 0.2	0.8± 0.3	**1.4 ± 0.4**	0.3 ± 0.1